NTNU – Trondheim
Norwegian University of
Science and Technology

Characterization of Cellular Effects of Insulin in SW982 Fibroblast-like Synoviocytes

Anide Johansen

Biotechnology (5 year)
Submission date: July 2014
Supervisor: Martin Tremen R. Kuiper, IBI

Norwegian University of Science and Technology
Department of Biology

Abstract

A Western diet is characterized by several components, but the main traits are a substantial consumption of red meats, refined carbohydrates and saturated fatty acids. Poor dietary choices and a low level of physical activity can quickly lead to lifestyle diseases like obesity and metabolic syndrome. It has previously been shown that the macronutrient composition of the diet affects the low-grade systemic inflammation in obese men. Both metabolic syndrome and obesity is linked to hyperinsulinemia and insulin resistance. Insulin signals through the insulin receptor (IR), which subsequently leads to many cellular responses including the activation of nuclear factor-κB (NF- κB) and induction of pro-inflammatory mediator production. Increasing body mass index has been linked to increasing disease activity scores (DAS28) for Rheumatoid Arthritis (RA) patients. RA is an autoimmune disease of the synovial membrane of joints, which becomes a hyperplastic, invasive tissue teeming with immunocompetent cells. This will eventually lead to excessive bone loss and chronic inflammation of the synovial membrane, a condition called synovitis.

The effect of chronic elevated levels of insulin on disease activity of RA is not yet known. Here, we investigate the potential of insulin to activate cytosolic phospholipase A_2α ($cPLA_2$α), which has been shown to be a key regulator of inflammation in RA, in a cell model for synovitis (SW982). In this master's thesis we also investigate a potential role for insulin in regulating proliferation and gene expression in SW982. More specifically, the time-dependent regulation of the genes insulin receptor (IR), insulin-like growth factor 1 receptor (IGF1R), c-Myc, c-Fos and interleukin 6 (IL-6) was investigated.

Detection of IR and IGF1R expression by real time quantitative polymerase chain reaction (RT-qPCR) in SW982 synoviocytes, validated for the first time that these cells express the respective receptors and that they are potentially susceptible to insulin signaling.

The activity of $cPLA_2$α in response to insulin was evaluated using a radioactive release assay in pre-labeled SW982 cells, which measures the activity of $cPLA_2$α by measuring the amount of arachidonic acid (AA) released from the cells. These tests showed that insulin did not increase the release of AA. However, this test did reveal a trend of decreased release of oleic acid (OA) in response to insulin. These results suggest a PLA_2 independent pathway for insulin signaling. Also, a pro-inflammatory role of insulin mediated through the hormone sensitive lipase (HSL) is speculated upon based on these results.

MTT viability assay was used to evaluate the effect of insulin on the metabolic activity of cultured SW982s. We found that insulin increases the metabolic activity by ~50% in a time, confluency and dose dependent manner. However, these results were not validated as

increased proliferation by flow cytometry. We speculate upon an activation of protein kinase B (PKB) by insulin, which signals increased survival of SW982 cells.

By RT-qPCR we show that insulin downregulates IR expression, and a similar trend is observed for IGF1R. Insulin induced no change in c-Myc expression, and induced a downregulation of c-fos after 12 hours. Further, insulin induced a time-dependent trend of increase in IL-6 gene expression. Insulin also induced variation in the expression of the previously accepted reference gene 18S.

More tests have to be conducted in order to validate/discard the hypotheses proposed in this study. Including the possible pro-inflammatory actions of insulin in synovial cells and other tissue, mediated through inhibition of HSL. The potential for insulin to induce hyper proliferation and increased survival of synovial cells through activation of PKB, and the potential for insulin to induce expression proliferative and inflammatory genes.

Sammendrag

En Vestlig diett karakteriseres gjerne ved flere komponenter, men i hovedtrekk domineres den av store mengder rødt kjøtt, raffinerte karbohydrater og mettet fett. Uheldige kostholdsvalg og et lavt nivå av fysisk aktivitet kan fort føre til livsstilssykdommer som overvekt og metabolsk syndrom. Det har tidligere blitt vist at kostholdets makronæringsstoffsammensetning påvirker den systemiske inflammasjonen hos overvektige menn. Både metabolsk syndrom og overvekt er forbundet med hyperinsulinemia og insulinresistens. Insulin signaliserer via insulinreseptoren (IR), som deretter fører til flere cellulære responser inkludert aktiveringen av transkripsjonsfaktor NF- κB (nuclear factor-κB) og induksjon av produksjon av pro-inflammatoriske mediatorer. Det har tidligere blitt vist at økende kroppsmasseindeks (BMI) sammenfaller med økende grad av sykdomsaktivitet (DAS28) hos pasienter med Revmatoid Artritt (RA). RA er en autoimmun sykdom i synovialmembranen i ledd, som blir til et hyperplastisk, invaderende vev som bugner av immunkompetente celler. Dette vil til slutt føre til en høy grad av tap av ben og kronisk inflammasjon i synovialmembranen, en tilstand som kalles synovitt.

Effekten av kronisk høye nivåer av insulin på sykdomsaktiviteten i RA er til nå uklar. I denne avhandlingen, utforsker vi insulins potensiale til å aktivere cytosolisk fosfolipase A_2 (cPLA$_2$α), som har blitt utpekt som en nøkkelregulator av inflammasjon i RA, i en cellemodell for synovitt (SW982). I denne avhandlingen utforsker vi også en potensiell rolle for insulin i reguleringen av proliferasjon og genuttrykk i SW982. Nærmere forklart, den tidsavhengige reguleringen av genene IR, insulin-liknende vekstfaktor 1 reseptor (IGF1R), c-Myc, c-Fos og interleukin 6 (IL-6).

Deteksjon av IR og IGF1R ble utført ved hjelp av sanntids kvantitativ polymerase kjedereaksjon (RT-qPCR) i SW982 synoviocytter, som for første gang validerte at disse cellene uttrykker de respektive reseptorene og at cellene potensielt er mottagelige for insulinsignalisering.

Aktiviteten til cPLA$_2$α i respons til insulin ble evaluert ved hjelp av et radioaktivt frigjøringsforsøk i merkede SW982 celler, som måler aktiviteten av cPLA$_2$α ved å måle mengden arakidonsyre (AA) som frigjøres fra cellene. Disse forsøkene viste at insulin ikke øker frigjøringen av AA. Men, disse testene avslørte en trend av reduksjon i frigjøringen av oljesyre (OA) i respons til insulin. Disse resultatene foreslår en PLA$_2$-uavhengig signaliseringskaskade for insulin. Basert på disse resultatene, ble det også spekulert i en pro-inflammatorisk rolle for insulin mediert gjennom en hormonsensitiv lipase (HSL).

MTT viabilitetsforsøk ble brukt til å evaluere effekten av insulin på metabolsk aktivitet hos kultiverte SW982. Vi observerte at insulin øker den metabolske aktiviteten med ~50% på en tids-, konfluens- og doseavhengig måte. Men, disse resultatene ble ikke validert som økt proliferasjon ved hjelp av flow cytometri. Likevel, spekulerer vi i en insulinavhengig aktivering av protein kinase B (PKB), som signaliserer til økt overlevelse i SW982.

Ved hjelp av RT-qPCR har vi vist at insulin nedregulerer uttrykket av IR, og at en liknende trend observeres for IGF1R. Insulin induserer ingen endring i uttrykk av c-Myc, og induserer en nedregulering av c-Fos etter 12 timer. Videre, insulin induserte en tidsavhengig trend av oppregulering i uttrykket av IL-6. Insulin induserte også variasjon i uttrykket av det etablerte referansegenet 18S.

Flere tester må utføres for å kunne bekrefte/avkrefte hypotesene i denne avhandlingen. Inkludert en mulig pro-inflammatorisk effekt av insulin i synovialceller og andre vev, mediert av inhiberingen av HSL. Insulins potensiale til å indusere hyperproliferasjon og økt overlevelse hos synovialceller gjennom aktivering av PKB, og potensialet for insulin til å indusere uttrykk av proliferative og inflammatoriske gener.

Preface

It's in my blood. I don't think this phrase could be any more applicable than in my case. Growing up in a family of professors has both positive and negative sides. On one hand you have the extreme expectations for academic achievement. But on the other hand you have a unique insight into the world of research and endless curiosity, driven by a creative, unstoppable mindset. In my case, this adolescence has left me with an insatiable desire and hunger for knowledge and plenty of motivation to reach my goals. It is safe to say that I would not be where I am today without my parents, Berit and Thorleif. Thank you for making sure I knew that only the sky was the limit.

I would also like to give a special thanks to my best friend and mental support, Anja. I would not have made it all the way without you. A huge thanks to my intellectual supervisors senior researcher, Dr. Astrid and Dr. Randi; you are two very strong and smart women and definitely great role models of mine. Thank you for being available at all times and for answering every question I threw your way. Last but not least, thank you Martin for being such a reliable, patient, available and incredibly knowledgeable supervisor!

Trondheim, July 2014

Anide Johansen

List Of Abbreviations

18S	Ribosomal 18S rRNA
AA	Arachidonic Acid
AATC	American Type Culture Collection
AC	Adenylate Cyclase
ALA	α-Linoleic Acid
AP-1	Activating Protein 1
ATP	Adenosine Triphosphate
B2M	Beta-2 Microglobulin
BEL	Bromoenol Lactone
BMI	Body Mass Index
BRC	Biological Resource Center
C-Peptide	Connecting Peptide
cAMP	Cyclic Adenosine Monophosphate
CCP	Cyclic Citrullinated Peptides
cDNA	Complimentary Deoxyribonucleic Acid
cGMP	Cyclic Guanosine Monophosphate
COX	Cutaneous Cyclooxygenase
$cPLA_2\alpha$	Cytosolic Phospholipase A_2 α
Cq	Quantification Cycle
CREBP	cAMP Response Element-Binding Protein
Ct	Threshold Cycle
CYP	Cytochrome P450
DAMP	Damage Associated Molecular Pattern
DAS28	Disease Activity Score, 28 Joints
DCV	Dense Core Vesicle
DGLA	Dihomo-gamma-linoleic Acid
DHA	Docosahexaenoic Acid
DHET	Dihydroxyeicosatrienoic Acid
DMEM	Dulbecco's Modified Eagle's Medium
DMEM10%	DMEM; 10% FBS, 3% Glutamine, 0.2% Gentamicin
DMSO	Dimethyl Sulfoxide
DNA	Deoxyribonucleic Acid
ECM	Extra-Cellular Matrix
EET	Epoxyeicosatrienoic Acid
ELISA	Enzyme-Linked Immunosorbant Assay
EPA	Eicosapentaenoic Acid
ER	Endoplasmic Reticulum
ETA	Eicotrioenic Acid

FBS	Fetal Bovine Serum
fBSA	Fatty Acid Free Bovine Serum Albumin
FLS	Fibroblast-Like Synoviocytes
FSL-1	TLR-2/6 Ligand
gDNA	Genomic Deoxyribonucleic Acid
GLUT4	Glucose Transporter 4
HDHA	Hydroxy-docosahexaenoic Acid
HEPE	Hydroxyeicosapentaenoic Acid
HETE	Hydroxyeicosatetraenoic Acid
HETrE	Hydroxyeicosatrienoic Acid
HODE	Hydroxyoctadecadienoic Acid
HPRT	Hypoxanthine-Guanine Phosphoribosyltransferase
HSC	Hematopoietic Stem Cells
HSL	Hormone Sensitive Lipase
ICAM	Intercellular Adhesion Molecule
IFN- γ	Interferon-Gamma
IGF1	Insulin-Like Growth Factor 1
IGF1R	Insulin-Like Growth Factor 1 Receptor
IKK	IKB Kinase
IL	Interleukin
iNOS	Nitric Oxide Synthase
INS	Insulin
$iPLA_2$	Ca^{2+} independent PLA_2
IR	Insulin Receptors
IRS1	Insulin Receptor Substrate 1
LA	Linoleic Acid
LDL	Low-Density Lipoprotein
LOX	Lipoxygenase
LT	Leukotriene
LTA_3	Leukotriene A3
LTA_4	Leukotriene A4
LTB_4	4-series Leukotrienes
LXA4	Lipoxin A4
Lyso-PC	Lyso-Phosphatidyl Choline
MAFP	Methoxy Arachidonyl Fluorophosphate
MAPK	Mitogen Activating Protein Kinase
MHC	Major Histocompatibility Complex
MMP3	Matrix Metalloproteinase
mRNA	Messenger Ribo Nucleic Acid
MTT	3,4,5 Dimethylthiazol-2,5 Diphenyl Tetrazolium

NaOH	Sodium Hydroxide
NF-κB	Nuclear Transcription Factor
NFATc1	Nuclear Factor of Activated T Cells
NIDDM	Non-Insulin Dependent Diabetes Mellitus
NIK	NFKB Inducing Kinase
OA	Oleic Acid
OD	Optical Density
$PACOCF_3$	Palmitoyl Trifluoromethyl Ketone
PAF	Platelet Activating Factor
Pam_3CSK_4	TLR2 Ligand
PAMP	Pathogen Associated Molecular Pattern
PC	Choline Phospholipids
PCR	Polymerase Chain Reaction
PD	Prostaglandin
PDE3B	Phosphodiesterase 3B
PDGF	Platelet Derived Growth Factor
PDK1	Phosphoinositide-dependent Kinase 1
PGD_2	Prostaglandin D2
PGE_2	Prostaglandin E2
PGF_2	Prostaglandin F2
PGF_2a	Prostaglandin F2alpha
PGI_2	Prostaglandin I2
PGJ_2	Prostaglandin J2
PGS	Terminal Prostanoid Synthase
PI3K	Phosphoinositide 3-Kinase
PIP_2	Phosphatidylinositol-4,5-bisphosphate
PIP_3	Phosphatidylinositol-3,4,5-trisphosphate
PKA	Protein Kinase A
PKA	Protein Kinase A
PKB	Protein Kinase B
PKC	Protein Kinase C
PKG	cGMP-dependent Protein Kinase
PLC	Phospholipase C
PTPN22	Protein Tyrosine Phosphatase, Non-Receptor Type 22
PUFA	Poly-Unsaturated Fatty Acids
QUEST-RA	Quantitative Patient Questionnaire Monitoring in Standard Clinical Care of Patients with RA
RANK	Receptor Activator of NF-KB
RANKL	Receptor Activator of NF-KB Ligand
RER	Rough Endoplasmic Reticulum

RNA	Ribo Nucleic Acid
ROS	Reactive Oxygen Species
rRNA	ribosomal RNA
RT-qPCR	Real Time Quantitative Polymerase Chain Reaction
RvD	Resolvin D-series
RvE	Resolvin E-series
SF	Serum Free
SF-DMEM	Serum free DMEM
SLC2A4	Solute Carrier Family 2A4
$sPLA_2$	Secretory PLA_2
SW982	Human Synovial Cell Line
TDMGlycerides	Tri-, di-, monoglycerides
TGF	Transforming Growth Factor
TGL	Triglyceride Lipase
THP1	Human Leukemic Monocyte Cell Line
TLR	Toll-Like Receptor
Tm	Melting Temperature
TNFα	Tumor Necrosis Factor Alpha
TXB2	Series-2 Thromboxane
WAT	White Adipose Tissue

Table Of Contents

1. Introduction

1.1 The Western Diet

A Western diet[1] is characterized by a substantial consumption of red meat, refined carbohydrates (with a high glycemic index) and saturated fatty acids, accompanied by the scarce content of micronutrients. The combination of a calorie dense diet and a sedentary life is a selling and effortless lifestyle among the urban population of the 21st century. The genetic makeup of humans determines the preferred way of living, which since the Paleolithic Era has been a pre-agricultural-revolution-lifestyle where the average Joe was a hunter-gatherer with significantly exceeding health markers, body composition and physical fitness compared to the modern average Joe[2]. The increasing interest for a western-type way of living was quickly accompanied by a series of illnesses commonly referred to as *lifestyle diseases*, also known as *diseases of longevity* or *diseases of civilization*. Lifestyle diseases may include several infamous conditions such as Alzheimer's disease[3], asthma, some cancers[4], coronary heart disease[4], type 2 diabetes[5], metabolic syndrome[6] and obesity[6]. When living on a western diet, where carbohydrates with a high glycemic index vastly dominate the macronutrient composition, the body is forced to constantly produce and secrete the growth hormone insulin in order to cope with elevated levels of blood sugar.

1.2 Insulin Resistance

1.2.1 Insulin

The primary structure of Insulin was elucidated in the mid 1950s by Fred Sanger, who later received the Nobel prize for his accomplishments.[7] Insulin is a two-chain, growth-promoting hormone[8], cleaved from a single-chain precursor. Initial translation of the insulin mRNA yields preproinsulin, which is a single polypeptide chain. Preproinsulin is cotranslationally translocated into the rough endoplasmic reticulum (RER), by the help of a 24-residue hydrophobic signal peptide at the N-terminal of the nascent chain.[7] Once inside the RER a peptidase will cleave the signal peptide to form the proinsulin, and chaperones will catalyze the folding of the hormone. After being folded, the proinsulin translocates to the Golgi, where it is transferred to immature secretory vesicles and subsequently cleaved into three fragments: connecting peptide (C-peptide), β-chain and α-chain (figure 1.2.1.1). In healthy individuals, insulin and C-peptide is secreted into the blood stream in equal amounts. Insulin hormone and connecting peptide is stored in dense core vesicles (DCVs) in the β-cells until the respective cell receives a signal to secrete the hormone.

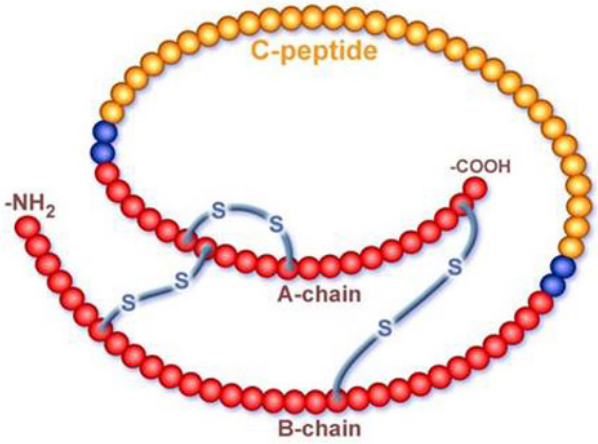

Figure 1.2.1.1: The detailed structure of proinsulin. Contains C-peptide, β-chain and α-chain.[9]

1.2.2 Insulin Secretion

When ingested, carbohydrates are dilapidated into sugar monomers (glucose), which reach cells throughout the body through the blood stream. Regardless of periods of feeding or fasting, plasma glucose levels in normal, healthy human beings remain in a range between 4 and 7 mM.[10] The presence of glucose in the blood causes β-cells in the pancreas (islets of Langerhans) to secrete insulin. Insulin binds to the insulin receptor (IR), causing the cell to bring more glucose transporters to the surface, subsequently empowering the cell to lower blood sugar levels through the uptake of glucose. Insulin stimulates the translocation of the glucose transporter GLUT4 from intracellular sites to the cell membrane.[10] The GLUT4 protein is encoded by the Solute Carrier Family 2A4 (SLC2A4) gene, and is important for maintaining glycemic homeostasis.[11] Insulin signaling occurs through activation of its tyrosine kinase receptor, which subsequently activates the insulin receptor subunit 1 (IRS1), which in turn activates phosphoinositide 3-kinase (PI3K) resulting in the activation of several proteins, including protein kinase B (PKB). The activation of PKB can lead to a variety of cellular responses, including promotion of cell cycle, inhibition of apoptosis and cellular transformation.[12] Secretion of insulin also inhibits hepatic glucose production, lipolysis and protein breakdown, and activates several metabolic pathways, like glycogen synthesis, glycolysis, glucose oxidation, *de novo* lipogenesis and protein synthesis.[13] Insulin is the primary regulator of cell metabolism, but not the only. Insulin-Like Growth Factor 1 (IGF-1) is a polypeptide with similar structure and function as insulin.[14] IGF-1 is also an essential growth-promoting peptide, and binds to the IGF1 Receptor (IGF1R). The binding affinity of IGF1 to IGF1R is high, likewise the binding affinity of insulin to IR is high. Even though these two growth hormones have their respective receptors, research suggests that they can bind to each other's receptors (*cross-binding*).[14] The cross-binding affinity of the growth hormones to the receptors is not as high (1/1000), as the hormones binding to their specific receptor.[14] The IR is a

heterotetramer tyrosine kinase receptor, made of two α- and two β-chains linked by disulfide bonds. The IR is activated upon binding of an insulin ligand to each αβ-dimer. After tetramerization the receptor autophosphorylates and an extrinsic kinase phosphorylates additional tyrosine residues for full activation. The response to insulin stimulation, the cell's sensitivity to insulin, depends on several aspects of cellular signaling, including the number of receptors on the surface of each cell and the affinity of ligand binding to the receptor. A decrease in a cell's sensitivity to a particular ligand is called desensitization.[15] Insulin holds the ability to desensitize its target cells to its actions through several mechanisms, including at receptor level and downstream targets.[16] A brief rise in insulin is stimulatory, while a chronic elevated level of insulin (>24h[16]) desensitizes the target cell and leads to generalized insulin resistance.[17] Twofold elevations of basal insulin levels are common in patients with insulin resistance associated with obesity or type 2 diabetes.[17]

1.2.3 Insulin Desensitization and Insulin Resistance

When the production and distribution of insulin in response to continuously high levels of blood sugar, is at an abnormally high rate, the insulin responding cells become desensitized and stops responding to insulin. Cells become resistant to insulin, which results in an elevation of blood sugar levels (hyperglycemia), and eliminates the ability of cells to take up important nutrients like glucose, amino acids and fatty acids. These events subsequently cause the β-cells to produce more insulin (hyperinsulinemia), which often is a precursor of insulin resistance. In people with insulin resistance, the liver might fail to reduce its production of glucose. In healthy individuals the liver reduces the production of glucose from glucagon, in response to the amount of circulating insulin. This will also cause the blood glucose to rise. There are several signs and symptoms of insulin resistance, including high blood sugar, inability to focus, increased blood triglyceride levels, depression and other. The associated risk factors include family history with type 2 diabetes, obesity, a tendency to store fat in the abdomen, hypertension, high triglyceride levels and others. Insulin resistance is also associated with and often seen as a precursor of other metabolic diseases like non-insulin dependent diabetes mellitus (NIDDM), obesity, hypertension, dyslipidemia and atherosclerotic cardiovascular disease.[18]

1.3 Obesity and Metabolic Inflammation

1.3.1 The Immune Response

The immune system protects the human body from the harmful effects of exposure to pathogens. The immune system is continuously learning to recognize new pathogens, while the pathogens are learning new ways to escape. Pathogens can enter the body in several ways and once inside the body, the immune system will recognize it as foreign and start the process of elimination; the immune response. An immune response includes the activation and recruitment of immune cells. Immune cells, like all blood cells, are derived from the pluripotent hematopoietic stem cells (HSCs) in the bone marrow.[19] HSCs are self-renewing and can differentiate along two different pathways, producing either myeloid progenitors or lymphoid progenitors. Myeloid progenitor cells can differentiate into dendritic cells, monocytes neutrophils, macrophages, eosinophils, basophils and erythrocytes. Lymphoid progenitor cells can differentiate into natural killer cells, T-cells and B-cells.[19]

The immune system is divided into two categories, depending on the onset of the response. The *innate* immune system is the first response to a pathogen invading an organism. The innate immune system is triggered by damage-associated molecular pattern molecules (DAMPs; the alarm signals of damaged cells) or by pattern recognition receptors (PRRs), which recognize pathogen-associated molecular patterns (PAMPs) associated with microbial pathogens and DAMPs.[20] Once the innate immune system is activated, an inflammation will occur. Inflammation is characterized by redness, pain, heat and swelling, which reflect the three major events of an inflammatory response: vasodilation (an increase in the diameter of blood vessels), increase in capillary permeability and an influx of phagocytes from the capillaries into the tissue.[19] A long cascade of events involving several chemical mediators initiates the inflammatory response. These mediators include chemicals released from damaged cells, pathogens and white blood cells, and some are also produced by plasma enzyme systems. Examples of pro-inflammatory chemicals include various serum proteins called acute-phase proteins (C-reactive protein), eicosanoids (prostaglandins and leukotrienes) and cytokines (interferons, interleukins and chemokines), released by infected cells.[21-23]

1.3.2 Obesity

Obesity is a modern world medical condition, associated with the accumulation of excess body fat to the point where it may have adverse effects on a person's health, life quality and life expectancy. Obesity is not only a personal issue, but also a disease with a huge negative impact on the nation's economy. The calculated direct and indirect costs in the United States for obesity related medical care in 2005 dollars, was a staggering $190 billion. This number accounts for 20.6% of the national health expenditures in the US, indicating that an obese person's medical costs will be $2751 higher than a normal weight person.[24] Being obese creates a major predisposition to several diseases, including atherosclerosis, certain cancers,

arthritis, type 2 diabetes and specific immune-mediated disorders.[25] The causal factors of obesity are many, highly complex and not fully elucidated. Such circumstances include energy consumption, activity level, genetics, meal macronutrient composition, and economic, social and environmental factors. Over the past several decades, the harmonic equilibrium between the aforementioned factors has shifted. A decrease in activity is coupled with an increase in caloric intake, fueled by easily accessible, cheap, calorie dense and pre-processed food items.[26] The unfortunate outcome of this is a lipid loading of the adipocytes, resulting in an increased mass of the human population, leaving 34.9% of the US adult population categorized as obese (Body Mass Index >30). [27]

1.3.3 Adipose Tissue

The most abundant cells in fat, or adipose tissue, are adipocytes. In addition to adipocytes, fat contains pre-adipocytes, endothelial cells, fibroblasts, leukocytes and macrophages.[28] The number of macrophages in adipose tissue is shown to correlate directly with obesity, and a low-grade inflammation of the adipose tissue has been characterized as a hallmark of both obesity and insulin resistance.[29] In mammals, adipose tissue is found in two forms; white and brown adipose tissue. These two types of fat have distinct tasks in the body. While white adipose tissue (WAT) is mainly used for the storage of excess energy, brown adipose tissue is applicable in the regulation of body temperature, has an elevated number of mitochondria and is primarily found in infants.[25]

WAT was previously thought to be an inert tissue, but it is now well established that adipose tissue holds important endocrine properties, producing and secreting numerous hormones, cytokines and chemokines.[30] The production and presence of the aforementioned pro-inflammatory molecules, has an unfortunate effect on the metabolic equilibrium in the body. Research has shown that pro-inflammatory molecules are associated with a sustained, but low-grade level of inflammatory changes that seem to arise from the daily challenges of nutritional excess.[31] This state of inflammation is called metabolic inflammation.

1.3.4 Metabolic Inflammation

Metabolic inflammation is a term frequently used to describe a low-grade systemic inflammation, characterized by the constant production of pro-inflammatory molecules like interleukin-6 (IL-6), nuclear transcription factor (NF-κB), leptin, tumor necrosis factor alpha (TNFα) and others.[31] Figure 1.3.4.1, shows some of the mediators of NF-κB activation and metabolic inflammation.

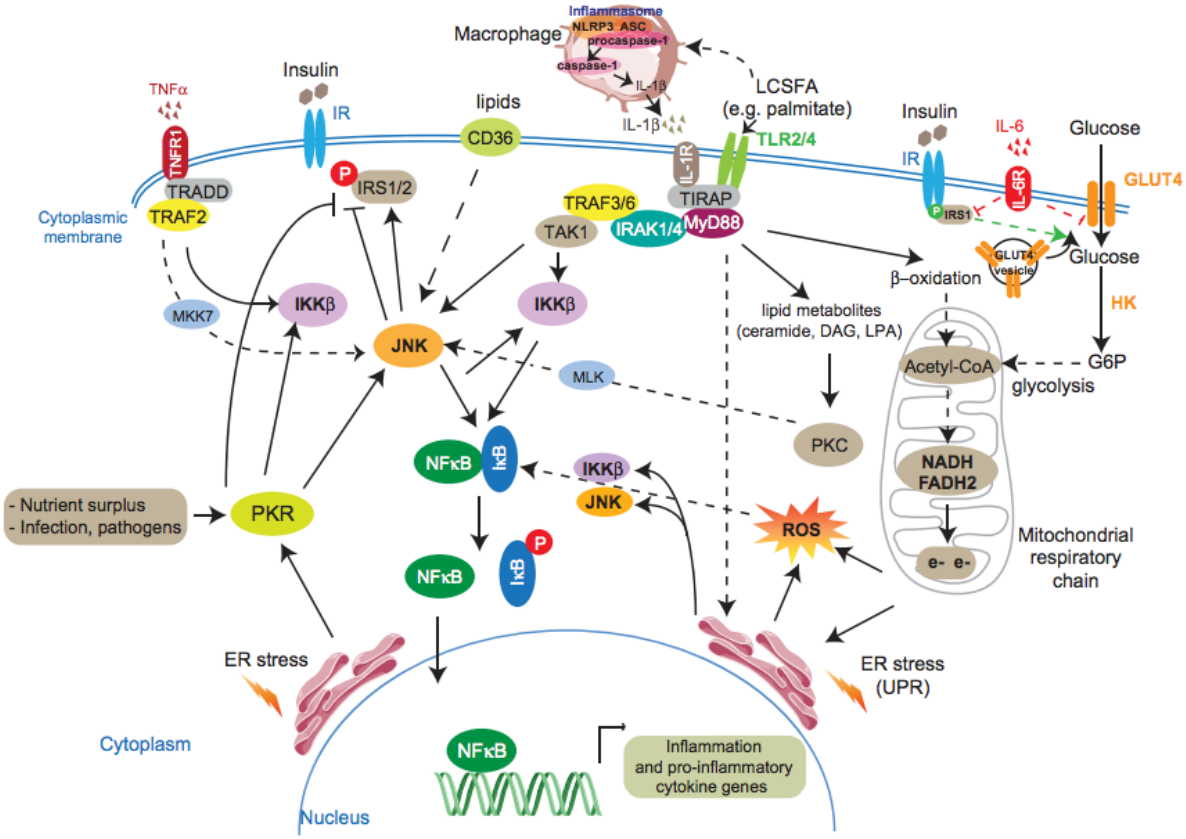

Figure 1.3.4.1: Mediators of NF-κB activation leading to the production of pro-inflammatory cytokine genes and a subsequent inflammation.[32]

Metabolic inflammation has several components; among these are endoplasmic reticulum (ER) stress, production of reactive oxygen species (ROS), production of pro-inflammatory cytokines and more. Activation of several signaling pathways have been associated with metabolic inflammation, including signaling through the insulin receptor (IR), which leads to induction of ER stress, production of ROS and the subsequent activation of NF-κB.[32, 33] The long-term effect of a low-grade systemic inflammation is the development of a cluster of chronic metabolic disorders, including obesity, type 2 diabetes and cardiovascular disease.[34]

1.3.5 Fatty Acids

Even though mammals are able to produce certain fatty acids from non-fat precursors like glucose and amino acids, this does usually not occur in humans. Because of the high content of fat (especially saturated and monounsaturated fatty acids) in the Western Diet, the human body does not produce fatty acids from non-fat precursors. However, the only fatty acids mammals absolutely cannot produce are the ones that have a double bond between the methyl terminus and carbon number nine in oleic acid (OA; 18:1n-9). This means that mammals neither can convert oleic acid into linoleic acid (LA; 18:2n-6), nor perform further oxidation of linoleic acid into α-linoleic acid (ALA; 18:3n-3).[35] LA and ALA are therefore termed essential fatty acids, and are found mainly in plants. Proceeding consummation, LA and ALA can be converted to arachidonic acid (AA; 20:4n-6), and eicosapentaenoic acid (EPA; 20:5n-3), docosapentaenoic acid (22:5n-3) and docosahexaenoic acid (DHA; 22:6n-3) by the pathways outlined in figure 1.3.6.1, respectively. EPA and DHA are mainly found in “oily fish” like herring, mackerel, tuna and sardines, and also in commercial products called “fish oils”. Studies show[36, 37] that human mononuclear immune cells (B- and T-lymphocytes, monocytes) contain 15-25% AA, 6-10% LA, 1-2% dihomo-γ-LA, and only 2-4% and 0,1-0,8% ALA and EPA/DHA, respectively. By increasing the dietary intake of n-3 fatty acids, the proportion of n-3 fatty acids in immune cells will increase at the expense of AA levels.[35] In cells with a high content of AA, this will be the primary precursor for eicosanoids produced in the cell. Eicosanoids are important in the regulation of inflammatory and immune response intensity and duration. Eicosanoids links fatty acids to immune function. EPA can inhibit the production of these pro-inflammatory eicosanoids, and is therefore a desired component of a healthy diet.[38]

1.3.6 Eicosanoids

Eicosanoids are derived from omega-3 (n-3) or omega-6 (n-6) fatty acids, where the omega-6 derived eicosanoids are mainly responsible for the induction of inflammation. The typical Western diet contains 20-25-fold more n-6 fatty acids than n-3 fatty acids.[38] The different types of eicosanoids include 2-series prostaglandins (PG; ex. PGE_2, PGD_2 and PGF_2), thromboxane and 4-series leukotrienes (LT; ex. LTB_4), and are produced from several precursors by the action of cutaneous cyclooxygenase (COX), terminal prostanoid synthase (PGS), lipoxygenase (LOX) and cytochrome P450 (CYP) enzymes. The precursor fatty acids from which the eicosanoids are produced include AA and the C-20 polyunsaturated fatty acids (PUFA) dihomo-γ-linoleic acid (DGLA; 20:3n-6) and EPA (20:5n-3).[39] Figure 1.3.6.1 shows a schematic overview of polyunsaturated fatty acids and the biosynthetic pathways of their oxygenated products.

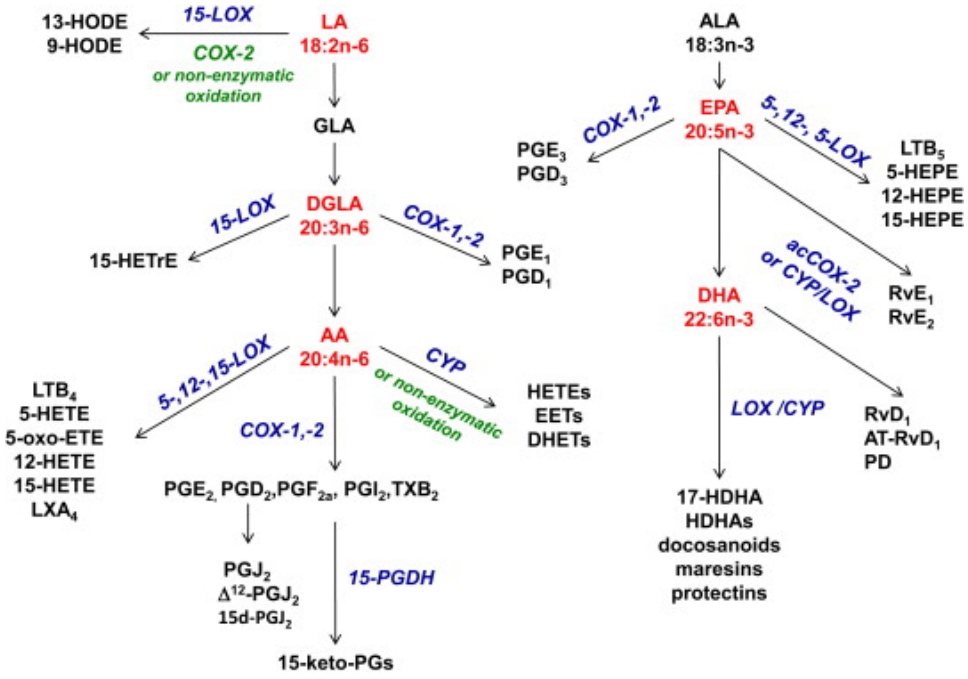

Figure 1.3.6.1: Schematic overview of polyunsaturated fatty acids and the biosynthetic pathways of their oxygenated products.[39] HODE: Hydroxyoctadecadienoic acid. HETrE: Hydroxyeicosatrienoic acid. HETE: Hydroxyeicosatetraenoic acid. EET: Epoxyeicosatrienoic acid. DHET: Dihydroxyeicosatrienoic acid. LXA4: Lipoxin A4. PGD2: Prostaglandin D2. PGF2a: Prostaglandind F2alpha. PGI2: Prostaglandin I2. TXB2: Series-2 thromboxane. PGJ2: Prostaglandin J2. HEPE: Hydroxyeicosapentaenoic acid. RvE: Resolvin E-series. RvD: Resolvin D-series. HDHA: Hydroxy-docosahexaenoic acid.

PGE_2 and LTB_4 are the two most studied eicosanoids. LTB_4 is a potent enhancer of inflammatory responses. LTB_4 enhances local blood flow, increases vascular permeability, promotes natural killer activity and enhances the production of pro-inflammatory cytokines like TNF-α, IL-1β, IL-6, IL-2 and IFN-γ.[40] PGE_2 is a biologically active immunoregulator and -activator[41, 42]. PGE_2 promotes immune cell influx to inflamed tissues and inflammatory angiogenesis, and is associated with several diseases, including Alzheimer's disease, RA and cancer.[43, 44] EPA can inhibit the synthesis of both PGE_2 and LTB_4 via competitive inhibition of the enzymes that catalyze the metabolism of AA, cyclooxygenase and 5-lipoxygenase, respectively.

Phospholipases are responsible for the mobilization of the different fatty acids. Phospholipase A_2 (PLA_2) enzymes catalyze the release of AA from the lipid bilayer. Ca^{2+} independent PLA_2 has previously been shown to catalyze the hydrolysis of choline phospholipids (PC), resulting in synthesis of monoacyl lysophosphatidylcholine (LPC).[45] The release of free fatty acids is mediated by a variety of lipases apart from the phospholipase A2 enzymes, including the hormone sensitive lipase (HSL) and triglyceride lipase (TGL). The TGL acts on triglycerides, whereas the HSL acts on tri-, di- and monoglycerides (TDMglycerides). [46] TGL has so far only

been found to be expressed in adipose tissue, while HSL is found to be expressed in various tissues, mainly in adipose and steroidogenic tissue.[47]

1.4 cPLA$_2$

PLA$_2$ is the principle lipolytic enzyme responsible for the release of AA and other PUFAs from membrane phospholipids.[48] There are more than 20 different human phospholipases in the PLA$_2$ family, located in the cytosol, the cell membrane and extracellularly, secreted from the cell. Other than cellular location, the enzymes differ in structure, molecular weight, substrate specificity, requirement for Ca^{2+} and mechanisms of action. Cytosolic PLA2α (cPLA2α) is considered to be the main lipolytic enzyme in the release of AA. To be specific, the cPLA2α enzyme hydrolyzes an arachidonyl group from the sn-2 position of glycerophospholipids, resulting in two products: AA and lysophospholipids. These two products have distinct, important tasks in cell signaling. Regulation of cPLA2α activity occurs on several different levels, including binding to lipid second messengers, phosphorylation induced kinases, de novo gene transcription and an increased intracellular Ca^{2+} level in response to pro-inflammatory stimuli.[49] Several factors have previously been shown to activate cPLA$_2$α and to stimulate release of AA, including ATP[50], thrombin[50], IL-1β[51, 52], TNFα[52], PAF[53] and lysophosphatidylcholine (lysoPC).[53]

As mentioned in chapter 1.3.4 and showed in figure 1.4.1, AA is one of the fatty acid precursors from which the pro-inflammatory eicosanoids are produced.

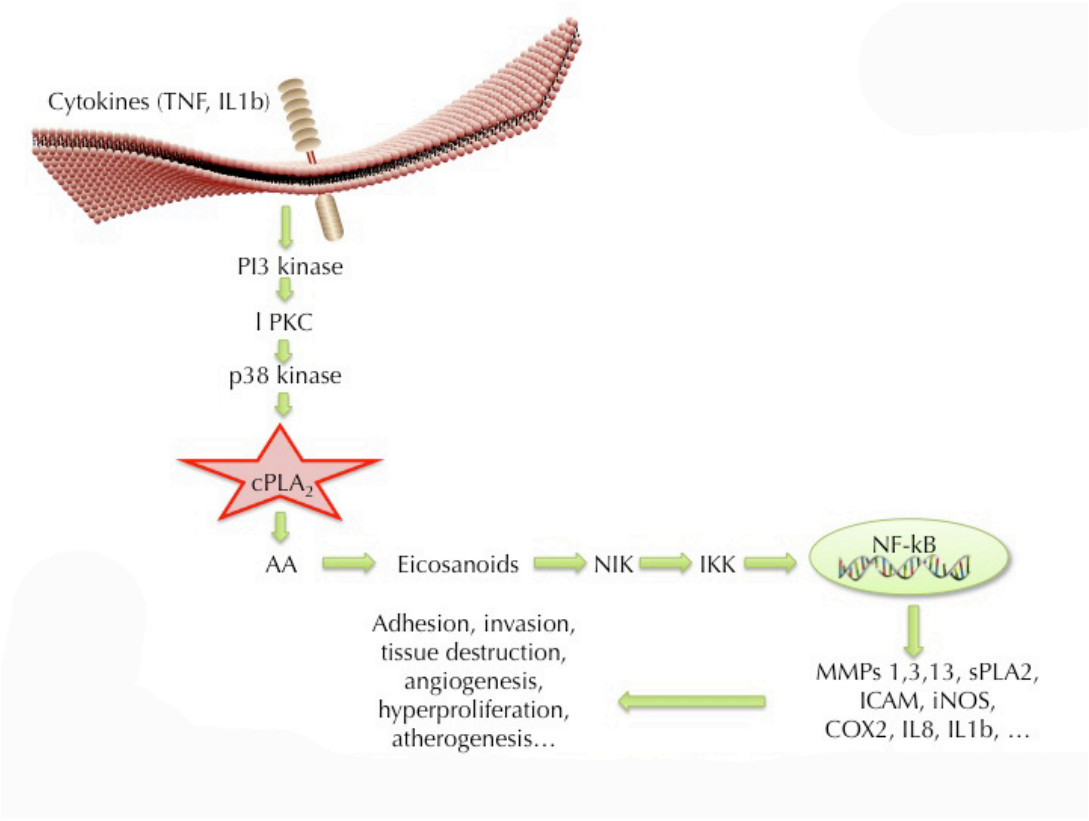

Figure 1.4.1: cPLA$_2$α releases AA from glycerophospholipids. AA is one of the fatty acid precursors for the pro-inflammatory eicosanoids. [49, 54] PI3 Kinase: Phosphoinositide 3-kinase. PKC: Protein kinase C. NIK: NFKB Inducing Kinase. IKK: IKB Kinase. MMP: Matrix Metalloproteinase. ICAM: Intercellular Adhesion Molecule. iNOS: Nitric Oxide Synthase.

The activity of cPLA$_2$α has been found to be upregulated in multiple inflammatory diseases like Psoriasis[55], Parkinson's Disease[56], Alzheimer's[57] and several types of cancers[58], including colorectal, small bowel and lung. Another inflammatory disease where cPLA$_2$α has been shown to play a role is Rheumatoid Arthritis (RA), an inflammatory disease of the joint. RA is an autoimmune and systemic inflammatory disease with a poorly understood etiopathogenesis.

1.5 Autoimmune Diseases

The immune system protects the human body from infections and diseases by recognizing foreign structures entering the body. Once recognized, the cells of the immune system continue to target and eliminate invading microbes, infected cells and tumors while ignoring healthy tissue. In some cases, for reasons still not understood, the immune system targets antigens of the host healthy tissue (self-antigens). This event is called autoimmunity and it is characterized by an abnormal immune reactivity in association with autoreactive B and T cell responses. Multiple factors are thought to contribute to the development of autoimmunity, including genetic, immunological, hormonal and environmental factors.[59] Why the immune system suddenly recognizes self-antigens as foreign is not fully elucidated. Some autoimmune responses are induced by pathogenic infection, where the pathogen proteins resemble proteins of the host, structurally. Predisposition to autoimmunity occurs when there are specific genetic variations in the allele(s) that controls antigen presentation by antigen-presenting cells for T-cell recognition.[60] In RA, circulating autoantibodies have been detected. A negative autoantibody test does not rule out RA, but a positive test does not occur in healthy patients. There are more than 80 types of autoimmune diseases, which can be divided into organ-specific illnesses (thyroid disease, type 1 diabetes etc) or systemic illnesses (RA, systemic lupus erythematosus etc).[61]

1.6 Rheumatoid Arthritis

Rheumatoid Arthritis (RA) is the third most common type of arthritis in the US, affecting approximately 1.3 million people in the US and about 1% of the world population.[62] RA is a systemic inflammatory and autoimmune disease of the synovial membrane that lines the non-weight bearing surface of joints. In RA, the quiescent and relatively acellular, healthy synovium becomes a hyperplastic, invasive tissue teeming with immunocompetent cells.[63] The chronic synovitis causes pain, swelling and loss of joint function due to degradation of cartilage and bone erosion.[49] In healthy joints the synovial membrane produces lubricating and nourishing synovial fluid and comprises two cell types; macrophage-like (Type A) and fibroblast-like (Type B) synoviocytes (FLSs).[64] In diseased joints, T cells and B cells will invade the synovial membrane resulting in a hyperplastic synovial tissue, which becomes invasive, destroying the articular cartilage and underlying bone (Fig. 1.6.1). In RA, the FLS will contribute to the elevation of produced pro-inflammatory cytokines (especially IL-1β) and molecule mediators of inflammation, as well as matrix metalloproteinases (MMPs), which are responsible for joint erosion.[65] It has also been stated that targeting the FLS might improve clinical outcomes in RA without suppressing systemic immunity.[63]

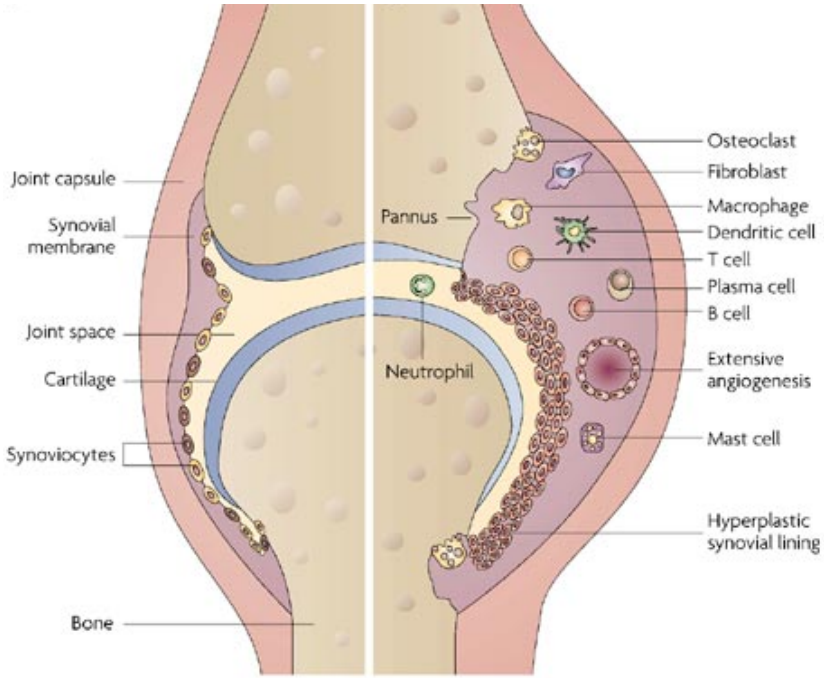

Figure 1.6.1: In a healthy joint (left side) a thin synovial membrane is seen, enclosing the synovial fluid. In RA (right side) the synovial membrane is hyperplastic and infiltrated by chronic inflammatory cells.[64]

A very important equilibrium in joints is that between bone formation and bone resorption. These repeated cycles of construction and destruction are controlled by osteoblasts and osteoclasts, respectively, and are important in the maintenance of bone mass.[66] An imbalance in bone remodeling, such as an excessive osteoclast-induced bone resorption can cause several diseases including osteoporosis, RA and cancer metastasis to the bone.[67] The regulation of differentiation and activation of osteoclasts is affected by several molecules, such as receptor activator of NF-κB ligand (RANKL), which activates RANK receptor. Once RANK is activated on osteoclast progenitor cells, the subsequent activation of TNF receptor-associated factors and several signaling cascades, including NF-κB, mitogen-activated protein kinase (MAPK), activating protein 1 (AP-1) and nuclear factor of activated T cells (NFATc1), leads to the formation of bone-resorbing osteoclasts.[67]

As mentioned in the previous chapter, there are multiple factors involved in the onset of an autoimmune disease like RA, even though the aetiology and pathogenesis of RA remains unsolved. In some patients, circulating autoantibodies have been detected. Such autoantibodies include rheumatoid factor and anti-cyclic citrullinated peptides (CCP), against the Fc region of other antibodies and against citrullinated epitopes on post-translationally modified proteins, respectively.[68] There is strong genetic linkage to chromosome 6, more specific the class II major histocompatibility complex (MHC) region.[69] There is also evidence of an association with the non-MHC gene PTPN22, which is a phosphatase that regulates T-cell activation. Even though there is evidence that genetic factors are related to an increased risk of RA, RA is a

multifactorial disease resulting from the interaction of both genetic and environmental factors. The sole environmental factor associated with RA is cigarette smoking.[70] Inflammation is mediated by pro-inflammatory cytokines (including TNFα, IL-1β, IL-6, IL-15 and IL-17) and tissue destructive enzymes (MMPs) in RA. T cells, macrophages, type B synoviocytes and bone-destructive osteoclasts produce these molecules, and all of these cells are involved in the pathology of RA.

1.7 An In Vitro Model for Synovitis

The SW982 synoviocyte cell line is a model for synovitis, and has previously been used to study RA.[65, 71-73] These are human fibroblast-like synoviocytes (FLSs), collected from a biphasic synovial sarcoma found in a 25-year-old Caucasian female. Leibovitz initiated the cell line in 1974 at the Scott and White Clinic, Temple, Texas.[74-76] According to immunohistochemical studies performed by McNearney et al, the SW982 cell line has characteristics consistent with the phenotype of type B synovial cell fibroblasts. Type B synoviocytes is the most abundant cell type in the RA synovium, together with synovial macrophages (type A synoviocytes) and infiltrating T lymphocytes.[77] SW982 cells can be purchased from the American Type Culture Collection (AATC), a private, non-profit biological resource center (BRC) and research organization.[78]

Animal cell culturing became a common laboratory technique in the mid-1900s, and today the technique also includes cultures of plants, fungi, insects and microbes, including viruses, bacteria and protists. When culturing animal cells, there are two different main types of cells; primary cells and cell lines. Primary cells are cultured directly from a subject (for example a skin sample) and have a limited lifespan. Immortalized or established cell lines, like the SW982 cell line, evades normal cellular senescence and can be studied for a longer period of time in vitro. There are many benefits of using primary FLSs from patients in the study of RA, but also several drawbacks, including difficulties to collect and establish. SW982 has been shown to express pro-inflammatory cytokines IL-6, IL-8 [79], IL-1β and Transforming growth factor (TGF)-β, and also matrix metalloproteinases (MMPs) 1, 2, 3 and 13[65], intracellular adhesion molecule-1 (ICAM-1) and COX-2. mRNA expression of these genes have been shown to be upregulated by stimulation with IL-1β.[65] Prof. Johansen and group showed in 2013 that TNF increases mRNA levels of MMP3 and IL-8.[49] Prof. Johansen and group also showed in 2014 that SW982 cells express a wide repertoire of PLA_2 enzymes. PLA_2 subgroups GIIA, GIVA, GVC, GV, GVIA, GVIB, GVIC, GVID, GVIF, GVIIA, GX and GXIIA were found to be expressed in cultured SW982s.[80] They also detected the expression of TLRs1-7 in SW982 synoviocytes. TLR2 expression was found to be upregulated by TNF, and TLR2 ligands Pam_3CSK_4 and FSL-1 were found to induce the activation of $cPLA_2$, which in turn regulates the expression and production of IL-6, IL-8 and COX2/PGE_2.[80]

1.8 Objectives

A pilot study published by Prof. Johansen and her group in 2013, studied the gene expression in blood in a group of obese men who had shifted from their normal diet to a strictly defined diet, with a fixed number of meals, serving sizes and macronutrient composition (decrease in dietary carbohydrates and an increase in dietary proteins). Already at day 1 of the intervention, there was a significant change (increase or decrease) in gene expression, which remained at that new level throughout the diet period of 28 days.[81] Genes that were downregulated in this period included genes associated with processes relying on B-lymphocyte activation. Genes involved in metabolic processes like protein modification and biosynthesis were found to be upregulated during the intervention pilot study.[81] Meaning that the macronutrient composition of the diet plays a role for the low-grade systemic inflammation.

In a 2010 quantitative patient questionnaire monitoring in standard clinical care of patients with rheumatoid arthritis (QUEST-RA) study, Dr. Jawaheer et al. analyzed a total of 5161 RA patients (4082 women and 1079 men), collecting complete data concerning their age, gender, BMI, disease duration and Disease Activity Scores based on a 28-joint count (DAS28 scores). The mean DAS28 scores among patients in different BMI categories increased with increasing BMI in most countries, as well as in the combined dataset for all countries.[82]

These findings underpin other similar studies[83-85], and may suggest that the caloric intake and the macronutrient composition of our diet influences the low-grade systemic inflammation in the body, and potentially has an effect on inflammatory diseases like RA. If a person with RA consumes a typical Western diet, relatively rich in dietary carbohydrates and scarce in dietary proteins, in amounts exceeding the daily caloric need, would this affect the disease activity? Would the excessive secretion of insulin affect the hyperplastic synovium, causing it to hyper proliferate?

A diet rich in carbohydrates will stimulate secretion of insulin. Are SW982s amenable to insulin stimulation? If dietary changes like the ones stipulated above, will downregulate genes associated with immunity, will excess amounts of insulin stimulate an upregulation of genes associated with immunity in fibroblast-like synoviocytes? Will insulin stimulation lead to hyper proliferation of fibroblast-like synoviocytes? Can the findings in the FLS' be the foundation of new dietary advices for patients suffering from RA?

2. Methods and Materials

2.1 Cell Culture

Fibroblast-Like Synoviocytes (SW982s) were purchased from the American Type Culture Collection (ATCC). Cell culturing medium (Dulbecco's modified eagle's medium; DMEM), L-glutamine, dimethyl sulfoxide (DMSO), Gentamicin solution and fatty acid free bovine serum (FBS) was purchased from Gibco. Cells were cultured in 75 cm^2 and 175 cm^2 cell culture flasks purchased form Sarstedt. Cells were cultured in Dulbecco's modified eagles medium (DMEM) with 10% Fetal Bovine Serum (FBS), 3% Glutamine and 1000 µL gentamicin added. This solution will be referred to as "DMEM10%" for the remaining of the thesis. Cells were subcultured twice every week and discarded at passage ~50 or earlier if there were signs of change of character. Signs of change of character could be morphological changes (smaller size, rounder edges) and a sudden change in the rate of mitosis. When the cells were used for stimulation experiments, they were plated in DMEM10% and left to settle for 24 hours (unless otherwise stated). The cells were then starved with starvation media, serum-free DMEM + 3% glutamine, from now on referred to as SF-DMEM. Starvation period was set to 24 hours (unless otherwise stated).

2.2 Growth Curve

A growth curve shows a model of the evolution of a cell population over time. Cells in culture grow either attached to a surface (anchorage dependent) or in suspension (anchorage independent). The SW982s grow attached to the surface in a monolayer, and follows a characteristic growth pattern of four phases: lag, log, stationary and decline phase. The lag phase is the first phase after seeding of the culture vessel. During this phase the cells grow slowly as they are still recovering from the stress of subculturing. As the cells settle down, they start dividing at a higher rate and enter the next phase: the log phase. During the log phase the cells experience an exponential growth until the entire growth surface is covered with cells. During the stationary phase, cell proliferation slows and stops. The cells enter a decline phase where cell viability and number decreases if the culture medium is not replaced and the cell are not subcultured.[86]

Confluency is a term used to describe the percentage of growth surface covered with cells. At 100% confluency, there is no available growth surface between the cells and the cells are confluent. Prior to 100% confluency, the cells are subconfluent and there is still available growth surface between the cells. At this stage they are still in the log phase. After the cells have become confluent, they enter post-confluency and are in the stationary phase. In this phase, the cells stop concentrating on mitosis and focus on the activities that are characteristic for fibroblast-like synoviocytes.

At day 0, cells (generation #41) were plated in 6 mL DMEM10% (DMEM containing 10% FBS, 1mL gentamicin and 3% glutamine) in T25 culture flasks at 25 000, 100 000, 250 000, 500 000 and 800 000 cells per flask. Cells were cultured for 8 days in a total of 32 T25 flasks (8 flasks per initial cell seeding). One flask of each cell seeding was studied and harvested each day starting at day 1, to determine confluency and cell number (using a Bürcher chamber). Each flask was counted one time with 3 technical replicates, cells were returned to their flask for determination of confluency each of the remaining days of the experiment. Any confluency below 40% was noted as "K<40%". A slope for the entire growth period and for the log-phase alone was determined using Excel.

A second growth curve experiment was conducted using the same culture flasks and otherwise identical experimental setup as for growth curve 1. This time, cells were plated at 25 000, 100 000, 250 000 and 500 000 in the used flasks, and an additional 8 new T25 flasks were plated with 800 000 cells per flask at day 0. One flask from each cell seeding was counted each day with 3 technical replicates, and the cells were subsequently returned to their flask for determination of confluency for the remaining of the 8 days.

2.3 Arachidonic Acid Release Assay

A release assay with radioactively labeled molecules has the purpose of measuring the ability of a given selection of cells to either take up or release the molecule in question. In the case of the fatty acid Release Assay performed on the SW982s, [^{3}H]-Arachidonic Acid and [^{14}C]-Oleic Acid is incorporated into the plasma membrane of the cells. Subsequently, the release of the respective fatty acids is measured, in response to a given stimuli. Release assays where the stimulant induces increased release of AA and not OA, may indicate an activation of the arachidonyl-specific cPLA2α enzyme.[52]

Release assay was performed on cells in subconfluent, confluent and post-confluent states plated in 48-well plates at 50 000 cells per well in 0.5 mL DMEM10%. The cells (generation #38-42) are left to grow until they reach the desired degree of confluency: 12, 24 and 72 hours respectively. After the growth period the cells were starved in 250 µL SF-DMEM for 24 hours. During starvation, 3.3 µL/mL [^{3}H]AA and 0.67 µL/mL [^{14}C]OA was added to the starvation media to label the cells. After starvation and labeling, the medium was removed and the cells were washed twice with 1 mL prewarmed SF-DMEM, the first wash containing 0.2% fatty acid free bovine serum albumin (fBSA). After washing, 160 µL stimulation medium was added to the wells and left on for 4, 8, 16, 24 or 48 hours. After stimulation the supernatant was transferred to individual 1.50 mL eppendorf tubes. The cells were lysed with 200 µL, 1M sodium hydroxide (NaOH) for 24 hours at 22°C. The supernatant was centrifuged for 5 min at 13200 rpm and 24°C. After centrifugation, the 160 µL of supernatant was transferred to 2 mL eppendorf tubes containing 1 mL scintillation fluid. Then the lysed cells were transferred to new 2 mL eppendorf

tubes containing 1 mL scintillation fluid. The samples were analyzed in a Wallac 1409 liquid scintillation counter.

Cells were stimulated with insulin suspended in SF-DMEM, at different concentrations for 4, 8, 16, 24 and 48 hours (for subconfluent cells), and 24 hours for confluent and post-confluent cells. All cells were treated with 1 μM insulin for the indicated hours. Cells stimulated for 48 hours were treated with 3 different concentrations of insulin; 0.3, 1 and 3 μM. SF-DMEM with or without IL-1β (10 μg/mL) were included as positive and negative controls, respectively.

2.4 MTT viability assay

The MTT viability assay is a semi-automated colorometric assay, invented by Mosmann in 1983.[87] MTT is an abbreviation for *3,4,5 dimethylthiazol-2,5 diphenyl tetrazolium*, and the assay is based on the ability of mitochondrial dehydrogenase enzymes of living cells to convert MTT to a purple formazan precipitate. These mitochondrial succinate dehydrogenases may reflect the number of viable cells present, but may also reflect the rate of cellular respiration. Therefore, the results should be validated by additional techniques as well. The resulting crystals are subsequently dissolved using dimethyl sulfoxide (DMSO) and the optical density of each well is measured using a multiwall plate reader.[87] This assay is simple, rapid and affordable, but will also render the cells non-viable meaning that repeat or complementary assays cannot be carried out on the same plate of cells.

For the “Timeline” assay, cells were plated in 96-well plates in DMEM10%. Cells were plated at 2500, 5000, 10 000, 15 000 and 25 000 cells per well, and starved after 24 hours, for 24 hours in SF-DMEM. After starvation cells were stimulated with 100 μL, 1 μM insulin. Some wells got SF-DMEM or DMEM10% as negative and positive controls, respectively. Cells were stimulated for 24, 36 or 48 hours. After stimulation the stimulation medium was removed and 100 μL MTT was added and left on for 2 hours. MTT was removed and 100 μL DMSO was added. The plates were analyzed in a plate reader at optical density of 550 and 595 nm.

For the “Dose Response” assay, cells were plated in 100 μL DMEM10% at 2500 and cells per well in a 96-well plate. Cells were starved with SF-DMEM after 24 hours, for 24 hours. Cells were stimulated with insulin (0.3-3 μM), SF-DMEM or DMEM10%, for 48 hours. After stimulation the protocol for “Timeline” assay was followed.

2.5 MTT Data Analysis Using Excel

All MTT data were analyzed using Microsoft Excel 2010, including fold changes, standard deviations and significance. The 2-tailed, paired student’s T-test was used for calculating statistical significance between means of biological replicates.

2.6 Flow Cytometry as a Validation for MTT

Flow cytometry is a rapid analysis based on optical and fluorescent measurements, yielding qualitative and quantitative information about cells. Flow cytometry can be used to analyze several different samples, including blood specimens, bone marrow, serous cavity fluids, cerebrospinal fluid, urine, solid tissue and cultured cells.[88] Flow cytometry can be used to analyze several different aspects of a cell, including cell size, cytoplasmic complexity, DNA/RNA content, and also membrane-bound and intracellular proteins. In order to measure the aforementioned characteristics, the specimen is pretreated with specific dyes that can bind to cellular components like DNA or RNA, such as propidium iodide, phycoerythrin, fluorescin or others.[88] In flow cytometry single cells from a sample pass through an illumination zone at ~300 cells per second (higher rates are possible). Electronically gated detectors measures the extent of light scattered, which results in the display of histograms of the number of cells possessing a certain quantitative property versus the channel number.[89]

Cells were plated in DMEM10% at 200 000 cells per well in a 6-well plate. Cells were starved in SF-DMEM after 24 hours, for 24 hours. After starvation the subconfluent cells were treated with 1.0 µM insulin for 48 hours. Cells were subsequently washed with PBS twice and treated with 0.5 mL trypsin for 2 min. 1.0 mL DMEM10% was added and the cells were transferred to a 15 mL centrifuge tube. Cells were spun at 700 rpm for 5 min, and the supernatant was discarded. Cells were carefully resuspended in 2.0 mL methanol (-20°C). Cells were subsequently spun at 700 rpm for 5 min, and resuspended in 1 mL RNase (200 µg/mL). Cells were spun again at 700 rpm for 5 min, and resuspended in propidium iodide (40 µg/mL). Samples were analyzed using a Becton Dickinson LSR at the institute of physics at NTNU.

2.7 RNA Isolation

Ribo Nucleic Acid (RNA) is a highly regulated and unstable, single stranded molecule with numerous biological functions. The messenger RNA (mRNA) is the cells' first step towards protein expression, and capturing the levels of mRNA at a specific time will reveal which genes are transcribed and how they are transcribed in relation to each other. RNA is extremely sensitive to degradation by RNases and therefore any handling of RNA should be quick, kept on ice, clean and performed the same way each time.

All RNA isolations were performed according to Qiagen's protocol for the RNeasy Mini Kit. Cells were lysed in 700 µL RLT lysis buffer, containing 1% Beta-Mercaptoethanol. The RNeasy Mini Kit is based on the use of spin columns to bind, wash and eluate total RNA from cells and tissues. Eluated RNA was kept on ice at all times and stored at -80 °C.

2.8 Nano Drop for Quality and Yield Assessment of RNA

The spectrophotometer NanoDrop ND-1000 uses UV light to make quantitative and qualitative assessments of nucleic acids and proteins. The NanoDrop measures absorbance between 200 and 350 nm. The absorbance at 260 nm is used to determine the concentration of RNA. Two ratios are important for assessing contamination of the RNA sample: 260/280 and 260/230. Both of these ratios should be at 2.0, and no less was accepted in this study. Ratios <2.0 indicate protein (or other components that absorb strongly at 280 nm) and carbohydrate contaminations, respectively. Through wavelength in a sample should be ~230 nm, and the peak at 260 nm. RNA concentrations >150 ng/µL was accepted for use in further analysis.

2.9 cDNA Synthesis

Complimentary DNA (cDNA) is a double stranded DNA molecule made from a RNA template, by reverse transcriptase and DNA polymerase. The cDNA molecule is more stable than RNA and therefore easier to analyze. Because cDNA is chemically identical to genomic DNA (gDNA), it is important to remove all potential gDNA contamination in the RNA sample before analyzing it.

cDNA synthesis was performed as stated in Qiagen's protocol, using reagents in Qiagen's *QuantiTect Reverse Transcription Kit.* For each cDNA sample, 1000 ng of RNA was used. This kit involves a step for gDNA removal, synthesis of cDNA and an end-reaction. Random primers are used in the conversion of mRNA to cDNA, meaning that cDNA is produced from all mRNA molecules in the sample. The whole process takes approximately 30 minutes.

RNA samples were thawed on ice (stored at -20°C), spun down briefly and RNA concentrations were measured with NanoDrop. 1000 ng of RNA was used in each cDNA reaction. 2 µL of gDNA wipeout buffer was added to a total of 12 µL of RNase-free H_2O and template RNA (varying amounts of the two depending of RNA concentration in sample), and incubated at 42°C for 2 minutes. After the incubation, 1 µL Quantiscript RT, 4 µL Quantiscript RT Buffer 5x and 1 µL RT Primer Mix was added to the samples, adding up to a totalt reaction volume of 20 µL.[90] This was incubated at 42°C for 15 minutes, and finally at 95°C for 2 minutes to stop the reaction. cDNA was stored at -20°C.

2.10 RT-qPCR

Since the invention of conventional polymerase chain reaction (PCR) 31 years ago, the method has been adapted several times for novel molecular biology approaches and is now able to detect minute amounts of nucleic acids.[91] The reverse-transcription real-time quantitative polymerase chain reaction (RT-qPCR) is a popular method for gene expression analysis, supporting protein expression data from proteomics-based assays, supporting phenotypic observations, validating micro-array experiments, monitoring biomarkers and more.[92, 93]

Several methods of qPCR and RT-PCR have been developed and several detection systems are used, including agarose gels, fluorescent labeling of PCR products with subsequent detection of laser-induced fluorescence using capillary electrophoresis or acrylamide gels, plate capture and sandwich probe hybridization.[94] The RT-qPCR process is based on a series of temperature changes, which are repeated 25-40 times. Each temperature defines the optimal temperature for DNA denaturation (95°C), binding of primers (55°C) and extension of single-stranded DNA molecules (72°C). The main difference between the conventional PCR and the RT-qPCR is the continuous quantification of PCR products in the latter. The RT-qPCR system detects the products at the end of each cycle by using a non-specific fluorescent dye, SYBR Green, which binds to double-stranded DNA. An increase in DNA product will cause increased fluorescence intensity, but the quantification of DNA is relative to an internal reference gene. At the end of an RT-qPCR process, the system allows you to analyze several aspects of the procedure, like the DNA melting temperature (*Tm*) of specific fragments, primer efficiency, the quantification cycle values (Cq) and the fluorescence for each sample plotted against the number of cycles on a logarithmic scale.[91]

cDNA samples were thawed and kept on ice, and prepared for analysis using the *QuantiTect SYBR Green RT-PCR Kit* from Qiagen. Each well was loaded with 5.0 µL cDNA (diluted 1:10), 10.0 µL SYBR Green I, 1.2 µL primer (forward + reverse) and 3.8 µL PCR grade water. Primer mixes with equal amount of forward and reverse primers, were prepared for target genes (INSR, IGF1R, c-Myc, c-Fos and IL-6) and for reference genes (18S ribosomal rRNA, hypoxanthine-guanine phosphoribosyltransferase (HPRT) and β2 microglobulin (B2M)). The plate was sealed and centrifuged before use. RT-qPCR was carried out on a Light Cycler 480 machine in 96-well plates. The Light Cycler has a program with cycling conditions obtained from the RT-qPCR primer assay handbook and included: denaturation for activation of DNA polymerase for 3 minutes at 95 °C (optimized by the PLA_2 group), 40 cycles of 15 seconds at 95°C for denaturation of double stranded cDNA, 40 seconds of 55°C for annealing of primer and single stranded DNA, 30 seconds of 72°C for extension of new DNA strand and quantification of fluorescence.

Table 2.10.1: Primers used in RT-qPCR experiments.

Entrez ID	Gene	Forward Primer	Reverse Primer
3643	INSR	CTGGATTCCGTGGAGGATAA	GCAGCCGTGTGACTTACAGA
3480	IGF1R	GCCGAAGGTCTGTGAGGAAGAA	GGTACCGGTGCCAGGTTATGA
100820712	c-Fos	GTGGGAATGAAGTTGGCACT	CCGGGGATAGCCTCTCTTAC
4609	c-Myc	AAAGGCCCCCAAGGTAGTTA	TTTCCGCAACAAGTCCTCTT
3569	IL6	TGTGTGAAAGCAGCAAAGAG	GCAAGTCTCCTCATTGAATCC
3251	HPRT	ATGGTCAAGGTCGCAAGC	ATTCATTATAGTCAAGGGCATATCC
567	B2M	GAATTCACCCCCACTGAAAA	AGCAAGCAAGCAGAATTTGG
100008588	18S	GTAACCCGTTGAACCCCATT	CCATCCAATCGGTAGTAGCG

The PLA_2 research group designed some of the primers used in the RT qPCR experiments in this master's thesis, and some were ordered directly from Sigma Aldrich.

The RT qPCR data were analyzed using LinReg and Microsoft Excel 2011.

2.11 RT-qPCR Data Analysis Using LinReg

LinReg is a program, which makes it easier to analyze the quantitative RT-qPCR data retrieved from the Light Cycler 480 after completion of the cycling process. LinReg determines baseline fluorescence and does a baseline subtraction, subsequently calculating the respective threshold cycle (Ct)-values and PCR efficiencies per sample, and also an average PCR efficiency per amplicon group. Data calculations from LinReg were further analyzed in Microsoft Excel.

2.12 RT-qPCR Statistics

All RT-qPCR data were analyzed in Microsoft Excel after baseline and Ct calculations in LinReg. The Ct is determined from a log-linear plot of the PCR signal versus the cycle number.[95] All cDNA samples were analyzed by RT-qPCR in duplicates, to control technical variability. Only technical duplicates varying with less than 0.5 cycles were included in further analysis. Reference genes, or housekeeping genes, were also analyzed with RT-qPCR, as an internal control gene to normalize the PCRs for the amount of RNA added to the reverse transcription reactions. Expression levels of samples were calculated as relative quantification, compared to untreated controls. The most common method for calculating the relative

expression is with the $2^{-\Delta\Delta Ct}$ equation, where one of several assumptions is that the amplification efficiencies of target and reference is approximately equal.[95] An other way to calculate the relative quantification of a target gene in comparison to a reference gene, is to determine the relative expression ratio (R) based on the specific primer efficiency and the Ct deviation of a sample versus control. This is then expressed in comparison to a reference gene[96]:

$$\text{Ratio (R)} = \frac{(E_{Target})^{\Delta Ct_{Target}^{(control-sample)}}}{(E_{Ref})^{\Delta Ct_{Ref}^{(control-sample)}}}$$

Mean Ct, variation of Ct and ΔCt was calculated in Microsoft Excel. Statistical significance was calculated based on the relative expression values of target genes and expression values of control genes in comparison to the mean value of the respective control genes, as described by Livak et al.[95] Statistical significance was investigated using a two-sample t-test, the Student's T-test, where the sample sizes and variance are equal. The degrees of freedom for this test is 2n-2, n is the sample size. The null hypothesis is that the means of two independent samples are equal. The chosen threshold for the calculated p-value is 0.05, and the null hypothesis is rejected whenever the p-value is < 0.05.

3. Results

3.1 Reuse of Culture Flasks Reduce Lag Phase in SW982 Cells

A growth curve for cells in culture commonly has three phases that are observed in the laboratory: the lag-phase, the log-phase and the stationary phase. During the lag-phase the increase in cell number will be none or small. During this phase the cells spend time and energy on metabolic activities like enzyme synthesis, cell-cell communication and attaching to the surface of the culture flask. Once the cells have established communication and produced proteins and enzymes for proliferation they transit into the log phase. During the log-phase the cells experience an exponential growth until there is no available surface left to grow on, or they are starved for serum. The SW982s are cells that grow in a monolayer and will stop proliferating once they occupy 100% of the growth surface. When the cells reach this stage they transition into the last phase: the stationary phase. During this phase the cells stop proliferation and differentiate, fulfilling specific functions. Do cells spend less time in the lag-phase when they are plated in used flasks?

Cells were seeded at 25 000, 100 000, 250 000, 500 000 and 800 000 cells per culturing flask in DMEM10%, and observed for the following 8 days. 8 culturing flasks were used per cell seeding, and for each day of the experiment one flask was counted using a Bürcher chamber. Confluency was determined before counting in every flask each day of the experiment. Cells with a low initial cell number spent longer time in the lag-phase, than the cells with a higher initial cell number. Cells plated at 25 000 cells per flask entered the log-phase at day 5, and stayed in this phase for the remaining 3 days of the experiment. Cells plated at 100 000 cells per flask entered the log-phase at day 3 of the experiment. Cell number reached a plateau at day 7 of the experiment, as they transitioned into the stationary phase. Cells plated at 250 000 cells per flask entered the log phase at day 2, and subsequently transitioned into the stationary phase at day 5. Cells plated at 500 000 cells per flask entered the log-phase at day 1. These cells stayed in the log-phase until day 5, when they entered the stationary phase. From day 7 to day 8 a slight decrease in cell number was observed, indicating that the cells entered the decline phase. Cells plated at 800 000 cells per flask started off in the log-phase, skipping the lag-phase. These cells had an exponential growth until day 4, where the number of cells started to decline slightly until the end of the experiment (figure 3.1.1).

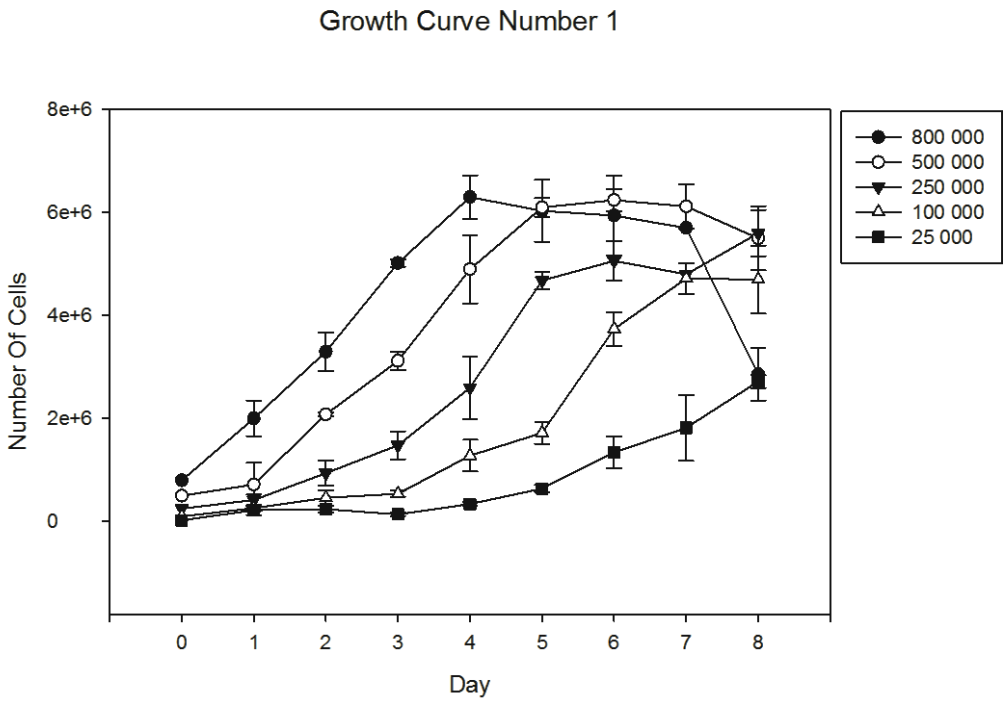

Figure 3.1.1: Growth curve for SW982s plated in T25 culture flasks at different cell number. Numbers indicate average number of cells per flask per day of the 8-day-experiment. Error bars indicate standard deviation after three technical replicates.

The slope of a linear model of the log phase of the growth curve was calculated for each initial cell seeding. Slopes for the log phase of the growth period increased with increasing cell seeding, but not proportionally with the number of cells. The slope for cells seeded at 800 000 cells is only ~2x the slope of cells seeded at 25 000 cells, even though there are ~32x cells. Slopes calculated for cells seeded at 25 000, 100 000, 250 000, 500 000 and 800 000, were based on days 4-8, 3-7, 2-6, 1-5 and 0-4, respectively. All slopes are presented as $x10^4$ and listed along with definitions of log phases in table 3.1.1.

Table 3.1.1: Slopes were calculated for the log phase of the growth curve experiment, for each initial cell seeding. The table lists the slope and each initial cell seeding, and the days defining the log phase are listed in the latter column.

Initial Cell Seeding	Slope Of Log Phase ($x10^4$)	Days Defining Log Phase
25 000	403	5-8
100 000	649	3-7
250 000	740	2-5
500 000	815	1-5
800 000	921	0-4

The confluency of the cells is a number explaining how many percent of the growth surface is covered with cells. Cell confluency below 40% is a very sparsely packed group of cells, where many of the cells may not have direct contact with other cells. Cell confluency at 100% is a very densely packed group of cells, where there is no growth surface available.

Cells plated at 25 000 cells per flask reached 40% confluency at day 4. These flasks showed a slight increase in confluency over the next couple of days, and had reached a confluency of 85% at day 8. Cells plated at 100 000 cells per flask reached 40% confluency at day 3, showing a slight increase over the next day, and subsequently reaching 100% confluency at day 8. Cells plated at 250 000 cells per flask reached 40% confluency at day 2 and had by day 6 reached 100% confluency, which it maintained throughout the remainder of the experiment. Both cells plated at 500 000 and 800 000 cells per T25 flask were at 40% confluency already at day 1, reaching a confluency of 100% at day 3. The cells remained at 100% confluency throughout the experiment (figure 3.1.2).

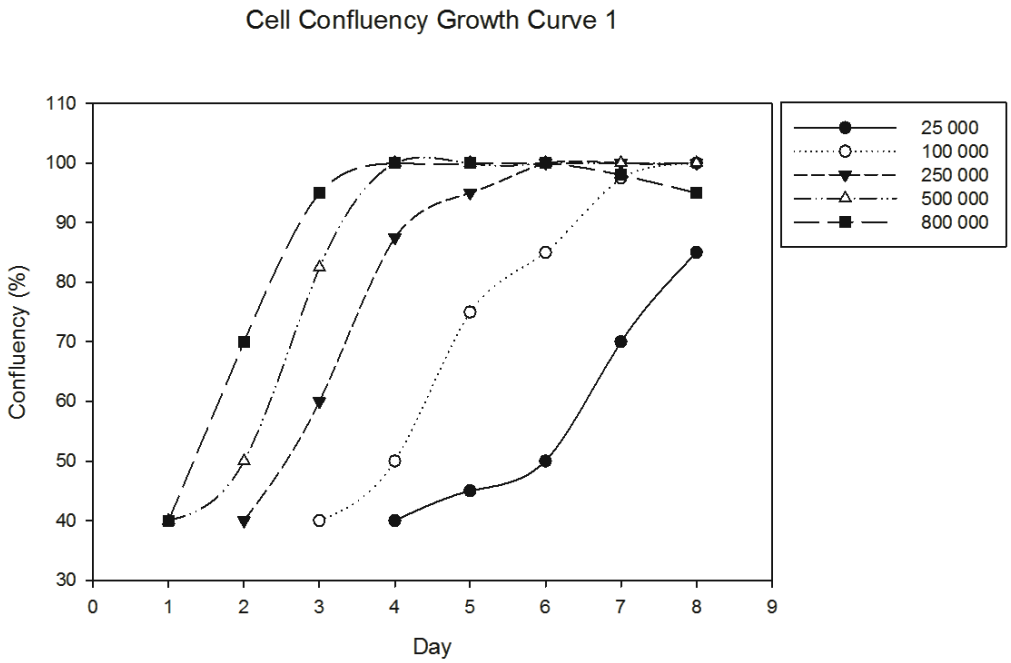

Figure 3.1.2: Progression of cell confluency per day of the 8-day growth curve experiment, one curve for each cell number plated. Shows the confluency of the T25 culture flasks behind figure 3.1.1, for the 8 days of the growth curve experiment. Cell confluences below 40% are referred to as “<40%”.

The T25 culture flasks applied in the first growth curve experiment were washed and reused to repeat the experiment. Hence, the new cells were introduced to an environment in which cells had already established cell-extracellular matrix (ECM) communication and proteins used to attach cells to the growth surface. The cells were plated in DMEM10% at four different cell numbers: 25 000, 100 000, 250 000 and 500 000. 8 flasks were used per cell number and for each day of the experiment, one flask was used to determine confluency and subsequently counted using a Bürcher chamber.

In the second growth-curve experiment no lag-phase was observed in used culture flasks. Cells plated at 25 000 reached the stationary phase at day 4, 2 days quicker than in the first experiment. Cells plated at 100 000 and 250 000 cells remained in the log-phase until day 3, and had a slight increase in cell number throughout the growth experiment. Compared to the first experiment, cells plated at 100 000 and 250 000 cells reached the stationary phase 4 and 2 days earlier in the second experiment, respectively. Cells plated at 500 000 cells had a steep linear growth curve the two first days, and had a slight increase in cell number until day 4, when it reached the stationary phase. In the first experiment, the growth was exponential until day 4 (figure 3.1.3).

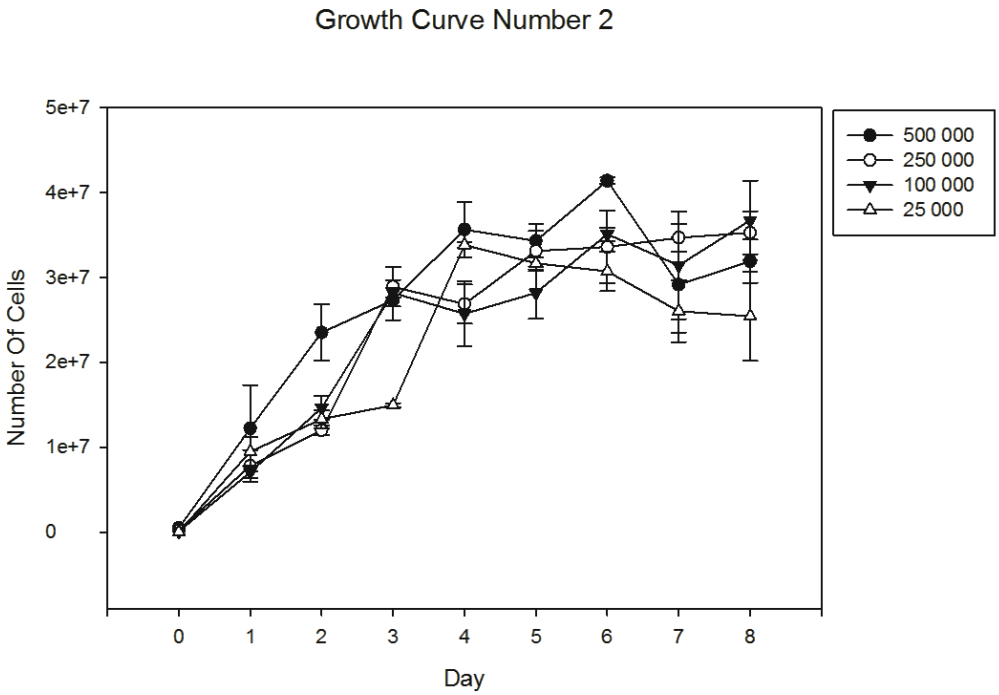

Figure 3.1.3: Growth curve for SW982s plated in T25 culture flasks at different cell number. Numbers indicate average number of cells per flask, per day of the 8-day-experiment. One biological replicate. Error bars indicate standard deviation after three technical replicates (3 counts).

Slopes were also determined for growth curve 2, as for growth curve 1. Slopes for the log-phase were calculated based on a linear model of the growth curve. For cells seeded at 25 000 cells per flask the slope of the log phase increased by 80%, in the second experiment, which was the biggest increase in slope. Cells seeded at 100 000 cells, had a much shorter log phase in the second experiment, and the slope of the log phase by 42% in the second experiment. Cells seeded at 250 000 cells produced a slope in the second experiment that was 31% higher than in the first experiment. Cells seeded at 500 000 cells exhibited a slope that was 41% higher in the second experiment than in the first experiment (table 3.1.2).

Table 3.1.2: Slopes were calculated for growth curve 2 based on a linear regression of the log phase of their growth period. Table presents initial cell seeding, slope for log phase and the days of the growth experiment defining the log phase.

Initial Cell Seeding	Slope Of Log Phase ($x10^4$)	Days Defining Log Phase
25 000	731	0-4
100 000	919	0-3
250 000	902	0-3
500 000	1151	0-2

As for growth curve 1, confluency was evaluated throughout the experiment of growth curve 2. Figure 3.1.4 shows the progression of confluency for the four cell numbers plated in the used T25 culture flasks. Cells plated at 25 000 cells per T25 reached 100% confluency at day 6. Cells plated at 100 000 cells reached 100% confluency at day 5. Both cell numbers reached 40% confluency at day 1. Cells plated at 250 000 and 500 000 cells per T25 flask, reached 40% confluency already the first day. Cells plated at 250 000 reached 100% confluency at day 5, and cells plated at 500 000 cells reached 100% confluency at day 3. Cells plated at 500 000 cells per flask started to decrease in confluency the last two days of the experiment (figure 3.1.4).

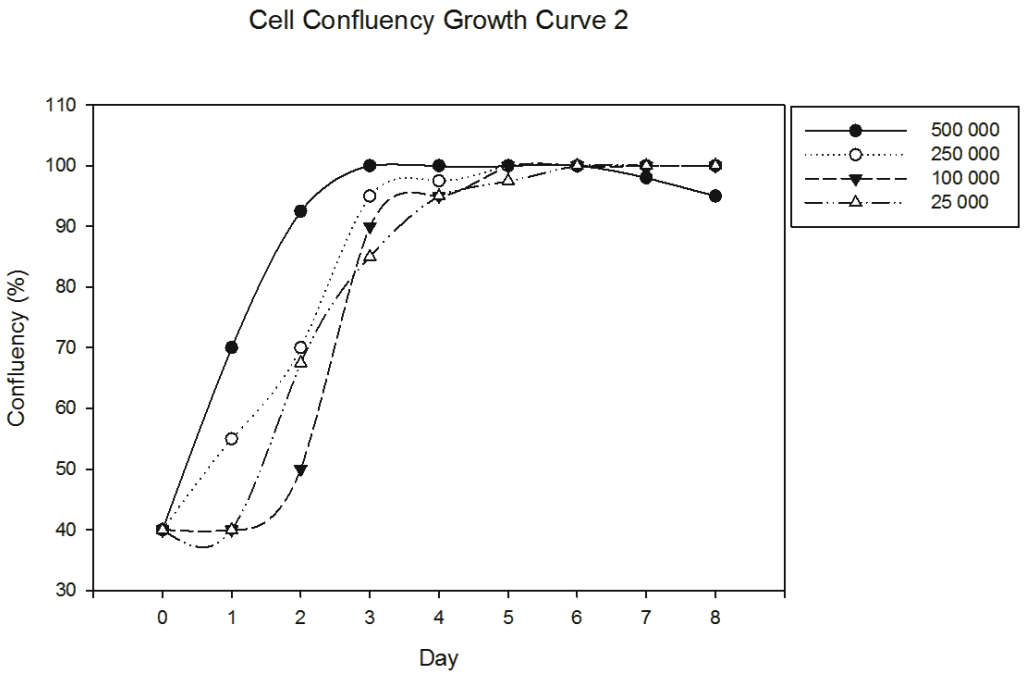

Figure 3.1.4: Progression of cell confluency per day of the second 8-day growth curve experiment, one curve for each cell number plated. Shows the confluency of the T25 culture flasks behind figure 3.1.1, for the 8 days of the growth curve experiment. Cell confluences below 40% are referred to as "<40%". One biological replicate.

Reuse of culture flasks for culturing SW982 cells can help minimize the lag-phase. This is helpful knowledge when performing experiments with cells in culture where cell confluency and differentiation is crucial.

3.2 The SW982 Cells Express IR and IGF1R

Insulin and Insulin-Like Growth Hormone 1 (IGF1) are two proteins with a high degree of homology. While IGF-1 is a known potent growth hormone, studies have shown that insulin also contains growth-promoting actions.[8] In order for any cell to be susceptible to growth promoting stimuli by either insulin or IGF1, it must express the respective receptors: insulin receptor (IR) and IGF-1 receptor (IGF1R). There is no published evidence on the SW982s expressing either of the two receptors. The aforementioned receptors were investigated by RT-qPCR analyses, and were found to be expressed in SW982 (figure 3.2.1).

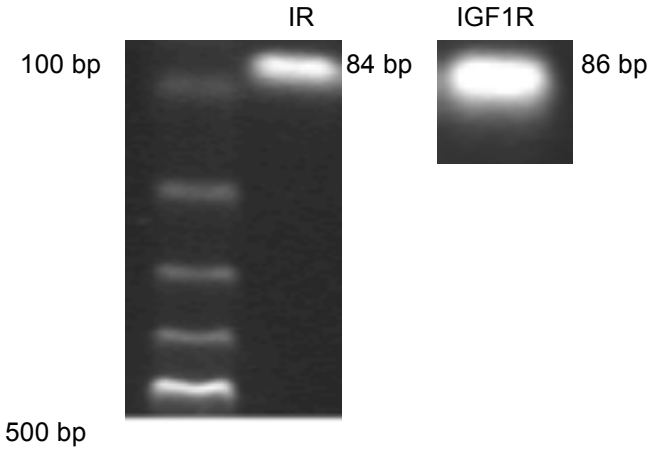

Figure 3.2.1: Gel electrophoresis showing the presence of IR in untreated, subconfluent SW982 cells (left band 84 bp, to the right of the ladder). Gel electrophoresis showing the presence of IGF1R in untreated subconfluent SW982 cell (right band, 86 bp).

The expected sizes of the RT-qPCR products are 84 bp for IR and 86 bp for IGF1R. A standard ladder (each band representing 100, 200, 300, 400, 500 bp from the top in figure 3.2.1) was used to determine and verify the size of each band. The gel electrophoresis can only be used as a qualitative verification of mRNA presence, not as a quantitative measurement of relative mRNA levels.

Ct values of IR and IGF1R detection in subconfluent SW982 cells were assessed using RT-qPCR. Ct values for IR were measured at cycle 26-27, and Ct values for IGF1R were measured at cycle 25-26. In comparison, reference gene HPRT was stable at Ct 22 throughout the experiment.

3.3 [^{3}H]AA Release in Response to Insulin Treatment in Subconfluent Cells

The selective release of AA is initiated mainly by cPLA$_2$α, which binds to natural membrane vesicles in a Ca^{2+}-dependent manner[50], but also sPLA$_2$s and iPLA$_2$s are involved in AA release.[97, 98] Release assays with cells pre-labeled with [^{3}H]AA and [^{14}C]OA may indicate the involvement of AA-selective or non-selective phospholipases, respectively.[52] By release assay, the ability of insulin to induce release of AA was measured. This was used as a method to determine if insulin co–induced proinflammatory activation of SW982 cells. Compared to untreated cells, insulin did not give any significant increase in AA release at 4, 8, 16, 24 or 48 hours of insulin treatment (figure 3.3.1), whereas the positive control clearly did. Averages in figure 3.3.1 are based on 2 biological replicates, mean fold change and SD can be found in appendix A.

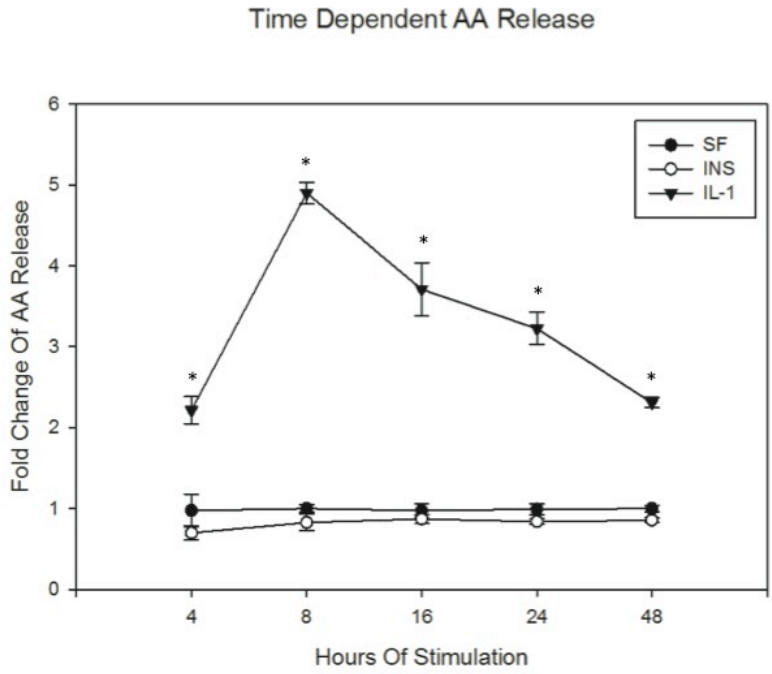

Figure 3.3.1: Insulin did not result in a significant increase of [^{3}H]AA release in [^{3}H]AA and [^{14}C]OA labeled SW982 cells treated with 1 µM insulin for 4, 8, 16, 24 and 48 hours, compared to control (set to 1). The presented results are averages of 2 biological replicates, with 3 technical replicates each.

Furthermore, in dose-response experiments, different concentrations (0.3 µM, 1 µM, 3 µM) of insulin treatment for 48 hours did not result in any increase in AA release in SW982 cells (figure 3.3.2). Averages in figure 3.3.2 are based on 3 biological replicates, mean fold change and SD can be found in appendix B.

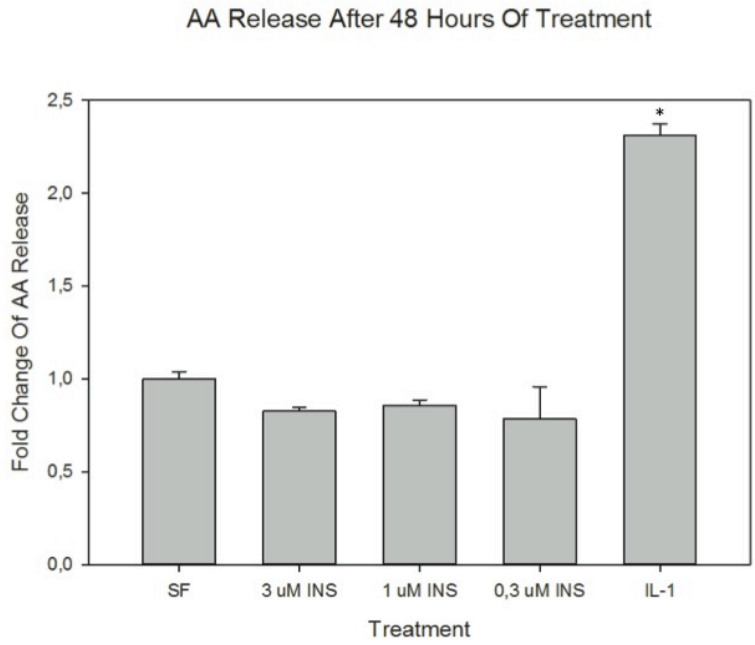

Figure 3.3.2: 48 hours of 0.3 µM, 1 µM and 3 µM insulin treatment in [^{3}H]AA and [^{14}C]OA labeled SW982 cells did not result in an increase in AA release, compared to control (set to 1). The presented results are averages of 3 biological replicates, with 3 technical replicated each.

Hence, it seems that insulin does not induce the release of AA in [^{3}H]AA and [^{14}C]OA pre-labeled SW982 cells.

3.4 [^{14}C]OA Release in Response to Insulin Treatment in Subconfluent Cells

Oleic acid (OA; 18:1n-9) is a non-essential fatty acid, which is consumed in substantial amounts in the typical Western diet.[38] OA and AA release has been shown to be increased by PAF in keratinocytes[99], and LysoPC stimulation in pre-labeled monocytes, expressing cPLA$_2$α, sPLA$_2$ and group VI iPLA$_2$.[97] Inhibitors SB204347, MAFP, BEL, PACOCF$_3$ of sPLA$_2$, cPLA$_2$α/group VI iPLA$_2$, cPLA$_2$α and group VI iPLA$_2$, respectively, have been shown to reduce release of AA and OA.[97, 99] Also, potent proinflammatory cytokines IL-1β[51] and TNFα[100] have been shown to induce release of AA.[52]

By radioactive release assay, the ability of insulin and IL-1β to induce release of OA was measured in [^{3}H]AA and [^{14}C]OA pre-labeled SW982 cells. It is well known in the lab that IL-1β causes a slight reduction in OA release compared to control.[101] A non-significant trend of

decreased release of OA was observed for all time points. A maximum of 40% reduction in OA release was observed after a 4-hour treatment with insulin, compared to control (figure 3.4.1). Averages in figure 3.4.1 are based on 2 biological replicates, mean fold change and SD can be found in appendix C.

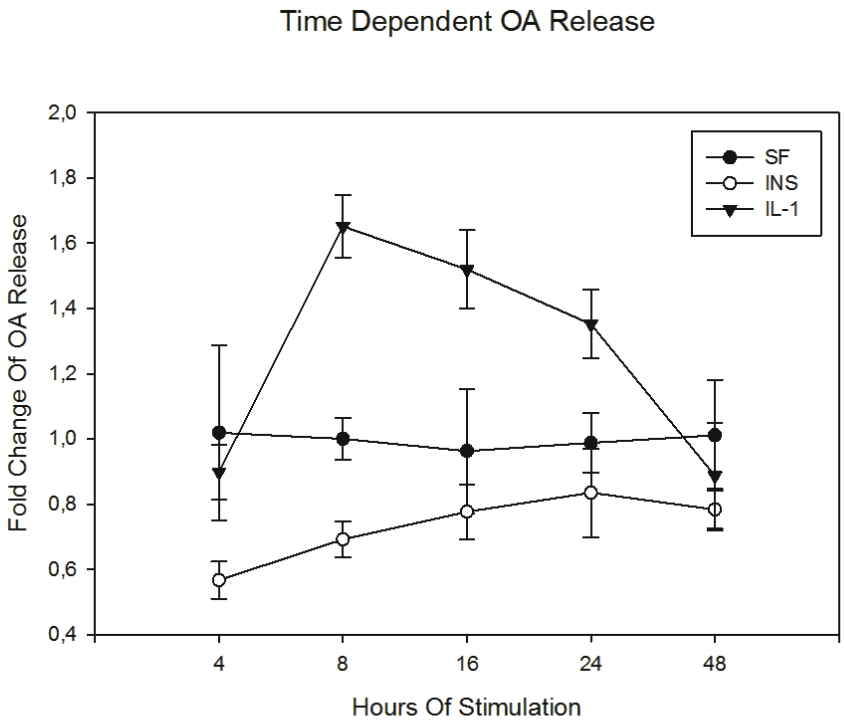

Figure 3.4.1: Insulin treatment resulted in a trend of decrease of [^{14}C]OA release in [^{3}H]AA and [^{14}C]OA labeled SW982 cells treated with 1 µM insulin for 4, 8, 16, 24 and 48 hours, compared to control (set to 1). The presented results are averages of 2 biological replicates, with 3 technical replicates each.

A trend of decreased OA release was also observed in dose-response experiments with 0,3 µM, 1 µM, 3 µM insulin for 48 hours (figure 3.4.2). Averages in figure 3.4.2 are based on 3 biological replicates, mean fold change and SD can be found in appendix D.

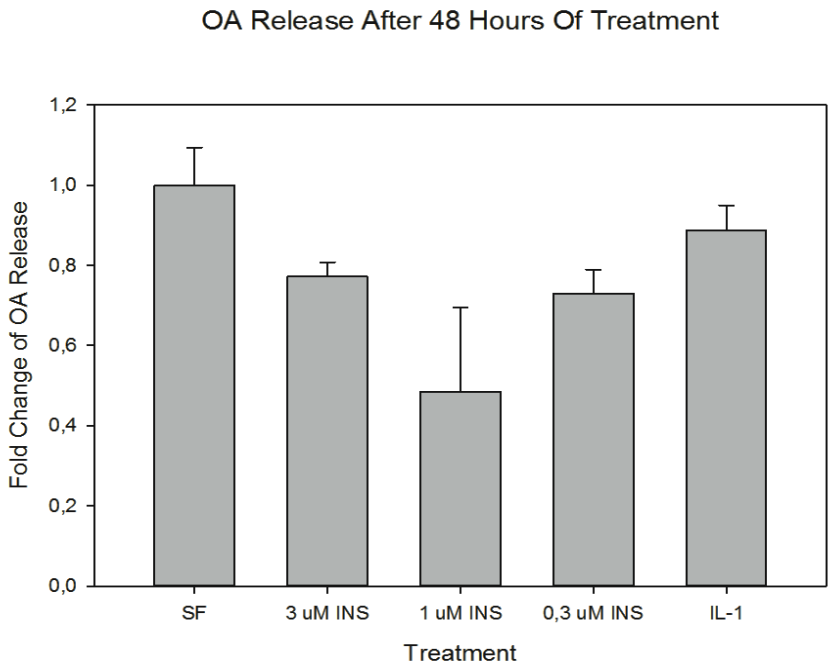

Figure 3.4.2: 48 hours of 0.3 µM, 1 µM and 3 µM insulin treatment in [^{3}H]AA and [^{14}C]OA labeled SW982 cells resulted in a decreased release of OA compared to control (set to 1). The presented results are averages of 3 biological replicates, with 3 technical replicates each.

Even though none of our results for OA release were significantly different from the control, a trend of decrease in OA release in a time and concentration dependent manner was observed after incubation with insulin in cultured SW982 cells.

3.5 [^{3}H]AA and [^{14}C]OA Release in Three States of Confluency

Having shown that in subconfluent cells insulin did not evoke AA-release, and tended to inhibit OA-release, we next asked if these effects could be dependent on cell confluency and cell differentiation. In most experiments on cultured cells, cells are experimented on in a post confluent state. A post confluent state will mimic the natural state of most cells in vivo. By radioactive release assay, [^{3}H]AA and [^{14}C]OA release was measured in pre-labeled confluent and post confluent SW982 cells. 24 hours of IL-1β treatment resulted in an increase in AA release significantly different from control (*) and insulin (#) treated cells, in both confluent and post confluent SW982 synoviocytes (figure 3.5.1). 24 hours of insulin treatment did not result in a significant increase in AA release in confluent or post confluent cells (figure 3.5.1).

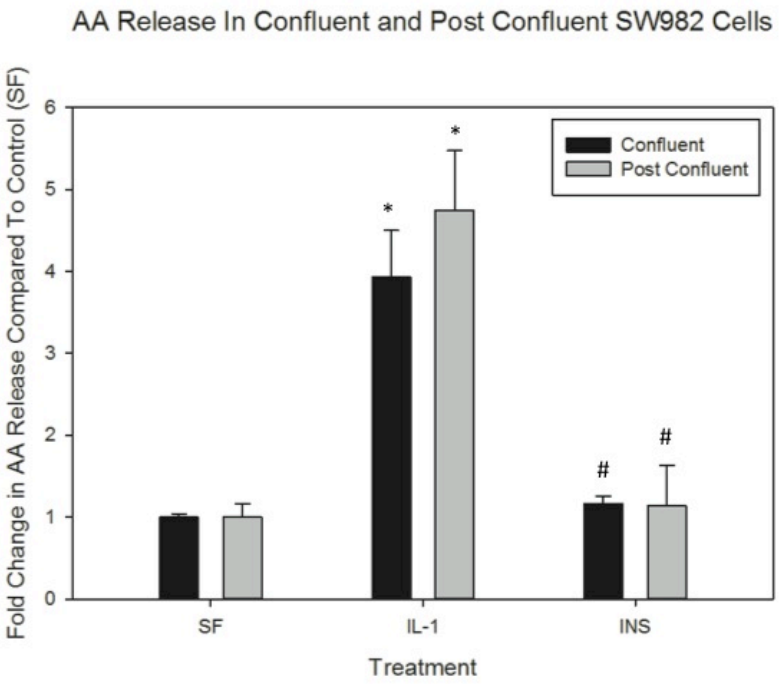

Figure 3.5.1: 24 hours of IL-1β treatment results in an increase in AA release, significantly different from control (*) and insulin treated cells (#). 24 hours of insulin treatment did not give a significant increase in AA release compared to control (set to 1). The presented results are averages of 2 biological replicates, with 3 technical replicates each.

Similarly, OA release was measured in confluent and post confluent cells treated with IL-1β or insulin for 24 hours. IL-1β treatment resulted in a significant decrease in OA release in post confluent cells, compared to control (*) and insulin treated cells (#) (figure 3.5.2). 24 hours of insulin treatment resulted in a decrease ($p>0.05$) in OA release in both confluent and post confluent cells.

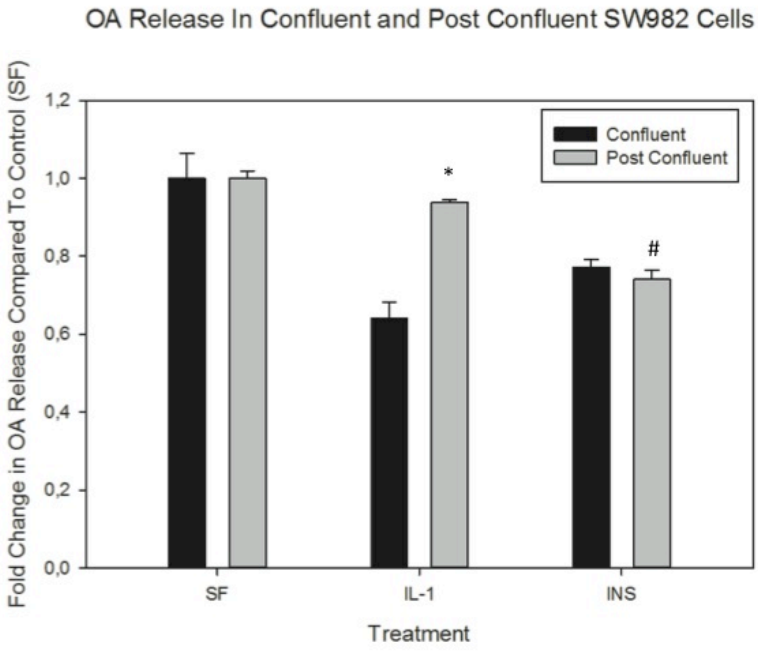

Figure 3.5.2: 24 hours of IL-1β treatment resulted in a decrease in OA release in post confluent cells, significantly different from control (set to 1) (*) and insulin treated cells (#). 24 hours of insulin treatment resulted in a decrease in OA release. The results are averages of 2 biological replicates, with 3 technical replicates each.

As for subconfluent cells, 24 hours IL-1β treatment in confluent and post confluent cells resulted in a significant increase in AA release compared to control and insulin treated cells. Also, like in subconfluent cells, 24 hours of insulin treatment resulted in a decrease ($p<0.05$) in OA release in confluent and post confluent cells.

3.6 Insulin Treatment Increases Metabolic Activity in SW982 Cells

One of the characteristics of an inflamed synovium in a rheumatic joint is an invasive, hyperplastic synovium with an abnormally high rate of proliferation.[102] Little is known about which extracellular stimuli increase the proliferative rate. Obesity has previously been linked to several conditions, like hyperinsulinemia –a compensatory response to insulin resistance.[103] Increased BMI is correlated with increased disease activity in RA patients.[82] Hence we asked if there is a link between an increased insulin level and the hyperplastic nature of the RA synovium?

In a MTT viability assay, vital enzymes catalyze MTT conversion. By MTT viability test, changes in metabolic activity in response to insulin were detected after 24, 36 and 48 hours of treatment. Fold change was measured in SW982 cells seeded at 2500, 5000, 10000, 15000 and 25000, compared to negative control (SF-DMEM). Results for fold change in metabolic activity after treatment with DMEM10%, positive control, is shown. After 24 hours of treatment, cells plated at 2500 cells had a fold change of 1.29 (+/-0.19) for insulin treatment and 1.59 (+/-0.12) for DMEM10% compared to the negative control. Cells plated at 5000 cells had a fold change of 1.16 (+/-0.09) and 1.80 (+/-0.16) for insulin and DMEM10% treatment, respectively. Cells plated at 10000 cells had a fold change of 1.26 (+/-0.32) for insulin and 1.70 (+/-0.09) for DMEM10% compared to the negative control. Cells plated at 15000 cells had a fold change of 1.17 (+/-0.13) and 1.57 (+/-0.04) for insulin and DMEM10% treatment, respectively. Cells plated at 25 000 cells had an average fold change of 1.10 (+/-0.11) and 1.40 (+/-0.03) after 24 hours of insulin and DMEM10% treatment, respectively (figure 3.6.1). Averages in figure 3.6.1 are based on 4 biological replicates, mean fold change and SD can be found in appendix E.

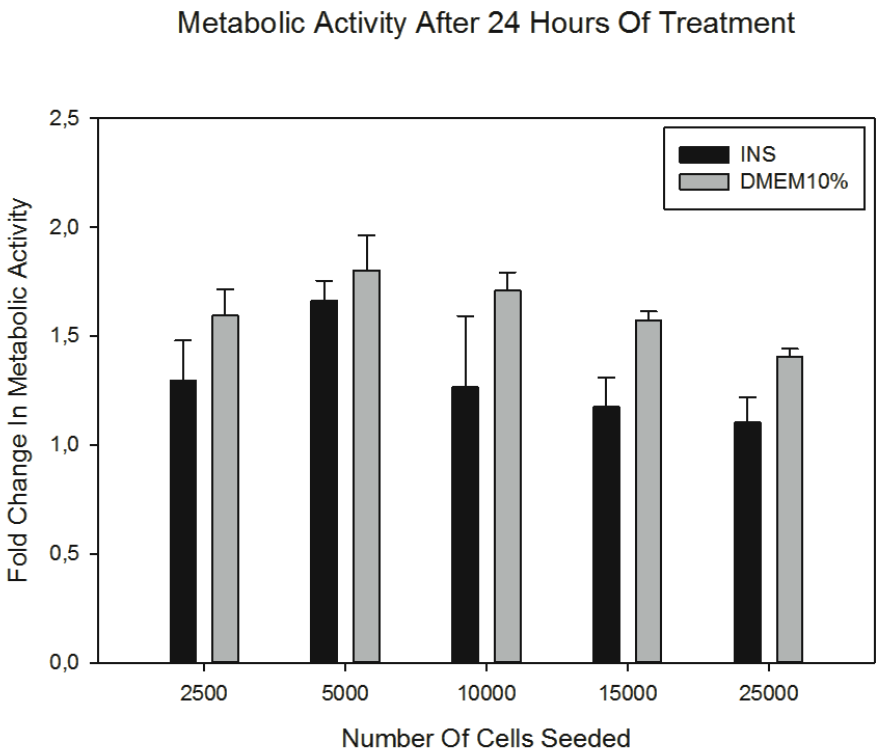

Figure 3.6.1: Increase in metabolic activity represented as average fold change compared to negative control (SF-DMEM, set to 1), based on 4 biological replicates with 6 technical replicates each. Cells were plated at 2500, 5000, 10000, 15000 and 25 000 cells per well in a 96-well plate, and treated with 1.0 µM insulin or DMEM10% for 24 hours.

After 36 hours of insulin or DMEM10% treatment, cells plated at 2500 cells showed a fold change of 1.30 (+/-0.22) and 1.94 (+/-0.16) respectively. Cells plated at 5000 cells showed a 1.26 (+/-0.26) and 2.74 (+/-0.04) fold change of increased metabolic activity after insulin and DMEM10% treatment, respectively. Cells plated at 10000 cells showed a fold change of 1.19 (+/-0.22) after insulin treatment and 2.37 (+/-0.26) after DMEM10% treatment. After 36 hours of the aforementioned treatments, cells plated at 15000 cells per well displayed a fold change of 1.17 (+/-0.26) and 2.06 (+/-0.06) respectively. Cells plated at 25 000 cells had an average fold change of 1.09 (+/-0.26) and 1.60 (+/-0.05) after 36 hours of treatment (figure 3.6.2). Averages in figure 3.6.2 are based on 4 biological replicates, mean fold change and SD can be found in appendix F.

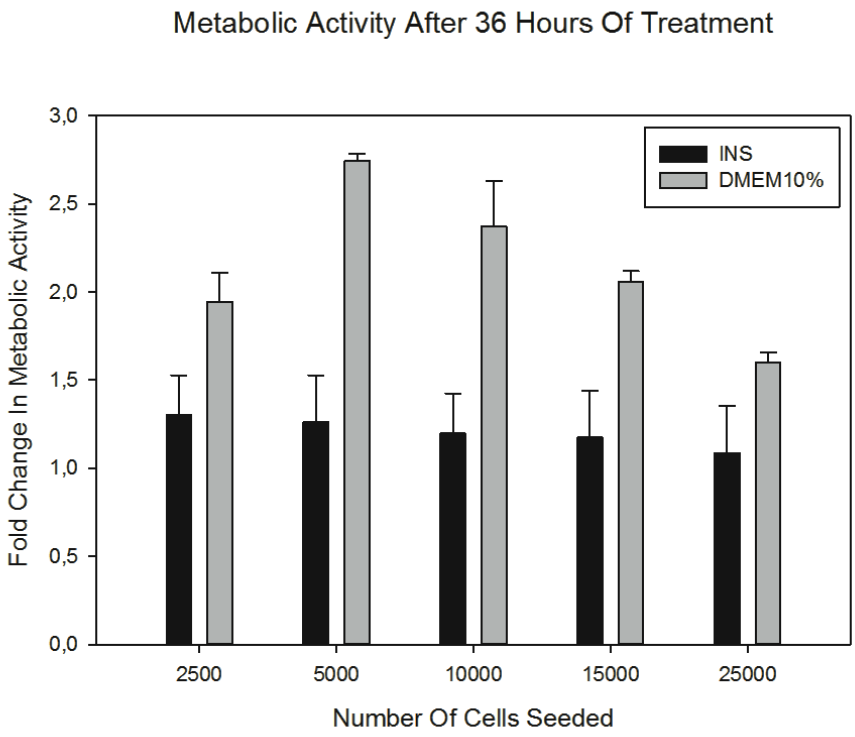

Figure 3.6.2: Increase in metabolic activity represented as average fold change compared to the negative control (SF-DMEM, set to 1), based on 4 biological replicates with 6 technical replicates each. Cells were plated at 2500, 5000, 10000, 15000 and 25 000 cells per well in a 96-well plate, and treated with 1.0 µM insulin or DMEM10% for 36 hours.

After 48 hours of insulin or DMEM10% treatment, cells plated at 2500 cells displayed an average fold change of 1.44 (+/-0.20) and 3.24 (+/-0.54), respectively. Cells seeded at 5000 cells displayed an average fold change of 1.30 (+/-0.13) and 2.81 (+/-0.19) with the same treatment. Changes in metabolic activity for cells seeded at 2500 and 5000 cells were statistically significant from control ($p<0.05$). Cells plated at 10000 cells per well, had an average fold change of 1,22 (+/-0.21) and 2.64 (+/-0.68) after 48 hours of insulin or DMEM10% treatment, respectively. The same treatment resulted in an average fold change of 1.20 (+/-

0.15) and 1.80 (+/-0.09), and 1.16 (+/-0.25) and 1.76 (+/-0.22) for cells plated at 15000 and 25 000, respectively (figure 3.6.3). Averages in figure 3.6.3 are based on 4 biological replicates, mean fold change and SD can be found in appendix G.

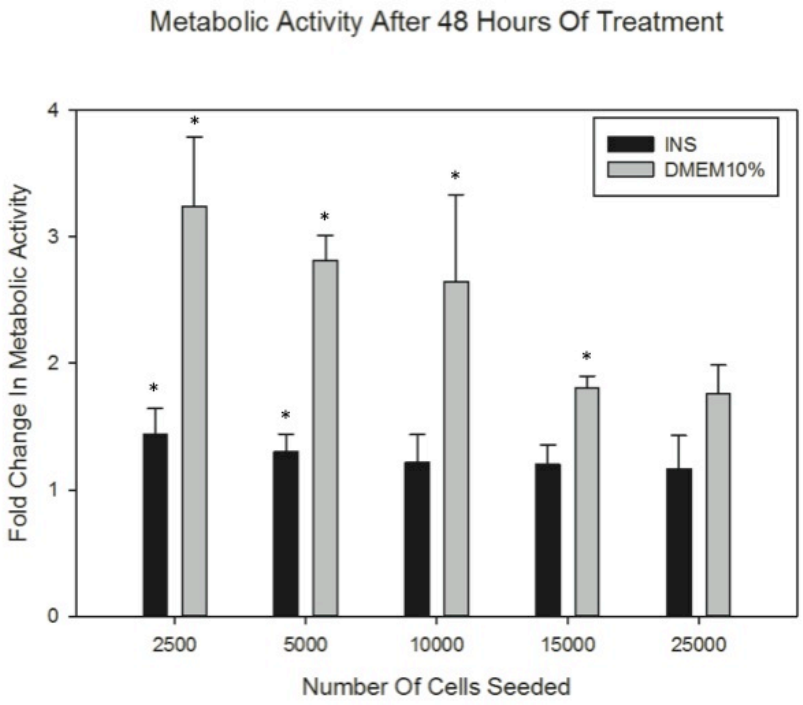

Figure 3.6.3: Increase in metabolic activity represented as average fold change compared to the negative control (SF-DMEM, set to 1), based on 4 biological replicates with 6 technical replicates each. Cells were plated at 2500, 5000, 10000, 15000 and 25 000 cells per well in a 96-well plate, and treated with 1.0 µM insulin or DMEM10% for 48 hours. * indicates significance ($p<0.05$).

Cells treated with 1 µM insulin for 48 hours gave an average fold change of metabolic activity of 1.44 (+/-0.20) and 1.30 (+/-0.13) for cells plated at 2500 and 5000 cells per well, respectively. These values represent an average increase in metabolic activity of 44% and 30% compared to the control, and are the largest increases in metabolic activity in this MTT experiment, also the only statistically significant results. These conditions (48 hours treatment, plating of 2500 and 5000 cells) will be examined further to pin down the perfect concentration of insulin treatment.

3.7 Optimizing Conditions for the MTT Viability Assay

Based on the results from the previous MTT viability assay, cells were plated at 2500 and 5000 cells per well in a 96-well plate, and treated with insulin for 48 hours. 3 insulin concentrations were used to define the most potent concentration: 3.0 µM, 1.0 µM and 0.30 µM insulin. Positive (DMEM10%) and negative (SF-DMEM) controls were included in the experiment.

Cells plated at 2500 cells per well and treated with 3.0 µM, 1.0 µM and 0.30 µM insulin, displayed significant ($p<0.05$) increases in metabolic activity compared to control, for all insulin concentrations and positive control. SW982 synoviocytes seeded at 2500 cells per well and treated with 3.0 µM insulin displayed a fold change of metabolic activity of 1.36 (+/-0.23) compared to control (figure 3.7.1). Similarly, treatment with 1 µM and 0.3 µM insulin resulted in fold changes of 1.51 (+/-0.22) and 1.30 (+/-0.18), respectively (figure 3.7.1). The two latter results were also significantly different from each other. Averages in figure 3.7.1 are based on 3 biological replicates, mean fold change and SD can be found in appendix H.

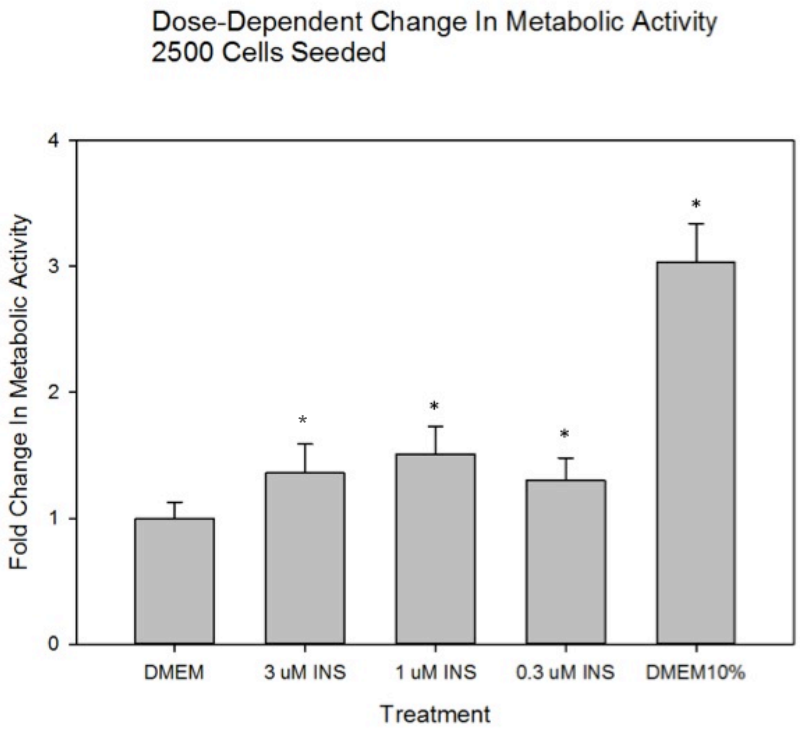

Figure 3.7.1: Increase in metabolic activity represented as average fold change compared to negative control (SF-DMEM, set to 1), based on 3 biological replicates, with 6 technical replicates per biological replicate. Cells were plated at 2500 cells per well in a 96-well plate, and treated with 3.0 µM – 0.3 µM insulin or DMEM10% for 48 hours. Significant ($p<0.05$) results labeled with *.

Cells plated at 5000 cells per well and treated with 3.0 µM, 1.0 µM and 0.3 µM insulin for 48 hours displayed significant increases in metabolic activity. The observed fold changes in metabolic activity for cells treated with 3.0 µM, 1.0 µM and 0.3 µM, were 1.21 (+/-0.15), 1.32 (+/-0.12) and 1.29 (+/-0.10) respectively (figure 3.7.2). All of the observed changes were statistically significant from the controls. Averages in figure 3.7.2 are based on 3 biological replicates, mean fold change and SD can be found in appendix I.

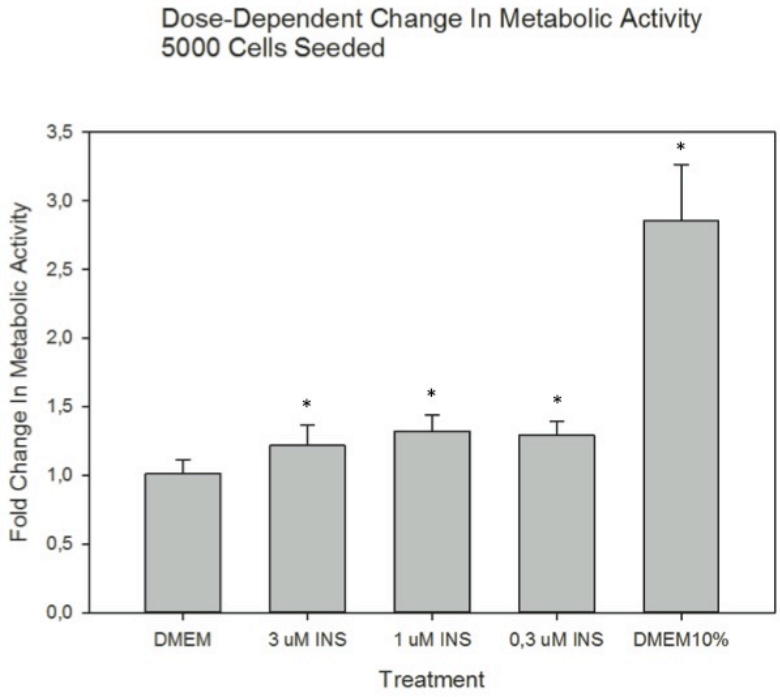

Figure 3.7.2: Increase in metabolic activity represented as average fold change compared to the negative control (SF-DMEM, set to 1), based on 3 biological replicates, with 6 technical replicates per biological replicate. Cells were plated at 5000 cells per well in a 96-well plate, and treated with 3.0 µM, 1.0 µM 0.3 µM insulin or DMEM10% for 48 hours. Significant ($p<0.05$) results labeled with *.

None of the insulin concentrations used in this experiment had cytotoxic effects on the SW982 synoviocytes. All insulin concentrations gave an increase in metabolic activity, however cells seeded at 2500 cells per well and treated with 1.0 µM insulin resulted in the largest increase in metabolic activity. For the remaining experiments using insulin stimulation, 1 µM insulin will be applied along with a degree of confluency corresponding to that observed at 2500 cells per 0.32 cm^2 (surface area of 1 well in a 96-well plate).

3.8 Flow Cytometry Could Not Validate Increased Proliferation In SW982

Insulin has previously been described as a potent growth factor in human cell cultures, including human hepatic stellate cells, human skin fibroblasts and human placental cells.[104-106] Insulin mediates the growth promoting effects through activation of PKB and more.[12] A MTT viability assay can be indicative of metabolic activity and proliferation, as it measures the conversion of MTT to formazan salts by mitochondrial enzymes.[107] In order to determine whether the increase in metabolic activity observed in MTT assays were due to increased metabolic activity or proliferation, flow cytometry was used to determine the proportion of cells in a proliferative state (G2, M or S phase) and non-proliferative state (G1 phase).

By flow cytometry cell cycle phase was determined in subconfluent SW982 synoviocytes stimulated with insulin. The proportion of cells in a non-proliferative state in samples stimulated with insulin were not different from control samples. The percentage of cells in G1 was 89.41%, 94.08% and 84.78% for cells treated with SF-DMEM, insulin and DMEM10%, respectively. Likewise, the percentage of cells in G2+M+S were 10.32%, 5.92% and 15.2% for cells treated with SF-DMEM, insulin and DMEM10%. Cells were stimulated with 1 µM insulin for 48 hours (figure 3.8.1). Numbers in figure 3.8.1 are based on one biological replicate, the other 2 replicates can be found in appendix J.

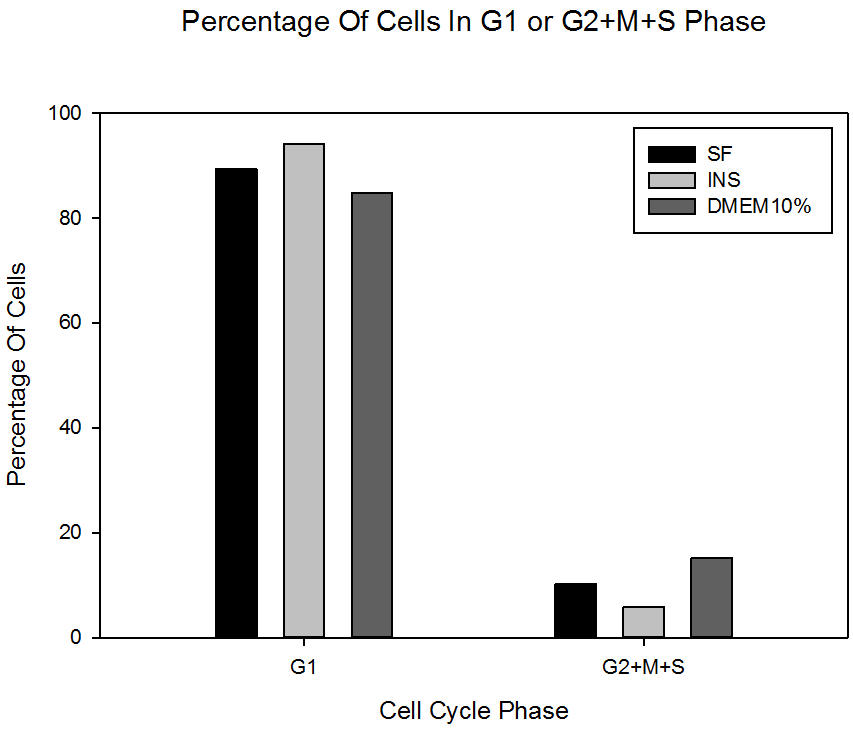

Figure 3.8.1: Cells stimulated with 1 µM insulin for 48 hours did not have a proportion of cells in a non-proliferative state (G1), different from control. Cells treated with DMEM10% had a higher proportion of cells in a proliferative state compared to control (G2+M+S). Results presented in the figure are based on one experiment, with a trend representative for 2 other biological replicates.

The flow cytometry assay could not validate that the insulin-induced change observed with the MTT assay was due to a change in rate of proliferation. 48 hours of 1 μM insulin treatment did not result in a change in the proportion of cells in a non-proliferative state.

3.9 Insulin Induces Changes in Gene Expression

In order to be receptive to the growth promoting effects of insulin stimuli, SW982 cells have to express the appropriate receptor for this kind of stimuli, the insulin receptor (IR). Also, it has previously been shown that the growth promoting actions of insulin, can be conducted by an additional receptor; the insulin-like growth factor 1 receptor (IGF1R).[108] c-Myc is a cellular oncogene and a marker for cell growth, proliferation, apoptosis and cellular metabolism. c-Myc has been shown to be regulated transcriptionally and post-transcriptionally, and mRNA levels have shown to be induced in quiescent rat skeletal muscle cells exposed to 3 hours of insulin.[109] c-fos is an early immediate proto-oncogene, with a rapidly induced transcription and a role in several cellular processes, like cellular growth.[110] c-fos mRNA levels have been shown to be induced by insulin stimulation after 15 min in rat white adipose tissue, with elevated mRNA levels lasting for 5 hours.[111] IL-6 is a pro-inflammatory cytokine, involved in the regulation of immune responses, hematopoiesis and inflammation.[112] IL-6 expression has been shown to be induced by insulin after 3 hours of 125 nM insulin treatment in LS14 human adipocytes.[113, 114]

HPRT[115], 18S[116] and B2M[117] have been shown to be promising reference genes in cell culture experiments where insulin is the stimulant.

The time-dependent, insulin-induced expression of IR, IGF1R, c-myc, c-fos and IL-6 was investigated with RT-qPCR in subconfluent SW982 synoviocytes. Cells were stimulated with insulin for 2, 4, 6, 12 and 24 hours, and change in gene expression was calculated relative to the square root of reference genes HPRT and B2M. 18S was excluded as a normalizing gene, as the 18S gene expression showed a tendency to vary with insulin incubation.

In this study, IR and IGF1R gene expression was significantly downregulated at 2 and 12 hours, and 12 hours respectively. A trend of negative regulation in response to insulin stimulation was observed at all time points, except for 24 hours, for both receptors (figure 3.9.1). Averages in figure 3.9.1 are based on 3 biological replicates, mean fold change and SD can be found in appendix K (IR) and L (IGF1R).

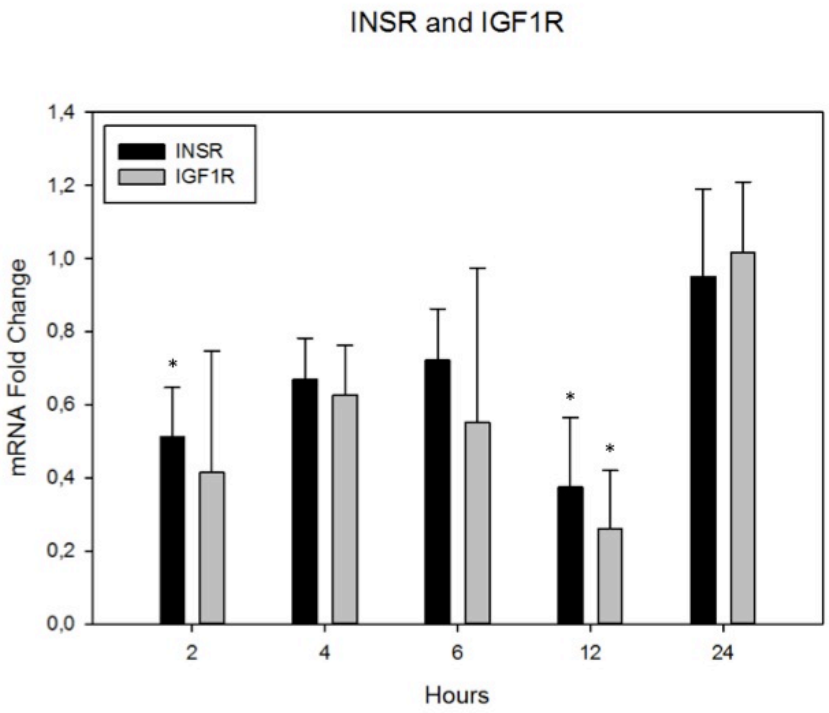

Figure 3.9.1: Regulation of INSR and IGF1R expression after 2, 4, 6, 12 and 24 hours of insulin stimulation (1 μM). Fold change in mRNA expression is relative to the square root of reference genes HPRT and B2M, and an average of 3 biological replicates. * indicates significance ($p<0.05$) compared to control (set to 1).

c-Myc expression was not significantly influenced by insulin stimulation compared to control (figure 3.9.2). Averages in figure 3.9.2 are based on 3 biological replicates, mean fold change and SD can be found in appendix M.

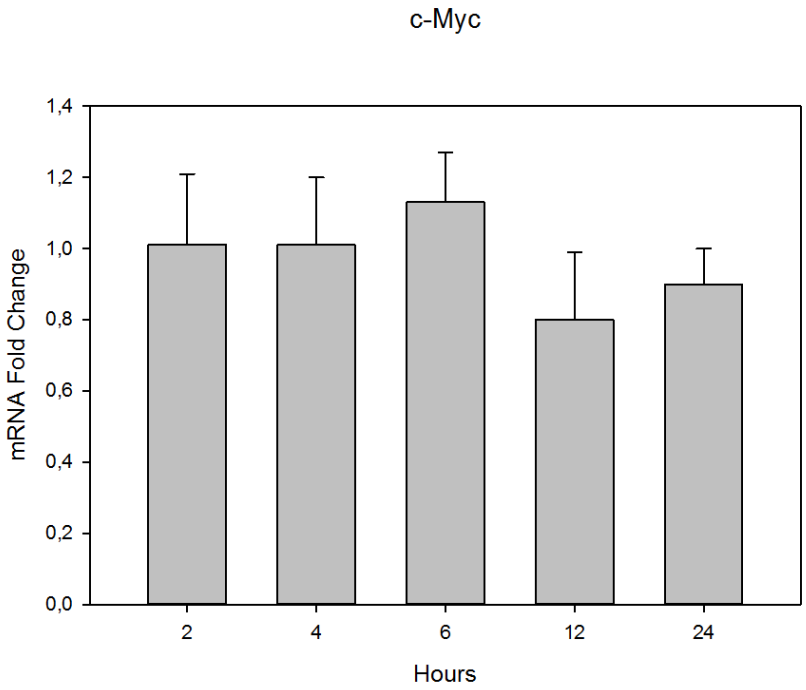

Figure 3.9.2: Regulation of c-Myc gene expression after 2, 4, 6, 12 and 24 hours of insulin stimulation (1 µM), compared to control (set to 1). Fold change in mRNA expression is relative to the square root of reference genes HPRT and B2M, and an average of 3 biological replicates.

c-fos gene expression was significantly downregulated after 12 hours of insulin stimulation. A negative regulation of c-fos gene expression was also observed at 2 hours, all though not statistically significant from the control. Gene expression was leveled to the control for the remaining time points, 4, 6 and 24 hours (figure 3.9.3). Averages in figure 3.9.3 are based on 3 biological replicates, mean fold change and SD can be found in appendix N.

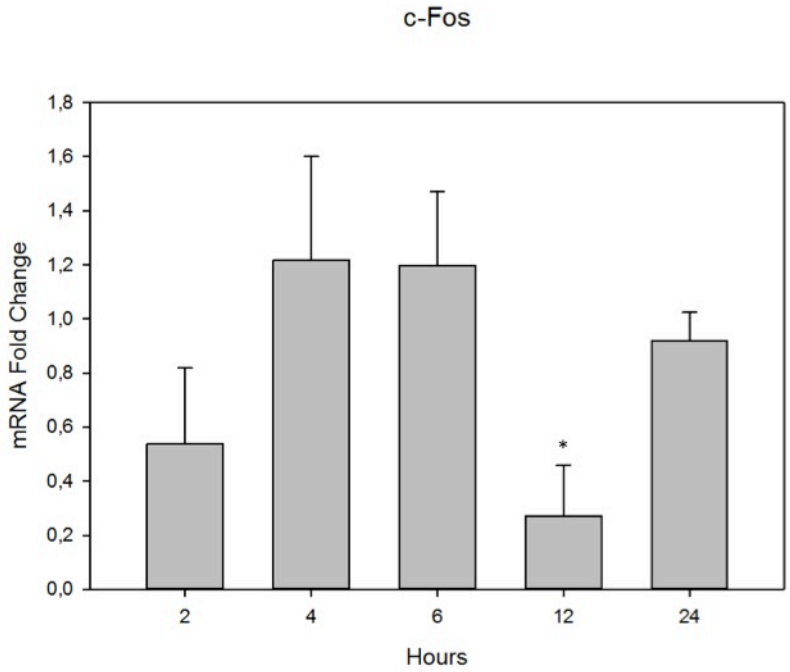

Figure 3.9.3: Regulation of c-Fos gene expression after 2, 4, 6, 12 and 24 hours of insulin stimulation (1 µM), compared to control (set to 1). Fold change in mRNA expression is relative to the square root of reference genes HPRT and B2M, and an average of 3 biological replicates. * indicates statistical significance ($p<0.05$) compared to normalizing control, set as 1.

A non-significant induction of 1.6 (+/-0.25) fold of IL-6 gene expression was observed after 2 hours of insulin stimulation in SW982s compared to control. The observed trend was still present at 4 hours, all though less prominent. IL-6 gene expression was not altered for the remaining time points of insulin stimulation (figure 3.9.4). Averages in figure 3.9.4 are based on 3 biological replicates, mean fold change and SD can be found in appendix O.

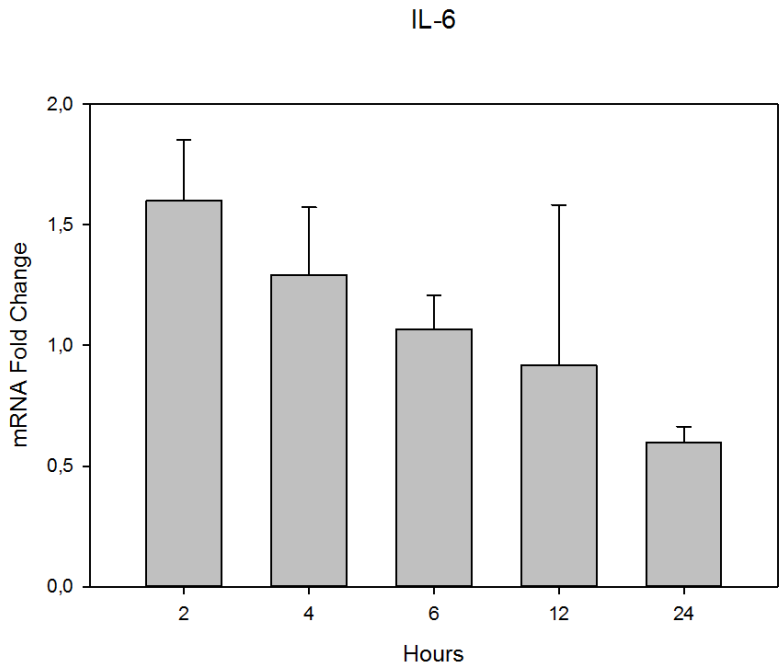

Figure 3.9.4: Regulation of IL-6 gene expression after 2, 4, 6, 12 and 24 hours of insulin stimulation (1 µM), compared to control (set to 1). Fold change in mRNA expression is relative to the square root of reference genes HPRT and B2M, and an average of 3 biological replicates.

18S was included in this study as a third reference gene, but was found to vary too much to be used as a reference gene. Therefore the fold change in mRNA levels compared to the two reference genes HPRT and B2M, are presented in figure 3.9.5. There were no significant regulations of 18S gene expression, but a trend was observed, where gene expression seemed to be induced after 4 hours of insulin stimulation and downregulated after 12 hours of insulin stimulation. Averages in figure 3.9.5 are based on 3 biological replicates, mean fold change and SD can be found in appendix P.

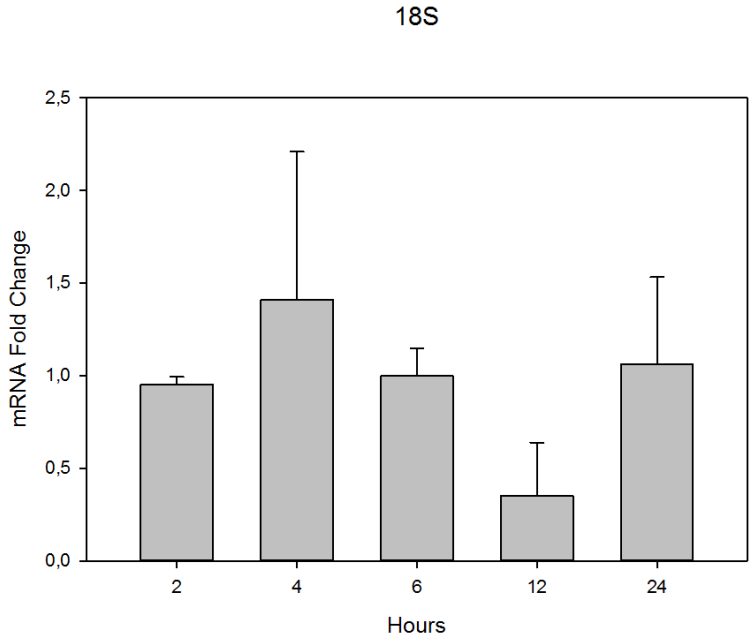

Figure 3.9.5: Regulation of 18S gene expression after 2, 4, 6, 12 and 24 hours of insulin stimulation (1 µM), compared to control (set to 1). Fold change in mRNA expression is relative to the square root of reference genes HPRT and B2M, and an average of 3 biological replicates.

This study may indicate a trend of downregulation of IR and IGF1R gene expression in response to insulin stimulation at 2, 4, 6 and 12 hours. Also, insulin was shown to induce a downregulation of c-Fos after 12 hours. Insulin did not affect c-Myc expression, but induced a trend of decreased IL-6 gene expression. Also, insulin induced variation in the expression of a previously accepted reference gene 18S.

4. Discussion

During the 2 years the work for this master's thesis was performed, the effect of the hormone insulin on SW982 cells was investigated. Several methods were utilized in order to investigate the effects on SW982 cells from different aspects. Arachidonic and oleic acid release assays were performed to investigate the time dependent effect of insulin stimulation on arachidonic and oleic acid release. Arachidonic acid release is mainly facilitated by $cPLA_2$, and can therefore be indicative of $cPLA_2$ activity. The release of oleic acid is facilitated by several enzymes, like $iPLA_2$, $sPLA_2$ and other lipases.[38, 98] The effect of insulin treatment on SW982 cells was also measured by MTT assays. Because the MTT assay measures the intracellular conversion of *3,4,5 dimethylthiazol-2,5 diphenyl tetrazolium* (MTT) to a formazan precipitate, an increase in the conversion can be indicative of an increase in metabolic activity or an increase in cell number and proliferation. In order to determine whether the effects of insulin observed with the MTT assay was due to an increase in metabolic activity or an increase in cell proliferation, flow cytometry was used to determine fraction of cells in a proliferative state.

In order to investigate the effect of insulin on the expression of some proliferation genes and one inflammatory gene, RT-qPCR was performed on cDNA samples with primers for 8 different genes (among these; 3 reference genes) from different time periods of insulin stimulation.

The SW982 synoviocytes utilized in these experiments were always in e subconfluent state at the time of treatment initiation (unless otherwise stated). Cells can be in three different states; subconfluent, confluent and post-confluent. This decision was made in order to mimic the natural, proliferative environment of the synovial lining of RA joints.

4.1 OA/AA Release

AA release is primarily mediated by the arachidonyl specific phospholipase, $cPLA_2$[50], and can be indicative of pro-inflammatory actions mediated through $cPLA_2\alpha$. AA release has previously been shown to be induced by several factors such as ATP, thrombin, IL-1, PAF and lysoPC.[50, 51, 53] We have shown that the rate of which AA is released is not affected by insulin stimuli. However, this is not necessarily synonymous with the fact that insulin does not have pro-inflammatory effects.

In this study we show that insulin stimulation decreases the release of OA, and has no effect on AA release. In 2004 Oestvang et al. showed that low-density lipoprotein (LDL) stimulation of cultured monocytes increases the release of both AA and OA through $sPLA_2$ activation.[118] Thus, this implies that the effect observed in this study by insulin on OA release, is not mediated by $sPLA_2$ activation, as it does not affect AA release. Similarly, Jorgensen et al. showed in 2010 that PAF induces the release of both AA and OA in human keratinocytes, through an $iPLA_2$ dependent mechanism.[99] Hence, this implies that insulin stimulated decrease in OA release is not mediated by $iPLA_2$ either. The HSL also mediates free fatty acid release and is activated by the accumulation of cAMP, which subsequently activates protein kinase A (PKA).[119] It has previously been shown that insulin inhibits HSL activation through a protein kinase B (PKB) dependent pathway, leading to the degradation of cAMP (figure 4.1.1).[120]

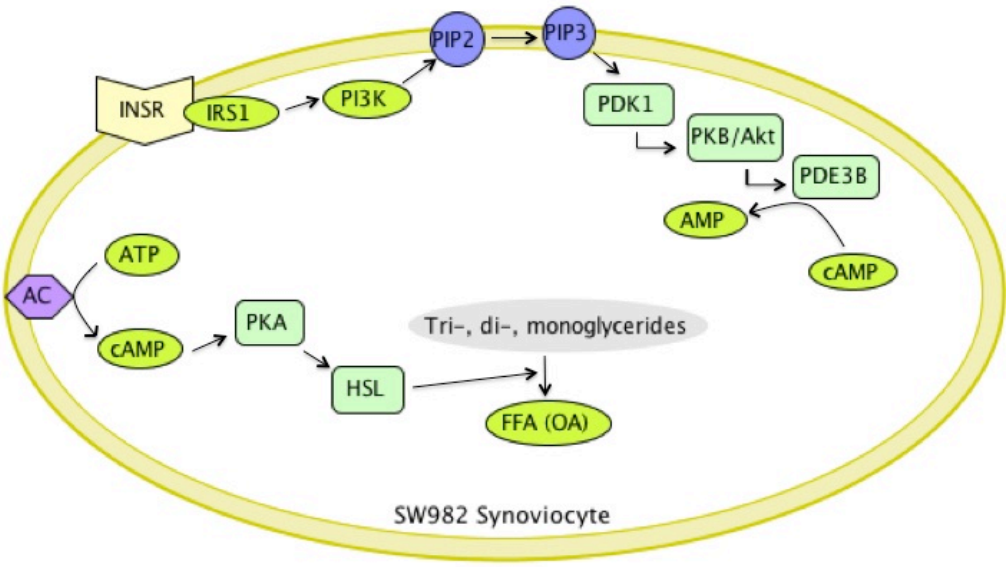

Figure 4.1.1: The activation and insulin-induced inhibition of HSL activity, by cAMP production and degradation, respectively. PIP2: Phosphatidylinositol-4,5-bisphosphate. PIP3: Phosphatidylinositol-3,4,5-trisphosphate. PDK1: Phosphoinositide-dependent Kinase 1. PDE3B: Phosphodiesterase 3B. AMP: Adenosine Monophosphate. cAMP: Cyclic AMP. AC: Adenylate Cyclase. PKA: Protein Kinase A.

Once released from phospholipids or TDMglycerides, OA is converted to n-9 eicotrioenic acid (ETA) by Δ5-desaturases. ETA can inhibit the production of the pro-inflammatory LTB_4s. ETA is a substrate for 5-lipoxygenase and is converted to LTA_3, which binds to LTA_4 hydrolase and thus inhibits the production of LTB_4 from LTA_4 (figure 4.1.2).[38] Inhibition of the production of the pro-inflammatory LTB_4 can be considered anti-inflammatory actions by ETA.

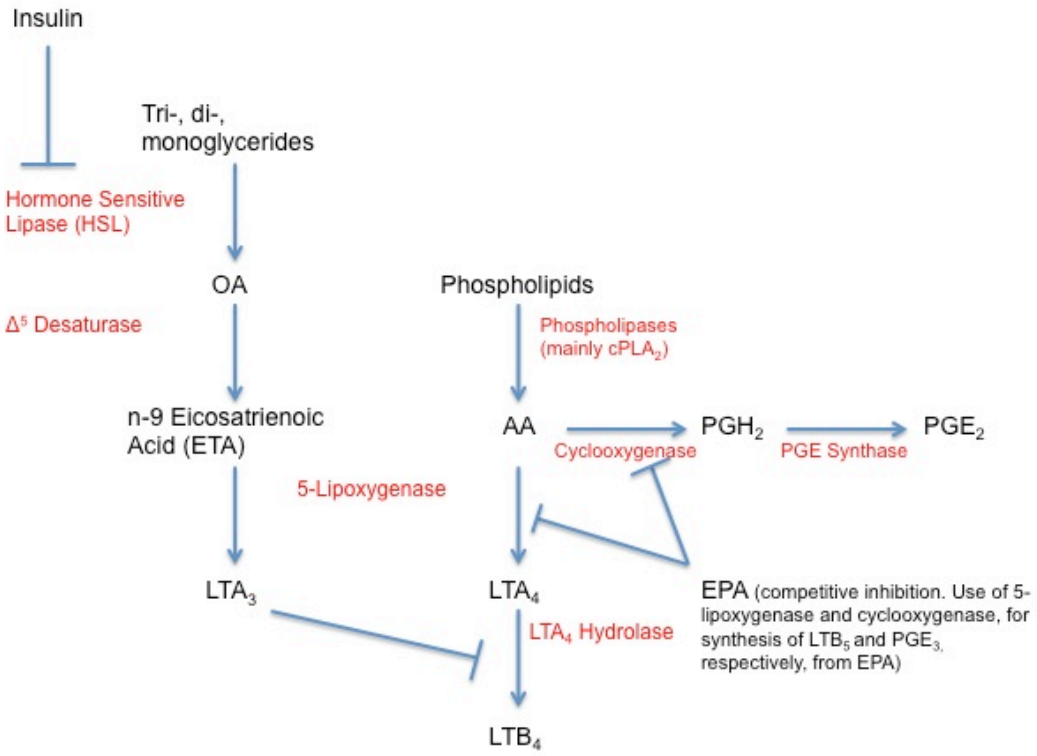

Figure 4.1.2: Production of LTA_3 follows the release of OA. LTA_3 further inhibits the production of pro-inflammatory LTB_4.

The n-3 eicopentaoenic acid (EPA; 20:5n-3) is derived from the essential fatty acid ALA, which is found in leafy greens, flaxseed and canola oils. The conversion of ALA to EPA is an extremely timely process in the human body, and the main source of EPA is through the diet (fish and n-3 fatty acid supplements). It is commonly known that EPA provides health benefits and has anti-inflammatory actions. One of the mechanisms through which EPA promotes anti-inflammatory actions is by competing for enzymes 5-lipoxygenase and cyclooxygenase with their common substrate AA, leading to a decrease in the production of LTB_4 and PGE_2, respectively. The fact that ETA affects the production of the pro-inflammatory LTB_4 through a similar mechanism as EPA, may point to similar anti-inflammatory effects of ETA. Because insulin inhibits the production of ETA, insulin may be labeled as pro-inflammatory.

One major source of oleic acid is olive oil. Olive oil is a central component of the Mediterranean diet, which is believed to be one of the healthier dietary choices.[121] It is currently not known why the Mediterranean diet is so beneficial, but it could be possible that parts of the explanation could be found in the anti-inflammatory actions of OA.

It is accepted that the hormone sensitive lipase releases OA from tri-, di- and monoglycerides.[46] It is an established theory that insulin inhibits the hormone sensitive lipase.[120] It is also an established theory that the n-9 ETA inhibits the production of LTB_4.[38] However, connecting the observed decrease in OA release with an inhibition of HSL is strictly a speculation. This is a hypothesis that would have to be thoroughly tested with a series of lab experiments. One way to do this could be to apply an inhibitor for HSL to the cell culture and perform the OA release experiment over again with insulin. If there was still a decrease in the release of OA in response to insulin, this could imply that the HSL is not responsible for the observed effects. Whether there is a connection between insulin stimulation and a decreased production of n-9 ETA is also only a speculation, which will have to be tested further. An enzyme-linked immunosorbant assay (ELISA) of the insulin-stimulated cells could reveal amounts of ETA in the cells relative to control cells. Also, an ELISA could measure whether the amount of LTB_4 was higher in insulin treated cells, than in control cells. To summarize, several tests have to be performed in order to verify/reject the hypothesis presented in this chapter. A clarification of the speculations in this chapter, could eventually lead to a dietary advice for RA patients, where a decreased consumption of carbohydrates would be preferable if insulin was labeled pro-inflammatory.

4.2 Positive Flow Cytometry Results in THP1 After Insulin Stimulation

The RA synovium is characterized by its hyperplastic nature. The inflamed synovium hyper proliferates while simultaneously secreting pro-inflammatory cytokines and cartilage destructive agents such as MMPs. The MTT assay revealed that insulin induces increased production of formazan crystals in subconfluent SW982 synoviocytes. Because the flow cytometry assay could not confirm, it could not be concluded that the observed increase indicated hyper proliferation. Cells used for flow cytometry were stimulated under the exact same conditions as cells in the MTT assay, 48 hours of 1 µM insulin in subconfluent cells. One possible explanation for why the flow cytometry assay was negative might be the duration of stimulation. When a cellular response is observed in the form of proliferation after 48 hours, it is possible that the change in expression of proliferative genes and shift in cell cycle phase occurs before the actual proliferation, and is no longer detectable at 48 hours. Jamal Naderi, a fellow master student in the lab, has studied the effect of insulin in monocytes (THP1), and observed a significant difference in cell cycle phase between quiescent cells and insulin stimulated quiescent cells after 24 hours.[122] The observable difference in cell cycle phase with flow cytometry is very little, with only a small percent difference in cells in dormant and proliferative phases.[123] For one treatment, for instance insulin, a couple of percent more cells in G1 means a couple of percent fewer cells in the proliferative phases (G2+M+S). Hence, Naderi's results may indicate that the 48-hour stimulation period used in the SW982 cells was too long, and that a potential difference in cell cycle phase was no longer detectable at this time.

One of the many enzymes activated by the insulin-signaling pathway is protein kinase B (PKB).[12] Activation of protein kinase B leads to the activation of several downstream signaling pathways, which affects the cell in different ways. Examples of cellular effects are increased proliferation and inhibition of apoptosis (figure 4.2.1).[12]

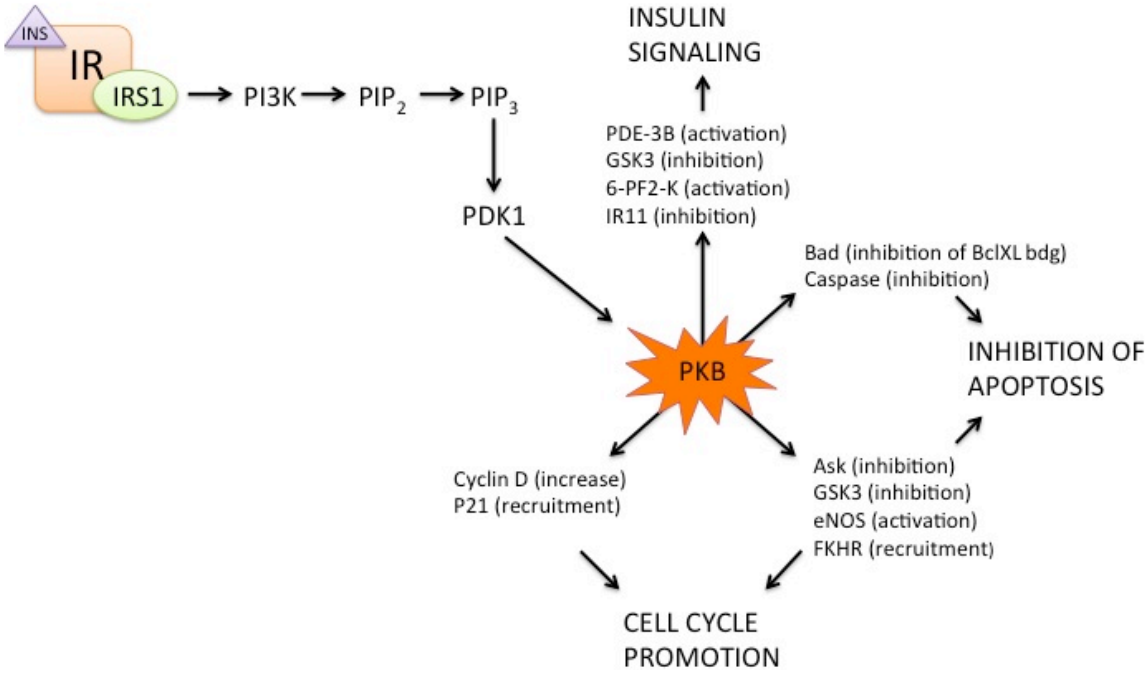

Figure 4.2.1: PKB can be activated by the insulin-signaling pathway, and lead to inhibition of apoptosis and cell cycle promotion.

Overexpression of constitutively activated PKB mutants promotes cellular transformation in many cell types, through inducing proliferation in growth-arrested cells and inhibiting apoptosis. This results in an artificially high rate of proliferation and cell survival, which characterizes both cancers and inflamed synovium. This could suggest a possible role for insulin signaling in both cancer and RA. PKB has previously been shown to be overexpressed in ovarian, breast and pancreatic cancers.[12] All of the aforementioned types of cancer have been related to obesity[124], which again is associated with insulin resistance and hyperinsulinemia.[124] For RA, DAS28 scores in RA patients increase with increasing BMI. These results may point to a central role for insulin in cancer and RA. In conclusion, the MTT results may be a result of insulin signaling through activation of PKB and inducing increased cell survival. Increased cell survival is not desirable in the hyperplastic synovial lining of RA joints.

4.3 A Trend of Downregulation of IR and IGF1R Gene Expression

It has previously been reported that the extracellular availability of the IR is decreased in response to insulin stimuli, by internalization and degradation of the IR after binding of insulin.[125] It has also been shown that extracellular stimuli can regulate the expression of IR[126, 127], and that also insulin downregulates the expression of IR and accelerates IR degradation, in pancreatic acinar cells.[127] Insulin has also been shown to reduce the number of IRs on the cell surface in cultured hepatocytes, fibroblasts and fat tissue explants.[128]
At chronically elevated levels, insulin is able to desensitize the IR through several mechanisms.[16]

In this study, we found that IR gene expression was significantly downregulated after 2 and 12 hours of insulin treatment. The overall trend for all time-points seemed to be downregulation of gene expression, except for 24 hours of insulin treatment, when the level was brought back to basal expression levels. One plausible explanation for the IR gene expression returning to basal levels at 24 hours might be that the target cell was desensitized, and the actions of insulin stimulation were abolished.

The IGF1R signals through multiple intracellular pathways by phosphorylation of Shc and insulin receptor substrate (IRS) -1, -2, -3, and -4, including the PI3K, Akt and the mitogen-activated protein kinase (MAPK) pathways.[129, 130] Activation of the aforementioned pathways plays a role in different cellular events, including cell growth, differentiation, migration and survival.[129] However, the IR and the IGF1R are able to trigger distinct cellular responses, even though they are able to activate similar signaling pathways and target the same intracellular substrates.[130] IGF1R gene expression has been reported to be regulated by various factors including IGF-1, platelet derived growth factor (PDGF), estrogen and LDL, in vascular smooth muscle cells.[129]

It has previously been shown that insulin can bind to the IGF1R and conduct its growth promoting activities through this receptor.[108] It is therefore not surprising that the same trend of gene regulation is observed for the IGF1R gene as for the IR gene. In this study, gene expression of IGF1R was found to be significantly downregulated after 12 hours of insulin stimulation, also the overall trend for IGF1R was a negative regulation of gene expression at 2, 4 and 6 hours of insulin stimulation. After 24 hours of insulin stimulation, the IGF1R gene expression returned to basal expression levels.

The fact that insulin stimulation resulted in a decreased expression of IR and IGF1R, indicates that the SW982 cells are amenable to insulin signaling and the cellular effects of insulin receptor and IGF1R pathways. The observed return to basal expression levels at 24 hours may indicate a desensitization of the receptors in response to insulin. The potential fact that SW982 cells are susceptible to the effects of insulin, means that every new discovery of insulin action in cells is a potential regulator of SW982 activity.

4.4 C-myc Gene Expression is Not Regulated by Insulin Stimulation

C-myc is a gene previously shown to be associated with cell proliferation, growth, apoptosis and metabolism. C-myc is regulated both transcriptionally and post-transcriptionally, and gene expression has been shown to be induced after 2-3 hours of insulin stimulation in quiescent rat skeletal muscle cells.[109, 131]

In this study we were not able to induce c-myc gene expression at any time-point of insulin incubation. In fact, it has previously been shown that insulin was unable to induce c-myc expression in fibroblasts, and that these fibroblasts were unable to arrest growth at low serum levels.[132] Fibroblasts constitutively overexpressing c-myc did not increase in cell number in culture, because of substantial cell death.[133] Therefore, one possible explanation to why we could not see an induction in c-myc gene expression in response to insulin incubation is that the SW982 cells were not quiescent. It is also possible that insulin did not affect the expression of proliferative genes.

4.5 C-fos Gene Expression is Downregulated by Insulin

C-fos is a proto-oncogene and the resulting protein, Fos, forms a dimer with Jun and binds to DNA-regulatory elements found in control regions of various genes. C-fos gene expression has been associated with cell cycle progression.[110] C-fos transcription has previously been shown to be rapidly induced by insulin incubation (1-2 hours) in chick embryonic lens epithelial cells, and is an immediate early-gene.[131]

In this study, no induction of c-fos gene expression was observed in response to insulin incubation at any time-points. In fact, c-fos gene expression was significantly downregulated after 12 hours of insulin stimulation.

C-fos transcription is regulated by phosphorylation of the transcription factor cAMP response element-binding protein (CREB)[134], which has been shown to be activated by insulin through a cGMP-dependent protein kinase or protein kinase G (PKG)-dependent manner.[114] Insulin has previously been shown to increase intracellular levels of cGMP[114], which should point to an induction of c-fos gene expression.

There might be several possible explanations to why c-fos gene expression was not induced as previously reported. One of them being, if c-fos is a marker of cell cycle progression and our cells were not in total quiescence, there would not be any induction of cell cycle promoting genes after incubation with insulin. Also, c-fos has previously been described to be constitutively highly expressed in the synovial tissue of RA.[135] Perhaps, this is why an induction of c-fos expression was not observed in our study. It is also possible that the induction of c-Fos gene expression occurred before 2 hours, and that the effect had faded already at 2 hours. Further investigations of the effect of insulin on c-Fos gene expression has to be conducted with RT-qPCR and shorter periods of insulin stimulation.

4.6 Time-dependent Trend of IL-6 Induction After Insulin Incubation

IL-6 is a marker for low-grade inflammation, a pro-inflammatory cytokine, involved in the regulation of immune responses, hematopoiesis and inflammation.[112] IL-6 expression has previously been shown to be induced (3-fold) in response to 3 hours of 125 nM insulin, in human adipocytes.[114] IL-6 gene expression is induced by insulin, through the same mechanism of PKG-CREBP activation as c-fos gene expression.[114]

Our study shows a time-dependent trend of non-significant induction of IL-6 gene expression after 2 hours (1.6 (+/-0.25) fold induction). The induction faded as the time of insulin incubation was lengthier, and was leveled to control after 6 hours of insulin incubation. A slight, non-significant, decrease in IL-6 gene expression was observed after 24 hours of insulin incubation. In order to be able to determine the regulation of IL-6 in response to insulin in SW982 cells, more experiments should be conducted in order to get significant results. It is important to know which effects insulin has on IL-6 gene expression, as an induction/decrease of IL-6 expression will have pro-inflammatory/anti-inflammatory effects on the synovial environment.

4.7 Regulation of 18S Gene Expression by Insulin

Ribosomes are the catalytic and regulatory centers of protein synthesis in cells. The ribosome is a large RNA-protein particle consisting of two subunits, the 60S and the 40S subunit, which together contains about 80 proteins and ribosomal RNA (rRNA). The small subunit, 40S, consists of the 18S rRNA and 32 ribosomal proteins.[136] The minimally regulated 18S rRNA has been validated several times as a good housekeeping gene and normalizing control in RT-qPCR experiments in various tissues and with different stimulants.[137-139] 18S rRNA has previously been used as a housekeeping gene in insulin stimulation experiments.[140, 141]

No significant changes in gene expression was detected for 18S in this experiment, but a substantial increase in gene expression was observed after 4 hours of insulin stimulation, also a substantial decrease in 18S gene expression was observed after 12 hours of insulin stimulation. These variations in gene expression were not observed for the other housekeeping genes, HPRT and B2M.

This might indicate that insulin affects the transcription of the 18S gene, and that this is no longer a suitable reference gene in experiments with insulin stimulation. The effects of insulin on 18S transcription has to be investigated further in order to reach a conclusion.

4.8 Choice of Cell Seed Number for Growth Curves

In order to determine the total number of cells to be seeded in each culture flask at day 0, the knowledge and experience of the senior researchers in the lab was exploited. Seeding cells at 5 different numbers was supposed to cover cell density from initially too scarce to initially too dense. Flasks seeded with 25 000 cells were expected to exhibit difficulties with proliferation, which they did. Cells seeded at 25 000 cells did not reach the log-phase until day 6, which was 5 days later than the first flasks to reach the log-phase. The hypothesis is that SW982 cells are dependent on direct and indirect cell-cell, and cell-extra cellular matrix (ECM) communication in order to initiate a proliferative state. Proteins that facilitate cell-cell communication include Cadherins, Selectins, Ig-like cell adhesion molecules and Integrins.[142] Proteins that facilitate communication between cell and ECM include Integrins and integral membrane proteoglycans on the cell surface, and structural glycoproteins (collagens, elastins etc) and proteoglycans in the ECM. Cells seeded at 25 000 cells had difficulties with initiation of proliferation, which can be a result of difficulties with cell-cell and cell-ECM communication. Seeding 25 000 cells in a new T25 culture flask is too scarce to observe a full growth curve, with 4 phases, in 8 days.

Culture flasks seeded with 800 000 cells at day 0 represent the other end of the scale, reaching the lag-phase already at day 1, subsequently transitioning into the stationary phase at day 4. Flasks seeded with 800 000 cells were hypothesized to reach the stationary phase at day 1 or 2 and subsequently transition into the decline phase at day 3 or 4, too early for this cell number to be ideal for observing a full growth curve with all 4 phases. This was not observed in this experiment. One reason why cells seeded at 800 000 cells per flask did not reach the lag-phase and stationary phase as rapid as hypothesized, can be due to the fact that these culture flasks were brand new. SW982 cells are dependent on cell-cell and cell-ECM communication in order to initiate proliferation, which takes some time to establish. Therefore, a second growth curve experiment was conducted, in the same culture flasks as used in growth curve experiment number 1. Indeed, here the results confirmed the initial idea that the use of used culture flasks, with an established network of cell-ECM proteins, reduces the lag-phase dramatically for all cell seedings.

4.9 Cell Confluency Reaches 100% Before Cells Enter The Stationary Phase

Culture flasks seeded with 500 000 cells at day 0, reached the stationary phase at day 5 in the first growth curve experiment. These same flasks reach 100% cell confluency at day 3, meaning that the number of cells increased even though there was no more available growth surface. This observation was accompanied by morphological changes in the cells. Cells that had just reached 100% confluency were the same size and shape as cells in the lesser confluency percentage. They had the characteristic shape of a fibroblast; a thin, oblong and elongated structure with a thicker center. After spending some time at 100% confluency, the cell shape changed to a smaller, rounder and more tightly packed cell. So, even though there was no more growth surface available, the cells acclimated to facilitate further cell proliferation.

4.10 Early log-phase entry in used culture flasks

In growth curve experiment number 2, cells were seeded at 4 different cell numbers at day 0, in culture flasks previously used in growth curve number 1. No lag-phase was observed for any of the cell numbers seeded, as they transitioned directly into log-phase during the first 24 hours after seeding. Flasks seeded with 25 000 cells reached the stationary phase 2 days quicker than in the first experiment. This may suggest that the SW982 cells are strongly dependent on anchoring, and that used culture flasks have a well-established coat of anchoring proteins to facilitate cell-ECM communication.

4.11 Decline Phase In Growth Curve Number 2

In growth curve number 1, the decline phase was only observed at day 8 for flasks seeded with 800 000 cells and 500 000 cells. In growth curve experiment number 2, the decline phase was observed already at day 7 for cells seeded at 500 000 cells. These flasks also had an abnormally high cell number at day 6. This could be due to an inaccurate number of cells being seeded at day 1, causing a delay in log-phase, or due to inaccurate counting of cells in the flask. Cells seeded at 25 000 cells had a slight decline in cell number already from day 4, though this decrease in cell number was not drastic enough to be labeled decline phase. There was not observed any decline phase for cells seeded at 100 000 and 250 000. These cells started off in the log-phase from day 0 and transitioned into the stationary phase during day 4, exhibiting a slight increase in cell number during the remaining days of the experiment.

In growth curve experiment number 2, the first flask to reach 100% confluency was the flasks seeded with 500 000 cells at day 0. Flasks seeded with 500 000 cells reached 100% confluency at day 3 and a decline in cell confluency was observed on day 7 and 8. This pattern was identical to what was observed in the first experiment. By day 6 all of the flasks had reached 100% confluency, which is very different from the confluency observed in the first experiment, where flasks seeded with 25 000 cells did not even reach 100% confluency. Flasks seeded with 500 000 cells reached 100% confluency at the same pace in experiment 2 as 1, while flasks seeded with 25 000-250 000 cells reached 100% confluency earlier in experiment 2 compared to experiment 1. These results may suggest that even though flasks seeded with 500 000 cells have enough cells to establish cell-cell communication at once both in experiment 1 and 2, they still need time to settle down and attach to the growth surface. The number of cells is not the rate-limiting factor in this case.

4.12 Insulin Concentration

Previous studies using insulin incubation in various in vitro cell cultures have reported using insulin concentrations ranging from 0.1 µM to 5.8 µM insulin.[114, 131, 143-146] A concentration of 1 µM insulin was chosen based on the fact that this concentration resulted in the largest increase in metabolic activity in cultured SW982 synoviocytes, and did not appear cytotoxic in any way. The reported levels of insulin in synovial fluid were 0.70 nmol/L and 0.202 nmol/L, in RA and OA joints, respectively.[147] In comparison, the level of insulin in RA synovial fluid is 0.00041 nM and the concentration of insulin used in these tissue culture experiments are 1000 nM.

Insulin and c-peptide are found in the synovial fluid of both RA and OA patients.[147] Rovensky et al. reported in 2005 that there were no significant differences in insulin levels of plasma and synovial fluid, between OA and RA patients.[147] The same group, reported in 2007 that levels of insulin in plasma and synovial fluid are increased in RA patients in comparison with OA patients.[148] OA patients have been reported to have higher levels of C-peptide and insulin in the synovial fluid than in plasma. RA patients, on the other hand, had higher concentrations of C-peptide and insulin in plasma than in the synovial fluid.[149]

4.13 Achieving the Same Degree of Cell Subconfluency in Every Experiment

In the tissue culture experiments performed in this thesis, cell confluency is crucial. All cells should be in a similar subconfluent state. After performing the MTT viability assay, a cell seeding of 2500 cells per well in a 96-well plate resulted in the largest increase in metabolic activity. A well in a 96-well plate has a surface area of 0.32 cm^2, a well in a 48-well plate is 0.95 cm^2 (used for release assays) and a 6-well plate has a growth surface of 9.5 cm^2 (used for RNA isolation). If the experiments had been based strictly on cells per cm^2 the numbers of cells seeded in each of the wells on the different plates would have been 7421 cells (48-well plates) and 74210 cells (6-well plates). But instead of seeding this number of cells, which would have been too scarce, 50 000 cells and 200 000 cells were seeded. Cell confluency is not only dependent on the number of cells seeded and the number of hours spent in the incubator, but also the fitness of the cells, the handling of the cells and the passage number. The higher the passage number is, the faster the cells tend to grow. If these cells have a rough handling before seeding, they tend to need more time to proliferate. Some batches of cells have a tendency to grow better than other. Together, these factors will determine the amount of time needed to get the cells to the wanted cell confluency. When the cells are stimulated they should be at a 50% confluency, subconfluent, where the cells only occupy 50% of the available growth surface. This was accomplished by closely and frequently studying the progression of cell proliferation and confluency with a microscope.

4.14 Technical Variation With MTT Viability Assays

The MTT viability assay measures the enzymatic conversion of MTT, and the accuracy of the assay is dependent on an equal environment throughout the plate, accuracy of cell seeding and reading of optical density (OD). In order to ensure the former, cells were not seeded in the outer most rows and columns of the plate. These wells were filled with PBS so that temperature and humidity conditions were the same for all wells. In order to ensure that approximately the same number of cells was seeded in each well a multi channel pipet was used. Also, the 6 pipet-tips were checked after adsorption of cell suspension, to ensure equal volumes of suspension. Cells have to be seeded evenly on the surface of each well, especially since confluency is an important factor in these experiments. If cells are spread unevenly on the growth surface, there will be areas with extreme subconfluency and areas with post confluency, which will not give us the results we are looking for; namely cellular effects in subconfluent cells. In order to overcome irregular reading of OD by the OD meter, the plate was read twice (forward and backward), to ensure that the same wells got the same densities. Lastly, in order to overcome any bias of the plate or OD meter, the different stimulations were moved around randomly on the plate.

There were no significant changes in the positive controls compared to the negative controls in most of the MTT viability assay, due to the fact that only two wells per experiment were sacrificed to positive controls, to verify that the assay had worked.

4.15 Technical Variation With Release Assays

All of the same factors regarding cellular aspects of the MTT viability assay are true for the release assay as well. In addition, there are technical variations specific for the release assay. In this assay we incorporate radioactively labeled fatty acids, AA and OA, into the cellular membranes of cultured cells. After incubation with radioactively labeled medium, we remove this and replace it with a non-labeled medium with a stimulant. We the measure the amount of radioactively labeled fatty acids released into the supernatant, and relate this to the amount of radioactively labeled fatty acids residing in the cells (lysed with NaOH). By relating the amount of fatty acids in the supernatant to the amount of fatty acids in the cells, we can overcome variations in number of cells in each well. Thus, we have to be careful to not get any cells in the supernatant, and vice versa. Also, it is important to collect all of the supernatant and afterwards, all of the lysed cells.

5. Conclusion

This thesis concerns the cellular effects of insulin on cultured, subconfluent SW982 synoviocytes. Several aspects of insulin actions were investigated, including the effect of insulin on metabolic activity, cellular proliferation, activation of $cPLA_2\alpha$ and regulation of IR, IGF1R, c-Myc, c-Fos and IL-6 gene expression. In addition, it was demonstrated that SW982 synoviocytes express IR and IGF1R.

Insulin incubation did not have any effect on AA release in subconfluent SW982 cells, suggesting that insulin did not activate $cPLA_2\alpha$ under the given conditions. A trend of decreased OA release was observed in response to a 48-hour treatment of insulin. The underlying mechanism for the observed decrease is unknown, but we humbly propose a mechanism involving the insulin induced inhibition of hormone sensitive lipase, as a reason for the observed decreased release of OA. Further, the ETA-inhibited production of the pro-inflammatory LTB_4 is presented, and as insulin decreases the release of OA, pro-inflammatory effects of insulin are speculated upon. If insulin could be labeled as pro-inflammatory, this could influence dietary advices for RA patients. Reducing the presence of a pro-inflammatory agent might potentially be beneficial for the disease activity of RA patients.

Incubating subconfluent SW982 cells with insulin resulted in a significant increase in metabolic activity after 48 hours. Flow cytometry could not validate an induction of proliferation by identifying differences in cell cycle phase. However, if an additional experiment with flow cytometry on subconfluent SW982s was conducted, with a shorter period of insulin treatment as performed by Naderi et al, we have strong believes that this could validate the observed increases in metabolic activity as hyper proliferation. A possible explanation for the observed effects of insulin is examined, where insulin induces cell cycle promotion and inhibits apoptosis, through activation of PKB. This might possibly place insulin responsible for increased survival of synovial cells.

Finally, insulin induced downregulation of IR, and the same trend was observed for IGF1R gene expression. Which might suggest that the SW982s are sensitive to insulin signaling through the IR and the IGF1R. Insulin induced no change in c-Myc expression, and induced a downregulation of c-fos after 12 hours. Further, insulin induced a time-dependent trend of increase in IL-6 gene expression. Insulin also induced variation in the expression of the previously accepted reference gene 18S.

More tests have to be conducted in order to validate/discard the hypotheses proposed in this study. Including the possible pro-inflammatory actions of insulin in synovial cells and other tissue, mediated through inhibition of HSL. The potential for insulin to induce hyper proliferation and increased survival of synovial cells through activation of PKB, and the potential for insulin to induce expression proliferative and inflammatory genes.

A potential validation of insulin as an inflammatory mediator in SW982 cells, a model for synovitis, could lead to novel dietary advices for RA patients concerning the macronutrient composition of their diet. If insulin were to be labeled an initiator of hyper proliferation and mediator of cell survival in synovial cells, this would be valuable information for physicians and RA patients in lowering the disease activity and possibly slowing disease progression.

6. Literature

1. Halton, T.L., et al., *Potato and french fry consumption and risk of type 2 diabetes in women.* American Journal of Clinical Nutrition, 2006. **83**(2): p. 284-290.
2. Cordain, L., et al., *Origins and evolution of the Western diet: implications of iodine and seafood intakes for the human brain - Reply.* American Journal of Clinical Nutrition, 2005. **82**(2): p. 483-484.
3. Berrino, F., *[Western diet and Alzheimer's disease].* Epidemiol Prev, 2002. **26**(3): p. 107-15.
4. Adlercreutz, H., *Western diet and Western diseases: some hormonal and biochemical mechanisms and associations.* Scand J Clin Lab Invest Suppl, 1990. **201**: p. 3-23.
5. Parillo, M. and G. Riccardi, *Diet composition and the risk of type 2 diabetes: epidemiological and clinical evidence.* Br J Nutr, 2004. **92**(1): p. 7-19.
6. Barnard, R.J. and S.J. Wen, *Exercise and diet in the prevention and control of the metabolic syndrome.* Sports Med, 1994. **18**(4): p. 218-28.
7. Steiner, D.F., *The Biosynthesis of Insulin*, ed. S.B. Seino, Graeme. 2008, Japan: Springer Japan.
8. Laron, Z., *Insulin--a growth hormone.* Arch Physiol Biochem, 2008. **114**(1): p. 11-6.
9. Cebix. *Biology of C-peptide*. 2012 [cited 2014 16.01.14]; Available from: http://www.cebix.com/index.php/science/c-peptide-biology.
10. Saltiel, A.R. and C.R. Kahn, *Insulin signalling and the regulation of glucose and lipid metabolism.* Nature, 2001. **414**(6865): p. 799-806.
11. Zanquetta, M.M., et al., *Recovery of insulin sensitivity and Slc2a4 mRNA expression depend on T3 hormone during refeeding.* Metabolism, 2013.
12. Lawlor, M.A. and D.R. Alessi, *PKB/Akt: a key mediator of cell proliferation, survival and insulin responses?* J Cell Sci, 2001. **114**(Pt 16): p. 2903-10.
13. Nakamura, M.T., B.E. Yudell, and J.J. Loor, *Regulation of energy metabolism by long-chain fatty acids.* Prog Lipid Res, 2013. **53C**: p. 124-144.
14. Conover, C.A., J.T. Clarkson, and L.K. Bale, *Physiological concentrations of insulin induce cellular desensitization to the mitogenic effects of insulin-like growth factor I.* Diabetes, 1994. **43**(9): p. 1130-7.
15. Lodish, H.e.a., *Molecular Cell Biology*. 7 ed. Vol. 7. 2013, New York: Katherine Ahr Parker. 1154.
16. Inoue, G., B. Cheatham, and C.R. Kahn, *Different pathways of postreceptor desensitization following chronic insulin treatment and in cells overexpressing constitutively active insulin receptors.* J Biol Chem, 1996. **271**(45): p. 28206-11.
17. Shanik, M.H., et al., *Insulin resistance and hyperinsulinemia: is hyperinsulinemia the cart or the horse?* Diabetes Care, 2008. **31 Suppl 2**: p. S262-8.
18. DeFronzo, R.A. and E. Ferrannini, *Insulin resistance. A multifaceted syndrome responsible for NIDDM, obesity, hypertension, dyslipidemia, and atherosclerotic cardiovascular disease.* Diabetes Care, 1991. **14**(3): p. 173-94.

19. Richard A. Goldsby, T.J.K., Barbara A. Osborne and Janis Kuby, *Immunology*. 5th ed, ed. J. Noe. 2003, New York: W.H. Freeman and Company. 551.
20. Tang, D., et al., *PAMPs and DAMPs: signal 0s that spur autophagy and immunity.* Immunol Rev, 2012. **249**(1): p. 158-75.
21. Watkins, L.R., S.F. Maier, and L.E. Goehler, *Immune activation: the role of pro-inflammatory cytokines in inflammation, illness responses and pathological pain states.* Pain, 1995. **63**(3): p. 289-302.
22. Pasceri, V., J.T. Willerson, and E.T. Yeh, *Direct proinflammatory effect of C-reactive protein on human endothelial cells.* Circulation, 2000. **102**(18): p. 2165-8.
23. Lone, A.M. and K. Tasken, *Proinflammatory and immunoregulatory roles of eicosanoids in T cells.* Front Immunol, 2013. **4**: p. 130.
24. Cawley, J. and C. Meyerhoefer, *The medical care costs of obesity: an instrumental variables approach.* J Health Econ, 2012. **31**(1): p. 219-30.
25. Tilg, H. and A.R. Moschen, *Adipocytokines: mediators linking adipose tissue, inflammation and immunity.* Nat Rev Immunol, 2006. **6**(10): p. 772-83.
26. Wright, S.M. and L.J. Aronne, *Causes of obesity.* Abdom Imaging, 2012. **37**(5): p. 730-2.
27. Ogden, C.L., et al., *Prevalence of childhood and adult obesity in the United States, 2011-2012.* JAMA, 2014. **311**(8): p. 806-14.
28. Fraser, J.K., et al., *Fat tissue: an underappreciated source of stem cells for biotechnology.* Trends Biotechnol, 2006. **24**(4): p. 150-4.
29. Hahn, W.S., et al., *Pro-inflammatory cytokines differentially regulate adipocyte mitochondrial metabolism, oxidative stress and dynamics.* Am J Physiol Endocrinol Metab, 2014.
30. Galic, S., J.S. Oakhill, and G.R. Steinberg, *Adipose tissue as an endocrine organ.* Mol Cell Endocrinol, 2010. **316**(2): p. 129-39.
31. Cai, D., *NFkappaB-mediated metabolic inflammation in peripheral tissues versus central nervous system.* Cell Cycle, 2009. **8**(16): p. 2542-8.
32. Dali-Youcef, N., et al., *Metabolic inflammation: connecting obesity and insulin resistance.* Ann Med, 2013. **45**(3): p. 242-53.
33. Ye, J., *Emerging role of adipose tissue hypoxia in obesity and insulin resistance.* Int J Obes (Lond), 2009. **33**(1): p. 54-66.
34. Hotamisligil, G.S., *Inflammation and metabolic disorders.* Nature, 2006. **444**(7121): p. 860-7.
35. Calder, P.C. and R.F. Grimble, *Polyunsaturated fatty acids, inflammation and immunity.* Eur J Clin Nutr, 2002. **56 Suppl 3**: p. S14-9.
36. Gibney, M.J. and B. Hunter, *The effects of short- and long-term supplementation with fish oil on the incorporation of n-3 polyunsaturated fatty acids into cells of the immune system in healthy volunteers.* Eur J Clin Nutr, 1993. **47**(4): p. 255-9.
37. Yaqoob, P., et al., *Encapsulated fish oil enriched in alpha-tocopherol alters plasma phospholipid and mononuclear cell fatty acid compositions but not mononuclear cell functions.* Eur J Clin Invest, 2000. **30**(3): p. 260-74.

38. James, M.J., R.A. Gibson, and L.G. Cleland, *Dietary polyunsaturated fatty acids and inflammatory mediator production.* Am J Clin Nutr, 2000. **71**(1 Suppl): p. 343S-8S.
39. Nicolaou, A., *Eicosanoids in skin inflammation.* Prostaglandins Leukot Essent Fatty Acids, 2013. **88**(1): p. 131-8.
40. Rola-Pleszczynski, M., et al., *Differential regulation of cytokine and cytokine receptor genes by PAF, LTB4 and PGE2.* J Lipid Mediat, 1993. **6**(1-3): p. 175-81.
41. Sakata, D., C. Yao, and S. Narumiya, *Prostaglandin E2, an immunoactivator.* J Pharmacol Sci, 2010. **112**(1): p. 1-5.
42. Sacco, K., et al., *The role of prostaglandin E2 in endometriosis.* Gynecol Endocrinol, 2012. **28**(2): p. 134-8.
43. Murakami, M., *Lipid mediators in life science.* Exp Anim, 2011. **60**(1): p. 7-20.
44. Kalinski, P., *Regulation of immune responses by prostaglandin E2.* J Immunol, 2012. **188**(1): p. 21-8.
45. McHowat, J. and M.H. Creer, *Lysophosphatidylcholine accumulation in cardiomyocytes requires thrombin activation of Ca2+-independent PLA2.* Am J Physiol, 1997. **272**(4 Pt 2): p. H1972-80.
46. Yeaman, S.J., et al., *The multifunctional role of hormone-sensitive lipase in lipid metabolism.* Adv Enzyme Regul, 1994. **34**: p. 355-70.
47. Kraemer, F.B., et al., *Detection of hormone-sensitive lipase in various tissues. I. Expression of an HSL/bacterial fusion protein and generation of anti-HSL antibodies.* J Lipid Res, 1993. **34**(4): p. 663-71.
48. Khanapure, S.P., et al., *Eicosanoids in inflammation: biosynthesis, pharmacology, and therapeutic frontiers.* Curr Top Med Chem, 2007. **7**(3): p. 311-40.
49. Sommerfelt, R.M., et al., *Cytosolic Phospholipase A2 Regulates TNF-Induced Production of Joint Destructive Effectors in Synoviocytes.* PLoS One, 2013. **8**(12): p. e83555.
50. Lin, L.L., A.Y. Lin, and J.L. Knopf, *Cytosolic phospholipase A2 is coupled to hormonally regulated release of arachidonic acid.* Proc Natl Acad Sci U S A, 1992. **89**(13): p. 6147-51.
51. Lerner, U.H. and T. Modeer, *Bradykinin B1 and B2 receptor agonists synergistically potentiate interleukin-1-induced prostaglandin biosynthesis in human gingival fibroblasts.* Inflammation, 1991. **15**(6): p. 427-36.
52. Leistad, L., et al., *Multiple phospholipase A2 enzymes participate in the inflammatory process in osteoarthritic cartilage.* Scand J Rheumatol, 2011. **40**(4): p. 308-16.
53. Oestvang, J., M.W. Anthonsen, and B. Johansen, *LysoPC and PAF Trigger Arachidonic Acid Release by Divergent Signaling Mechanisms in Monocytes.* J Lipids, 2011. **2011**: p. 532145.
54. Berit Johansen, M.O. *Avexxin*. 2010; Available from: http://www.avexxin.com.
55. Andersen, S., et al., *Elevated expression of human nonpancreatic phospholipase A2 in psoriatic tissue.* Inflammation, 1994. **18**(1): p. 1-12.
56. Lee, H.J., et al., *Brain arachidonic acid cascade enzymes are upregulated in a rat model of unilateral Parkinson disease.* Neurochem Res, 2010. **35**(4): p. 613-9.

57. Stephenson, D.T., et al., *Cytosolic phospholipase A2 (cPLA2) immunoreactivity is elevated in Alzheimer's disease brain.* Neurobiol Dis, 1996. **3**(1): p. 51-63.
58. Cummings, B.S., *Phospholipase A2 as targets for anti-cancer drugs.* Biochem Pharmacol, 2007. **74**(7): p. 949-59.
59. Sfriso, P., et al., *Infections and autoimmunity: the multifaceted relationship.* J Leukoc Biol, 2010. **87**(3): p. 385-95.
60. Atassi, M.Z. and P. Casali, *Molecular mechanisms of autoimmunity.* Autoimmunity, 2008. **41**(2): p. 123-32.
61. Molina, V. and Y. Shoenfeld, *Infection, vaccines and other environmental triggers of autoimmunity.* Autoimmunity, 2005. **38**(3): p. 235-45.
62. Gibofsky, A., *Overview of epidemiology, pathophysiology, and diagnosis of rheumatoid arthritis.* Am J Manag Care, 2012. **18**(13 Suppl): p. S295-302.
63. Bartok, B. and G.S. Firestein, *Fibroblast-like synoviocytes: key effector cells in rheumatoid arthritis.* Immunol Rev, 2010. **233**(1): p. 233-55.
64. Strand, V., R. Kimberly, and J.D. Isaacs, *Biologic therapies in rheumatology: lessons learned, future directions.* Nat Rev Drug Discov, 2007. **6**(1): p. 75-92.
65. Chaiwongsa, R., et al., *Active compound of Zingiber cassumunar Roxb. down-regulates the expression of genes involved in joint erosion in a human synovial fibroblast cell line.* Afr J Tradit Complement Altern Med, 2012. **10**(1): p. 40-8.
66. Lee, D.G., et al., *The bone regenerative effects of fucosterol in in vitro and in vivo models of postmenopausal osteoporosis.* Mol Nutr Food Res, 2014.
67. Ma, X., et al., *Jolkinolide B inhibits RANKL-induced osteoclastogenesis by suppressing the activation NF-kappaB and MAPK signaling pathways.* Biochem Biophys Res Commun, 2014.
68. Klareskog, L., et al., *A new model for an etiology of rheumatoid arthritis: smoking may trigger HLA-DR (shared epitope)-restricted immune reactions to autoantigens modified by citrullination.* Arthritis Rheum, 2006. **54**(1): p. 38-46.
69. Begovich, A.B., et al., *A missense single-nucleotide polymorphism in a gene encoding a protein tyrosine phosphatase (PTPN22) is associated with rheumatoid arthritis.* Am J Hum Genet, 2004. **75**(2): p. 330-7.
70. Padyukov, L., et al., *A gene-environment interaction between smoking and shared epitope genes in HLA-DR provides a high risk of seropositive rheumatoid arthritis.* Arthritis Rheum, 2004. **50**(10): p. 3085-92.
71. Chang, J.H., et al., *Validity of SW982 synovial cell line for studying the drugs against rheumatoid arthritis in fluvastatin-induced apoptosis signaling model.* Indian J Med Res, 2014. **139**(1): p. 117-24.
72. Lv, F., et al., *The role of Act1, a NF-kappaB-activating protein, in IL-6 and IL-8 levels induced by IL-17 stimulation in SW982 cells.* Pharm Biol, 2013. **51**(11): p. 1444-50.
73. Matsuo, K., et al., *Arthritogenicity of annexin VII revealed by phosphoproteomics of rheumatoid synoviocytes.* Ann Rheum Dis, 2011. **70**(8): p. 1489-95.

74. Yamazaki, T., et al., *Phenotypic characterization of a human synovial sarcoma cell line, SW982, and its response to dexamethasone.* In Vitro Cell Dev Biol Anim, 2003. **39**(8-9): p. 337-9.
75. Fogh, J., W.C. Wright, and J.D. Loveless, *Absence of HeLa cell contamination in 169 cell lines derived from human tumors.* J Natl Cancer Inst, 1977. **58**(2): p. 209-14.
76. Tsuji, F., et al., *Effects of mitogen-activated protein kinase inhibitors or phosphodiesterase inhibitors on interleukin-1-induced cytokines production in synovium-derived cells.* Immunol Lett, 1999. **68**(2-3): p. 275-9.
77. Tran, C.N., S.K. Lundy, and D.A. Fox, *Synovial biology and T cells in rheumatoid arthritis.* Pathophysiology, 2005. **12**(3): p. 183-9.
78. ATCC. *American Type Culture Collection*. 2014; Available from: http://www.lgcstandards-atcc.org/.
79. Sugiyama, R., et al., *Defect of suppression of inflammasome-independent interleukin-8 secretion from SW982 synovial sarcoma cells by familial Mediterranean fever-derived pyrin mutations.* Mol Biol Rep, 2014. **41**(1): p. 545-53.
80. Randi M Sommerfelt, A.J.F., Trine Skuland, Berit Johansen, *Cytosolic Phospholipase A2 modulates TLR2 signaling in synoviocytes*, N.U.o.S.a. Technology, Editor. 2014.
81. Brattbakk, H.R., et al., *Balanced caloric macronutrient composition downregulates immunological gene expression in human blood cells-adipose tissue diverges.* OMICS, 2013. **17**(1): p. 41-52.
82. Jawaheer, D., et al., *Gender, body mass index and rheumatoid arthritis disease activity: results from the QUEST-RA Study.* Clin Exp Rheumatol, 2010. **28**(4): p. 454-61.
83. Esposito, K., et al., *Effect of a mediterranean-style diet on endothelial dysfunction and markers of vascular inflammation in the metabolic syndrome: a randomized trial.* JAMA, 2004. **292**(12): p. 1440-6.
84. Sharman, M.J. and J.S. Volek, *Weight loss leads to reductions in inflammatory biomarkers after a very-low-carbohydrate diet and a low-fat diet in overweight men.* Clin Sci (Lond), 2004. **107**(4): p. 365-9.
85. Calder, P.C., et al., *Dietary factors and low-grade inflammation in relation to overweight and obesity.* Br J Nutr, 2011. **106 Suppl 3**: p. S5-78.
86. ATCC, *ATCC Animal Cell Culture Guide*. 2014.
87. Sargent, J.M. and C.G. Taylor, *Appraisal of the MTT assay as a rapid test of chemosensitivity in acute myeloid leukaemia.* Br J Cancer, 1989. **60**(2): p. 206-10.
88. Brown, M. and C. Wittwer, *Flow cytometry: principles and clinical applications in hematology.* Clin Chem, 2000. **46**(8 Pt 2): p. 1221-9.
89. Kolesik, M., et al., *Space-time resolved simulation of femtosecond nonlinear light-matter interactions using a holistic quantum atomic model: application to near-threshold harmonics.* Opt Express, 2012. **20**(14): p. 16113-28.
90. Qiagen, *QuantiTect Reverse Transcription Handbook*. 2009. p. 11-13.
91. Bustin, S.A., et al., *The MIQE guidelines: minimum information for publication of quantitative real-time PCR experiments.* Clin Chem, 2009. **55**(4): p. 611-22.

92. VanGuilder, H.D., K.E. Vrana, and W.M. Freeman, *Twenty-five years of quantitative PCR for gene expression analysis.* Biotechniques, 2008. **44**(5): p. 619-26.
93. Taylor, S., et al., *A practical approach to RT-qPCR-Publishing data that conform to the MIQE guidelines.* Methods, 2010. **50**(4): p. S1-5.
94. Heid, C.A., et al., *Real time quantitative PCR.* Genome Res, 1996. **6**(10): p. 986-94.
95. Livak, K.J. and T.D. Schmittgen, *Analysis of relative gene expression data using real-time quantitative PCR and the 2(-Delta Delta C(T)) Method.* Methods, 2001. **25**(4): p. 402-8.
96. Pfaffl, M.W., *A new mathematical model for relative quantification in real-time RT-PCR.* Nucleic Acids Res, 2001. **29**(9): p. e45.
97. Oestvang, J., M.W. Anthonsen, and B. Johansen, *Role of secretory and cytosolic phospholipase A(2) enzymes in lysophosphatidylcholine-stimulated monocyte arachidonic acid release.* FEBS Lett, 2003. **555**(2): p. 257-62.
98. Huwiler, A., et al., *The omega3-polyunsaturated fatty acid derivatives AVX001 and AVX002 directly inhibit cytosolic phospholipase A(2) and suppress PGE(2) formation in mesangial cells.* Br J Pharmacol, 2012. **167**(8): p. 1691-701.
99. Jorgensen, K.M., et al., *Platelet activating factor stimulates arachidonic acid release in differentiated keratinocytes via arachidonyl non-selective phospholipase A2.* Arch Dermatol Res, 2010. **302**(3): p. 221-7.
100. Hoeck, W.G., et al., *Cytoplasmic phospholipase A2 activity and gene expression are stimulated by tumor necrosis factor: dexamethasone blocks the induced synthesis.* Proc Natl Acad Sci U S A, 1993. **90**(10): p. 4475-9.
101. Feuerherm, A.J.S., R.M., *Oleic Acid Release In Response To IL-1B*, A. Johansen, Editor. 2014.
102. Hitchon, C.A. and H.S. El-Gabalawy, *The synovium in rheumatoid arthritis.* Open Rheumatol J, 2011. **5**: p. 107-14.
103. Buettner, C., *Is hyperinsulinemia required to develop overeating-induced obesity?* Cell Metab, 2012. **16**(6): p. 691-2.
104. Svegliati-Baroni, G., et al., *Insulin and insulin-like growth factor-1 stimulate proliferation and type I collagen accumulation by human hepatic stellate cells: differential effects on signal transduction pathways.* Hepatology, 1999. **29**(6): p. 1743-51.
105. Flier, J.S., P. Usher, and A.C. Moses, *Monoclonal antibody to the type I insulin-like growth factor (IGF-I) receptor blocks IGF-I receptor-mediated DNA synthesis: clarification of the mitogenic mechanisms of IGF-I and insulin in human skin fibroblasts.* Proc Natl Acad Sci U S A, 1986. **83**(3): p. 664-8.
106. Boileau, P., et al., *Dissociation between insulin-mediated signaling pathways and biological effects in placental cells: role of protein kinase B and MAPK phosphorylation.* Endocrinology, 2001. **142**(9): p. 3974-9.
107. van Meerloo, J., G.J. Kaspers, and J. Cloos, *Cell sensitivity assays: the MTT assay.* Methods Mol Biol, 2011. **731**: p. 237-45.
108. Banskota, N.K., et al., *Characterization of induction of protooncogene c-myc and cellular growth in human vascular smooth muscle cells by insulin and IGF-I.* Diabetes, 1989. **38**(1): p. 123-9.

109. Endo, T. and B. Nadal-Ginard, *Transcriptional and posttranscriptional control of c-myc during myogenesis: its mRNA remains inducible in differentiated cells and does not suppress the differentiated phenotype.* Mol Cell Biol, 1986. **6**(5): p. 1412-21.
110. Hunt, S.P., A. Pini, and G. Evan, *Induction of c-fos-like protein in spinal cord neurons following sensory stimulation.* Nature, 1987. **328**(6131): p. 632-4.
111. Olson, A.L. and J.E. Pessin, *Regulation of c-fos expression in adipose and muscle tissue of diabetic rats.* Endocrinology, 1994. **134**(1): p. 271-6.
112. Akira, S., et al., *Biology of multifunctional cytokines: IL 6 and related molecules (IL 1 and TNF).* FASEB J, 1990. **4**(11): p. 2860-7.
113. Fasshauer, M., et al., *Interleukin (IL)-6 mRNA expression is stimulated by insulin, isoproterenol, tumour necrosis factor alpha, growth hormone, and IL-6 in 3T3-L1 adipocytes.* Horm Metab Res, 2003. **35**(3): p. 147-52.
114. LaPensee, C.R., E.R. Hugo, and N. Ben-Jonathan, *Insulin stimulates interleukin-6 expression and release in LS14 human adipocytes through multiple signaling pathways.* Endocrinology, 2008. **149**(11): p. 5415-22.
115. Rosa, S.C., et al., *Expression and function of the insulin receptor in normal and osteoarthritic human chondrocytes: modulation of anabolic gene expression, glucose transport and GLUT-1 content by insulin.* Osteoarthritis Cartilage, 2011. **19**(6): p. 719-27.
116. Aljada, A., et al., *Insulin inhibits the expression of intercellular adhesion molecule-1 by human aortic endothelial cells through stimulation of nitric oxide.* J Clin Endocrinol Metab, 2000. **85**(7): p. 2572-5.
117. Mohn, K.L., et al., *Immediate-early gene expression differs between regenerating liver, insulin-stimulated H-35 cells, and mitogen-stimulated Balb/c 3T3 cells. Liver-specific induction patterns of gene 33, phosphoenolpyruvate carboxykinase, and the jun, fos, and egr families.* J Biol Chem, 1990. **265**(35): p. 21914-21.
118. Oestvang, J., et al., *Modification of LDL with human secretory phospholipase A(2) or sphingomyelinase promotes its arachidonic acid-releasing propensity.* J Lipid Res, 2004. **45**(5): p. 831-8.
119. Kawamura, M., et al., *Hormone-sensitive lipase in differentiated 3T3-L1 cells and its activation by cyclic AMP-dependent protein kinase.* Proc Natl Acad Sci U S A, 1981. **78**(2): p. 732-6.
120. Stralfors, P. and R.C. Honnor, *Insulin-induced dephosphorylation of hormone-sensitive lipase. Correlation with lipolysis and cAMP-dependent protein kinase activity.* Eur J Biochem, 1989. **182**(2): p. 379-85.
121. Gotsis, E., et al., *Health Benefits of the Mediterranean Diet: An Update of Research Over the Last 5 Years.* Angiology, 2014.
122. Jamal Naderi, A.F., Thanh Ngyuen, Berit Johansen, *Cellular effect of insulin on proliferation of monocytes* 2014, The FASEB Journal.
123. Feuerherm, A.J., et al., *Platelet-activating factor induces proliferation in differentiated keratinocytes.* Mol Cell Biochem, 2013. **384**(1-2): p. 83-94.
124. Calle, E.E. and R. Kaaks, *Overweight, obesity and cancer: epidemiological evidence and proposed mechanisms.* Nat Rev Cancer, 2004. **4**(8): p. 579-91.
125. Sbraccia, P., et al., *Insulin down-regulates insulin receptor number and up-regulates insulin receptor affinity in cells expressing a tyrosine kinase-defective insulin receptor.* J Biol Chem, 1990. **265**(9): p. 4902-7.

126. Maestro, B., et al., *Stimulation by 1,25-dihydroxyvitamin D3 of insulin receptor expression and insulin responsiveness for glucose transport in U-937 human promonocytic cells.* Endocr J, 2000. **47**(4): p. 383-91.
127. Mamula, P.W., et al., *Regulating insulin-receptor-gene expression by differentiation and hormones.* Diabetes Care, 1990. **13**(3): p. 288-301.
128. Marshall, S. and J.M. Olefsky, *Effects of insulin incubation on insulin binding, glucose transport, and insulin degradation by isolated rat adipocytes. Evidence for hormone-induced desensitization at the receptor and postreceptor level.* J Clin Invest, 1980. **66**(4): p. 763-72.
129. Delafontaine, P., Y.H. Song, and Y. Li, *Expression, regulation, and function of IGF-1, IGF-1R, and IGF-1 binding proteins in blood vessels.* Arterioscler Thromb Vasc Biol, 2004. **24**(3): p. 435-44.
130. Dupont, J., et al., *Insulin and IGF-1 induce different patterns of gene expression in mouse fibroblast NIH-3T3 cells: identification by cDNA microarray analysis.* Endocrinology, 2001. **142**(11): p. 4969-75.
131. Rampalli, A.M. and P.S. Zelenka, *Insulin regulates expression of c-fos and c-jun and suppresses apoptosis of lens epithelial cells.* Cell Growth Differ, 1995. **6**(8): p. 945-53.
132. Alexandrow, M.G., et al., *Overexpression of the c-Myc oncoprotein blocks the growth-inhibitory response but is required for the mitogenic effects of transforming growth factor beta 1.* Proc Natl Acad Sci U S A, 1995. **92**(8): p. 3239-43.
133. Evan, G.I., et al., *Induction of apoptosis in fibroblasts by c-myc protein.* Cell, 1992. **69**(1): p. 119-28.
134. West, A.E., E.C. Griffith, and M.E. Greenberg, *Regulation of transcription factors by neuronal activity.* Nat Rev Neurosci, 2002. **3**(12): p. 921-31.
135. Firestein, G.S., *Evolving concepts of rheumatoid arthritis.* Nature, 2003. **423**(6937): p. 356-61.
136. Doudna, J.A. and V.L. Rath, *Structure and function of the eukaryotic ribosome: the next frontier.* Cell, 2002. **109**(2): p. 153-6.
137. Schmittgen, T.D. and B.A. Zakrajsek, *Effect of experimental treatment on housekeeping gene expression: validation by real-time, quantitative RT-PCR.* J Biochem Biophys Methods, 2000. **46**(1-2): p. 69-81.
138. Thellin, O., et al., *Housekeeping genes as internal standards: use and limits.* J Biotechnol, 1999. **75**(2-3): p. 291-5.
139. Selvey, S., et al., *Beta-actin--an unsuitable internal control for RT-PCR.* Mol Cell Probes, 2001. **15**(5): p. 307-11.
140. Sartipy, P. and D.J. Loskutoff, *Monocyte chemoattractant protein 1 in obesity and insulin resistance.* Proc Natl Acad Sci U S A, 2003. **100**(12): p. 7265-70.
141. Krogh-Madsen, R., et al., *Insulin stimulates interleukin-6 and tumor necrosis factor-alpha gene expression in human subcutaneous adipose tissue.* Am J Physiol Endocrinol Metab, 2004. **286**(2): p. E234-8.
142. Lynne Cassimeris, V.R.L., George Piopper, *Lewin's CELLS*. 2nd ed.
143. Fukuda, H., T. Noguchi, and N. Iritani, *Transcriptional regulation of insulin receptor gene promoter in rat hepatocytes.* Biochem Biophys Res Commun, 2001. **280**(5): p. 1274-8.
144. Crettaz, M., et al., *Insulin receptor regulation and desensitization in rat hepatoma cells. The loss of the oligomeric forms of the receptor*

correlates with the change in receptor affinity. J Biol Chem, 1984. **259**(18): p. 11543-9.
145. Gavin, J.R., 3rd, et al., *Insulin-dependent regulation of insulin receptor concentrations: a direct demonstration in cell culture.* Proc Natl Acad Sci U S A, 1974. **71**(1): p. 84-8.
146. Elgin, R.G., W.H. Busby, Jr., and D.R. Clemmons, *An insulin-like growth factor (IGF) binding protein enhances the biologic response to IGF-I.* Proc Natl Acad Sci U S A, 1987. **84**(10): p. 3254-8.
147. Rovensky, J., et al., *Hormone concentrations in synovial fluid of patients with rheumatoid arthritis.* Clin Exp Rheumatol, 2005. **23**(3): p. 292-6.
148. Macho, L., et al., *[Levels of hormones in plasma and in synovial fluid of knee joint of patients with rheumatoid arthritis].* Cas Lek Cesk, 2007. **146**(3): p. 292-6.
149. Rovensky, J., et al., *Peptide hormones and histamine in plasma and synovial fluid of patients with rheumatoid arthritis and osteoarthrosis.* Endocr Regul, 2005. **39**(1): p. 1-6.

Appendix

A. All biological replicates (n=2) for the representative experiment in figure 3.3.1.

Table A.1 Mean AA release fold changes after insulin incubation for 4, 8, 16, 24 and 48 hours. * indicates results significantly different from control ($p<0.05$), which was set to 1.

Treatment	4h	8h	16h	24h	48h
1 µM INS	0.70	0.83	0.87	0.84	0.86
±SD	0.09	0.10	0.06	0.03	0.03
IL-1β 10 ng/mL	2.22*	4.90*	3.71*	3.22*	2.31*
±SD	0.17	0.14	0.32	0.20	0.06

B. All biological replicates (n=3) for the representative experiment in figure 3.3.2.

Table B.1 Mean AA release fold changes after insulin incubation for 48 hours, three different insulin concentrations. * indicates results significantly different from control ($p<0.05$), which was set to 1.

Treatment	48h
0.3 µM INS	0.82
±SD	0.02
1 µM INS	0.86
±SD	0.03
3 µM INS	0.78
±SD	0.17
IL-1β 10 ng/mL	2.31*
±SD	0.06

C. All biological replicates (n=2) for the representative experiment in figure 3.4.1.

Table C.1 Mean OA release fold changes after insulin incubation for 48 hours, three different insulin concentrations.

Treatment	4h	8h	16h	24h	48h
1 μM INS	0.56	0.69	0.77	0.83	0.78
±SD	0.06	0.05	0.08	0.14	0.06
IL-1β 10 ng/mL	0.89	1.65	1.52	1.35	0.89
±SD	0.08	0.09	0.12	0.11	0.16

D. All biological replicates (n=3) for the representative experiment in figure 3.4.2.

Table D.1 Mean OA release fold changes after insulin incubation for 48 hours, three different insulin concentrations.

Treatment	48h
0.3 μM INS	0.78
±SD	0.04
1 μM INS	0.78
±SD	0.06
3 μM INS	0.74
±SD	0.06
IL-1β 10 ng/mL	0.89
±SD	0.16

E. All biological replicates (n=4) for the representative experiment in figure 3.6.1.

Table E.1 Mean fold changes of metabolic activity measured by MTT assay, after insulin incubation for 24 hours. Different number of cells seeded.

Number of Cells Seeded	24h
2500	1.29
±SD	0.19
5000	1.16
±SD	0.09
10 000	1,26
±SD	0.33
15 000	1.18
±SD	0.13
25 000	1.10
±SD	0.11

F. All biological replicates (n=4) for the representative experiment in figure 3.6.2.

Table F.1 Mean fold changes of metabolic activity measured by MTT assay, after insulin incubation for 36 hours. Different number of cells seeded.

Number of Cells Seeded	36h
2500	1.31
±SD	0.22
5000	1.26
±SD	0.27
10 000	1,19
±SD	0.23
15 000	1.18
±SD	0.26
25 000	1.09
±SD	0.27

G. All biological replicates (n=4) for the representative experiment in figure 3.6.3.

Table G.1 Mean fold changes of metabolic activity measured by MTT assay, after insulin incubation for 48 hours. Different number of cells seeded. * indicates results significantly different from control ($p<0.05$), which was set to 1.

Number of Cells Seeded	48h
2500	1.44*
±SD	0.20
5000	1.31*
±SD	0.13
10 000	1,22
±SD	0.21
15 000	1.20
±SD	0.16
25 000	1.16
±SD	0.26

H. All biological replicates (n=3) for the representative experiment in figure 3.7.1.

Table H.1 Mean fold changes of metabolic activity measured by MTT assay, after incubation with different concentration of insulin for 48 hours. Cells seeded at 2500 cells per well. * indicates results significantly different from control ($p<0.05$), which was set to 1.

Treatment	48h
0.3 µM INS	1.30*
±SD	0.18
1 µM INS	1.51*
±SD	0.22
3 µM INS	1.36*
±SD	0.23
DMEM10%	3.04*
±SD	0.31

I. All biological replicates (n=3) for the representative experiment in figure 3.7.2.

Table I.1 Mean fold changes of metabolic activity measured by MTT assay, after incubation with different concentration of insulin for 48 hours. Cells seeded at 5000 cells per well. * indicates results significantly different from control ($p<0.05$), which was set to 1.

Treatment	48h
0.3 µM INS	1.29*
±SD	0.10
1 µM INS	1.32*
±SD	0.12
3 µM INS	1.22*
±SD	0.15
DMEM10%	2.85*
±SD	0.41

J. Each of the biological replicates, where number 1 is presented in figure 3.8.1.

Table J.1 Percent of cells in G1 and G2+S+M for each of the biological replicates from the flow cytometry experiment. Biological replicate number 2.

Treatment	G1	G2+M+S
SF-DMEM	89.41	10.32
1 µM INS	94.08	5.92
DMEM10%	84.78	15.2

Table J.2 Percent of cells in G1 and G2+S+M for each of the biological replicates from the flow cytometry experiment. Biological replicate number 2.

Treatment	G1	G2+M+S
SF-DMEM	78.34	16.32
1 µM INS	79.84	13.74
DMEM10%	65.65	22.14

Table J.3 Percent of cells in G1 and G2+S+M for each of the biological replicates from the flow cytometry experiment. Biological replicate number 3.

Treatment	G1	G2+M+S
SF-DMEM	85.12	13.65
1 μM INS	80.19	10.87
DMEM10%	83.6	15.93

K. All biological replicates (n=3) for the representative experiment in figure 3.9.1.

Table K.1 Mean fold changes of IR mRNA levels, after incubation with insulin for 2, 4, 6, 12 and 24 hours. * indicates results significantly different from control ($p<0.05$), which was set to 1.

Treatment	2h	4h	6h	12h	24h
1 μM INS	0.51*	0.67	0.72	0.38*	0.95
±SD	0.14	0.11	0.14	0.19	0.24

L. All biological replicates (n=3) for the representative experiment in figure 3.9.2.

Table L.1 Mean fold changes of IGF1R mRNA levels, after incubation with insulin for 2, 4, 6, 12 and 24 hours. * indicates results significantly different from control ($p<0.05$), which was set to 1.

Treatment	2h	4h	6h	12h	24h
1 μM INS	0.41	0.62	0.55	0.26*	1.01
±SD	0.33	0.13	0.42	0.16	0.19

M. All biological replicates (n=3) for the representative experiment in figure 3.9.3.

Table M.1 Mean fold changes of c-Myc mRNA levels, after incubation with insulin for 2, 4, 6, 12 and 24 hours.

Treatment	2h	4h	6h	12h	24h
1 μM INS	1.01	1.06	1.13	0.80	0.85
±SD	0.20	0.19	0.14	0.19	0.10

N. All biological replicates (n=3) for the representative experiment in figure 3.9.4.

Table N.1 Mean fold changes of c-Fos mRNA levels, after incubation with insulin for 2, 4, 6, 12 and 24 hours. * indicates results significantly different from control ($p<0.05$), which was set to 1.

Treatment	2h	4h	6h	12h	24h
1 μM INS	0.54	1.21	1.20	0.39*	0.91
±SD	0.28	0.38	0.27	0.18	0.11

O. All biological replicates (n=3) for the representative experiment in figure 3.9.5.

Table O.1 Mean fold changes of IL-6 mRNA levels, after incubation with insulin for 2, 4, 6, 12 and 24 hours.

Treatment	2h	4h	6h	12h	24h
1 μM INS	1.6	1.29	1.06	0.91	0.60
±SD	0.25	0.28	0.14	0.66	0.07

P. All biological replicates (n=3) for the representative experiment in figure 3.9.6.

Table P.1 Mean fold changes of 18S mRNA levels, after incubation with insulin for 2, 4, 6, 12 and 24 hours.

Treatment	2h	4h	6h	12h	24h
1 μM INS	0.95	1.41	0.99	0.35	1.06
±SD	0.04	0.79	0.15	0.28	0.47